NTNU – Trondheim
Norwegian University of
Science and Technology

Modelling and Control of the Secondary Combustion Chamber in an Energy from Waste Plant

Kristin Guldberg

Master of Science in Engineering Cybernetics
Submission date: June 2012
Supervisor: Morten Hovd, ITK
Co-supervisor: Sigurd Lone, Energos

Norwegian University of Science and Technology
Department of Engineering Cybernetics

Problem description

Title: Modelling and control of the secondary combustion chamber in an energy from waste plant.

This thesis is given in cooperation with Energos and Cybernetica and is a continuation of a project work conducted in the final semester of 2011.

The task is to do preparatory work for model based control of the secondary combustion chamber of an Energos energy from waste plant.
This includes:

- Further development of the simulation model for the secondary chamber, among others to include heat transfer with the walls of the furnace.
- State the control problem for the model predictive controller reflecting the desired process behaviour.
- Identify control variables, manipulated variables and measurements.
- Identify relevant constraints in the operation conditions.
- Implementation and simulation of the model in Cybernetica's tools.
- Implementing a Kalman filter in Cybernetica's tool ModelFit and use available measurements for parameter and state estimation.

Abstract

Thermal conversion of municipal and industrial waste is an environmentally friendly way to recover energy from waste. There are many governmental requirements regarding air emissions from such processes. A tight control is required for the operation of the combustion chamber as there are many unknown disturbances, the biggest being the composition of the waste. Classic PID controllers will only just provide the required control, hence model predictive control, MPC, was proposed to optimise the control. This thesis covers the preparatory work for the implementation of MPC.

This report describes how a transient model of the secondary combustion chamber was derived. The model consists of material and energy balances for six control volumes with a simplified approach the combustion reaction. The report also gives a short description of the entire process in a typical Energos energy from waste plant and some basics on MPC and Kalman filtering.

Model simulations were performed in Cybernetica's software ModelFit. Operational data from an Energos plant was used as input to the model and measured outputs were compared to predicted outputs. Parameter estimation was also performed using the process data. The implementation of model predictive control for this system was considered.

A first order divided difference Kalman filter was implemented in ModelFit for model updating that improved the accuracy of the predictions. This is an important step on the way towards MPC.

Sammendrag

Termisk konvertering av husholdnings- og industielt avfall er en miljøvennig måte å gjenvinne energi fra avfallet. Det finnes mange statlige krav når det gjelder utslipp fra slike søppleforbrenningsanlegg. En stram regulering er nødvending for driften av forbrennigskammeret siden det finnes mange ukjente forstyrrelser, den største er sammensetningen av avfallet. Klassiske PID regulatorer vil kun tilby det nødvendige regulering for å drive anlegget, derfor ble modell basert regulering, MPC, foreslått for å optimalisere prosessen. Denne oppgaven dekker forberedende arbeid for implementering av MPC.

Denne rapporten beskriver hvordan en transient modell av sekundærkammeret i en Energos forbrenningsovn ble utviklet. Modellen består av material- og energibalanser for seks kontrollvolum med en forenklet tilnærming til forbrenningskinetikken. Rapporten gir også en kort beskrivelse av hele prosessen i et typisk "energi fra avfall" Energosanlegg samt litt grunnleggende om MPC og Kalmanfilter.

Modellsimuleringene ble gjort i Cyberneticas software ModelFit. Loggedata fra et Energosanlegg ble brukt som inngangadata til modellen og måledata ble sammenlignet med beregnede verdier. Parameterestimering ble utført basert på loggedataene. Implementering av model basert regulering ble vurdert.

Et første ordens divided difference Kalmanfilter ble implementert i ModelFit for modelloppdateringer. Dette forbedret nøyaktigheten til de beregnede verdiene og er et viktig skritt på veien mot MPC.

Preface

This is a final year Master thesis at NTNU, Department of Engineering Cybernetics, done in cooperation with Energos and Cybernetica. The work is based on preliminary work done during my final year project last semester. The task was to look at the possibilities and challenges related to model based control of the secondary combustion chamber of an Energos energy from waste plant. Preparatory work for MPC was conducted. This was done because it's expected that model based control will improve the performance.

The modelling was more challenging than first expected and some problems were encountered, making the project a great experience with a steep learning curve.

The report has an introductory part, theoretical part, a part presenting the results, a part discussing the results and finally some conclusions and suggestions to further work.

I would like to take this opportunity to thank Energos for an interesting problem, Cybernetica for letting me use their tools and for guiding me on the way, in particular thanks to Andreas for explaining all the basics, Ruben for technical assistance and Halgeir for decision making. Thanks also to my supervisors Morten and Sigurd for always giving quick responses.

In addition I have to thank my "family" in Abels gate for making life bearable, especially thanks to Pablo for standing living with me.

Trondheim, June 2012

Kristin Guldberg

Contents

Nomenclature

i	Index for control volumes
j	Index for components
r	Index for reactions
M	Molar mass of mixture, [g mol^{-1}]
R	Universal gas constant, [J $K^{-1}mol^{-1}$]
ΔH_f	Heat of formation, [J mol^{-1}]
A	Area, [m^2]
U_{htc_w}	Heat transfer coefficient [W m^{-2} K^{-1}]
V_i	Volume of control volume i, [m^3]
$\vec{e}$	Outward normal unit vector
c	Number of components, here: 7
m	Mass, [kg]
m_w	Mass of wall, [kg]
v	Number of control volumes, here: 6
C_p	Heat capacity, for constant pressure, [J $mol^{-1}K^{-1}$]
C_{th_w}	Thermal mass of wall, [J K^{-1}]
E	Energy, [J]
F_{SG_i}	Molar flow out of control volume i, [mol s^{-1}]
F_{air_i}	Molar flow of air into control volume i, [mol s^{-1}]

H	Enthalpy, [J]
R_t	Thermal resistance, [$m^2K\ W^{-1}$]
T_s	Temperature of the sensors, [K]
T_w	Temperature of the walls, [K]
U	Internal energy, [J]
W	Work done by system, [J]
$[j]$	Concentration of species j, [mol m^{-3}]
$\dot{Q}$	Heat transferred to or from wall, [J]
$\dot{m}$	Mass flow, [kg s^{-1}]
ω_r	Rate of reaction r, [mol $m^{-3}s^{-1}$]
ρ	Density, [kg m^{-3}]
$\vec{\Omega}_i$	Reaction rates of all components in volume i, [mol $m^{-3}s^{-1}$]
$\vec{n}$	Molar holdup of each species, [mol]
$\vec{x}_i$	Molar fraction of gas leaving control volum i
$\vec{x}_{air_i}$	Molar fraction of air entering control volume i
e	Energy per mass, [J kg^{-1}]
h	Enthalpy, [J mol^{-1}]
k_g	Heat conductivity, gas, [W m^{-1} K^{-1}]
k_w	Heat conductivity, wall, [W m^{-1} K^{-1}]
n_j	Molar holdup of species j, [mol]
n_{tot_i}	Total molar holdup of all species in control volume i, [mol]
u	Internal energy per mol, [J mol^{-1}]
v	Process noise
v_m	Mean velocity, [m s^{-1}]

w Measurement noise

x_j Molar fraction of species j

C Programming language (unless context indicates use as temperature unit)

CSTR *Continuously Stirred Tank Reactor*

DAE *Differential Algebraic Equation*

EKF *Extended Kalman Filter*

GNU *GNU is Not Unix*, free software operating system

GSL *GNU Scientific Library*, software library written in C

MPC *Model Predictive Control*

ODE *Ordinary Differential Equation*

PID Classic controller

SPKF *Sigma Point Kalman Filter*

List of Figures

List of Tables

Chapter 1

Energy from waste

1.1 Introduction

The world today suffers from a general waste and energy problem; the amount of waste and the demand for energy are both increasing. An energy from waste plant is a step in the direction of finding a solution to this problem by converting waste to energy. Such a plant provides an environmentally friendly alternative to landfill by converting possibly environmentally hazardous components into harmless compounds [1]. It also offers a significant volume reduction of the waste and removes the nuisance from odour and leakages to the local surroundings. The released combustion heat is used for district heating and/or electricity production. The alternative energy source is mainly fossil fuel that has far higher pollutant air emissions per kilowatt hour produced [1]. Additionally, the plant provides a local solution for local waste problems and is hence relatively small with a low visual impact. A local solution also minimises the transportation needs [2].

Some schematics and a brief description of the process of a typical plant can be found in appendix A. It is recommended to read this now if the reader is unfamiliar with the process, especially in order to understand the role of the secondary combustion chamber which is the target of this work.

The largest uncertainty in the combustion process is the ever changing fuel quality of the waste, such as water content and mean calorific value, which are not available for on-line measurement. It is desirable to have a stable temperature inside the furnace and also stable and low pollutant air emissions of the flue gas leaving the plant (to be discussed later). Consequently a good control system is needed to decide at any time how much waste to be fed into the plant and how much air to be injected to the combustion. The idea behind this project is to contribute to the improvement and optimisation

of the current control system of the combustion process. This by doing preparatory work for the implementation of model predictive control, e.g. modelling and simulating the process and considering the possible benefits from an implementation of a model predictive controller.

1.2 Scope and goals

This report focuses only on the secondary combustion chamber of an Energos energy from waste plant (no. 5 in Figure A.2) where the syngas produced in the primary chamber is burned. Model predictive control, MPC, is to be considered as the current control system based on PID controllers has some limitations. However, the goal of this project is not to have a product ready for implementation, but rather a study of the system and how model predictive control might improve control performance. In order to implement a model predictive controller, the process has to be modelled. The model derived during my final year project last semester [3] was used after some improvements and changes.

Only the main combustible species like methane, hydrogen and carbon monoxide are taken into account in the combustion reactions. The reaction kinetics were also drastically simplified to get an acceptable run time.

The aspects of interest are the temperature and composition out of the furnace which are being simulated and compared to process data.

Cybernetica's CENIT user interface was used for implementation of the model. Model fitting and simulations were done using Cybernetica's simulation platform ModelFit.

The goals are:

- to have an accurate yet simple enough model that can be used for testing model predictive control strategies
- to assess the validity of the model and fit it to process data by parameter and state estimation (Kalman filter)
- to define the control problem and consider how MPC can be implemented into the already existing control system

Chapter 2

Model development

This chapter will cover model development and the the relevant theory behind it. A description of the implementation plus some basics on Kalman filtering and MPC are also included.

From the previous modelling work done on this process [3] we have expressions for the change in molar hold-up and change in temperature. The Reynolds transport theorem (see Appendix B) was applied to the conservation laws for conservation of mass and energy. The derivations of this are included here (as parts of section 2.2) as they form an important part of the model.

The model was previously programmed and simulated in Matlab. During the current work the model was changed and improved and the changes first tested in Matlab. When working satisfactory the entire model was reimplemented using the programming language C.

Last semester the model was simulated with some assumed constant inputs, this time real process data was used.

2.1 System description

In this section we will take a closer look at the part of the process that forms our system, namely the secondary combustion chamber.

Inputs and outputs

The syngas produced in the primary combustion chamber flows directly into the secondary chamber for combustion. In addition to this there are also four other inlets to the secondary chamber: two injections of recirculated flue gas

with a temperature of approx. 150° C and two injections of secondary air[1] of approx. 25° C. The recirculated flue gas is denoted R1 and R2, and the secondary air S1 and S2. This notation will be used throughout the report. Figure 2.1 shows approximately where the injections happen.

Leaving the chamber is flue gas of approx. 900° C. The residence time in the secondary chamber is approximately 4 seconds.

Chemical components

Measurements of the composition of the syngas produced during the gasification process at Energos facilities [4] shows that the gas consists mainly of seven components:

$$\begin{bmatrix} CH_4 \\ CO \\ CO_2 \\ H_2 \\ H_2O \\ O_2 \\ N_2 \end{bmatrix} \tag{2.1}$$

This syngas composition vector includes combustion species, nitrogen and traces of oxygen from gasification air, combustion products and vaporised water from the waste. Concentration of other combustible species, i.e. longer-chain aliphatic hydrocarbons and tars are small, and therefore not considered in this model.

The injected air is assumed to consist of 21% oxygen and 79% nitrogen (dry basis). The recirculated flue gas composition is equal to the composition going out of the chamber (with a small time delay) and is measured. It is desirable and common that methane, hydrogen and carbon monoxide is fully combusted in the process, so typically the flue gas consists only of the combustion products, CO_2 and H_2O, and air, O_2 and N_2. The kinetic reactions will be described in the next section.

Control volumes

When analysing fluid motion, we might take one of two paths: (1) seeking to describe the detailed flow pattern at every point (x, y, z) in the field or (2) working with a finite region, making a balance of flow in versus flow out, and determining gross flow effects such as the force or torque on a body or

[1] The air injected to the primary chamber is denoted primary air, and the air injected into the secondary chamber is denoted secondary air, they are both normal air taken from the bunker halls for the waste.

the total energy exchange [5]. The second method is the control volume or large scale approach and is what was chosen for this model.

Figure 2.1 shows a sketch of the simplified physical setup of the combustion chambers used in this model. The primary chamber is at the bottom of the figure and the secondary chamber at the top. The secondary chamber is divided into six control volumes as shown in the figure below.

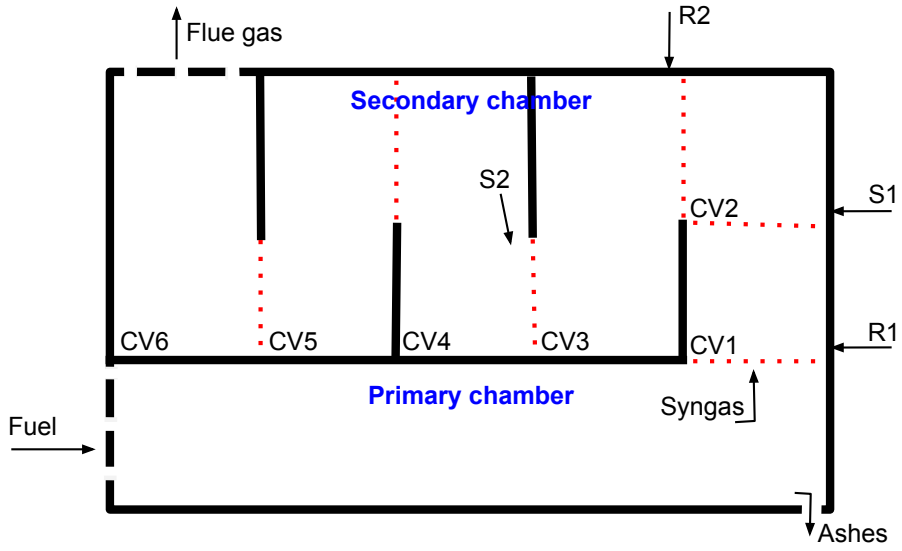

Figure 2.1: Combustion chambers with control volumes

The black lines are the walls of the furnace with dashed lines at the fuel inlet and flue gas outlet. CV1-CV6 denote control volumes 1-6 and the division of the control volumes are shown by the red dotted lines. R1/2 and S1/2 stand for recirculated flue gas and secondary air, respectively.

Each control volume is idealised as a continuously stirred tank reactor, CSTR, and the chamber is thus regarded as a series of CSTRs. A CSTR is ideal in the sense that it is assumed to have an instant and perfect mixing, i.e. the concentration, temperature, pressure etc. is the same over the entire volume. This also means that what goes out of each control volume is exactly the same as what's inside it.

Measurements

In the primary chamber and control volume 2,3,5 and 6 of the secondary chamber there are temperature sensors. In addition to this the composition of the flue gas going out to stack is measured and thus known. However, the composition of the syngas from the primary chamber is constantly changing

and always unknown. The measurements are used to estimate the composition of the syngas. The temperatures and flow rates of the recirculated flue gas and secondary air are also known. The flow out of the chamber is measured and based on that the flow into the chamber is calculated.

The components analysed just before the stack are: CO, CO_2, H_2O and O_2. CH_4 and H_2 are assumed to be 0. N_2 compensates for errors by assuming that the percentage of it is the total minus what has been measured of other components, i.e. if the components are measured in percent then $N_2 = 100\% - CO - CO_2 - H_2O - O_2$.

Assumptions and simplifications

The inputs to the system are somewhat simplified in the sense that the syngas is assumed to have only seven components, flue gas only four and the air assumed to be very 'clean' and consist of only oxygen and nitrogen. Experiments and calculations done by Energos [4] shows that this is a realistic simplification. Depending on the waste coming in, there could be small amounts of other unknown species, but these other possible components would be impossible to model. The amount would anyway be so small that it's unlikely that it would affect the calculations significantly.

Another assumptions regarding the injected air and recirculated flue gas is that their temperature is constant. This is based on information given by Energos. In the real plant these temperatures are nearly constant, and the variation would only be some degrees up/down which would not affect calculations significantly.

The division in control volumes is also a simplification. Here the flow goes from one control volume to the next, i.e. only one directional movement. Using a CSTR model means that we only look at mean values for the entire control volume and hence miss local gradients, e.g. "hot spots"[2].

The mean pressure of the chamber is assumed to be constant just below one atmosphere, meaning that the flue gas fan just before the chimney is assumed to be infinitely fast in its operation controlling the pressure in the system by adjusting the flow throughput.

All compositions are measured in volumetric percentages, but when the gas is assumed ideal volume percentage equals molar percentage. Assuming

[2]Here meaning a smaller region with quite high temperature compared to the rest of the volume.

ideal gas is common in systems with high temperatures and low pressures like this.

2.2 The mathematical model

The model derived is a first principles model, i.e. physical and chemical properties are used to model the system. Classic conservation laws are used to find mass and energy balances. There are some complex mechanisms which are difficult to model with high degree of confidence. These are simplified with some assumptions or replaced by unknown parameters which are estimated from process data.

The important aspect of the model is that it should be sufficiently simple to run in an on-line application, yet capture the main process nonlinearities. Another important thing to consider is the process noise.

This section covers the derivation of the first principles model in more detail whereas the next section explains how the unknown parameters are estimated. The main result from [3] are the equations for state updates of the molar holdup and gas temperature derived from the mass and energy balance, (2.16) and (2.38).

2.2.1 Combustion kinetics

This subsection describes the combustion kinetics used in the previous work [3]. These kinetic reactions require a lot of computation and are therefore best suited for a simulation purpose model where there are no real-time requirements. This project is however intended for control purposes and the kinetics had to be further simplified. The original combustion kinetics are included for a better understanding of the problem faced while using them and the need for a simpler solution. The reader is welcome to skip this part and jump directly to section 2.2.2 that describes the simplified kinetics currently used.

The components listed in (2.1) are modelled to react according to the following four reactions from [6] and [7]:

$$CH_4 + O_2 \rightarrow CO + H_2O + H_2 \tag{I}$$

$$CO + H_2O \leftrightarrow CO_2 + H_2 \tag{II}$$

$$2\ H_2 + O_2 \rightarrow 2\ H_2O \tag{III}$$

$$CO + \frac{1}{2}O_2 \rightarrow CO_2 \tag{IV}$$

Each reaction has the following reaction rate in moles per unit time per unit volume [8] where the subindex of the reaction rate denotes which of the four reactions, (I-IV), it belongs to:

$$\omega_I = k_{1f}[CH_4][H] \tag{2.2}$$

$$\omega_{II} = k_{2f}[CO][OH] - k_{2b}[CO_2][H] \tag{2.3}$$

$$\omega_{III} = k_{3f}[O_2][H][M] \tag{2.4}$$

$$\omega_{IV} = k_{4f}[CO][O_2] \tag{2.5}$$

The Arrhenius equation gives the constants k:

$$k = Ae^{-E_a/RT} \tag{2.6}$$

where A is a constant and E_a, activation energy in joules, are given for each reaction, found in table C.1. R is the gas constant $R = 8.3144621$ J K^{-1} mol^{-1}. $[j]$ denotes the concentration of species j in moles per unit volume, M represents a third body [9]:

$$[M] = [CH_4] + 1.2[CO] + 2.4[CO_2] + 2.5[H_2] + 16[H_2O] + [O_2] + [N_2] \tag{2.7}$$

and $[H]$ and $[OH]$ are given by

$$[H] = \left(1 - \frac{k_{3f}[M]}{k_{4f}}\right)^{1/2} K_H[O_2]^{1/2}[H_2]^{3/2}/[H_2O] \tag{2.8}$$

$$[OH] = \left(1 - \frac{k_{3f}[M]}{k_{4f}}\right)^{1/2} K_{OH}[O_2]^{1/2}[H_2]^{1/2} \tag{2.9}$$

where $K_H = 1.27e^{2997/T}$ and $K_{OH} = 5.97e^{-4696/T}$ are equilibrium constants [7]. It's important to note that for computations a cutoff must be incorporated at the crossover temperature $T_c \approx 810$°C, given by $k_{3f}[M] = k_{4f}$ which leads to $[H] = [OH] = 0$ and therefore $\omega_{III} = \omega_{II} = \omega_I = 0$, i.e. no reactions will happen for $T < T_c$. It can also be seen that if $k_{3f}[M] > k_{4f}$ equations

(2.8) and (2.9) will have a complex result, which is not a physically possible amount for a molar concentration. The crossover temperature is calculated for a given typical composition [9], and will vary depending on the composition.

By looking at which of the four reactions (I-IV) the different species appear and simply summing the reaction rates for those reactions, we get the following reaction rates for each of the seven components in the component vector (2.1):

$$\vec{\Omega} = \begin{bmatrix} -\omega_I \\ \omega_I - \omega_{II} - \omega_{IV} \\ \omega_{II} + \omega_{IV} \\ \omega_I + \omega_{II} - 2\omega_{III} \\ \omega_I - \omega_{II} + 2\omega_{III} \\ -\omega_I - \omega_{III} - \frac{1}{2}\omega_{IV} \\ 0 \end{bmatrix} \tag{2.10}$$

This set of rates is valid for each control volume. The reaction rates are defined positive as formation rates, i.e. positive for the creation of each species, thus the rates for the combustible species will have a negative sign as they are consumed. No reactions are modelled for nitrogen[3], hence the reaction rate for nitrogen equals zero, as can be seen from the last element in the reaction rate vector (2.10).

2.2.2 Simplification of reaction kinetics

The combustion model turned out to be very stiff[4] because of the very fast reaction rates. It was only possible to simulate it if the reaction rates were reduced with a factor of 10^6 and the integration time set to 10^{-6}s. Still the model was running very slowly, far below real-time speed, which is not acceptable for an on-line MPC application. Hence the model needed further simplifications. This was done by removing the reactions rates, i.e. by assuming that the kinetics is so fast that it can be considered instantaneous. The reaction equations were simplified even more and a steady-state calculation was used to find the final composition assuming everything is burned.

[3]No reactions involving nitrogen are modelled. The production of NO_x is not a concern in today's plants and is hence not part of the scope for this project.

[4]A stiff equation is a differential equation for which certain numerical methods for solving the equation are numerically unstable, unless the step size is taken to be extremely small. It is difficult to define stiffness, but the main idea is that the equation includes some terms that can lead to rapid variation in the solution. Typically this is due to large variations in the system's different time constants.

To make the implementation easier we assume that hydrogen burns first, thereafter methane and finally carbon monoxide, provided sufficient amounts of oxygen, which is assumed to be the case at steady-state. The water-gas-shift reaction (II) is assumed to always be at equilibrium. The three following reactions then describe the kinetics of the system:

$$H_2 + \frac{1}{2}O_2 \rightarrow H_2O \tag{2.11}$$

$$CH_4 + \frac{3}{2}O_2 \rightarrow CO + 2H_2O \tag{2.12}$$

$$CO + \frac{1}{2}O_2 \rightarrow CO_2 \tag{2.13}$$

The reactions occur in this order, chosen based on knowledge of the process. It is well-known that a mix of hydrogen and oxygen gas will result in a large combustion rate, especially at these high temperatures, and simulations [3] also show that hydrogen burns quickest[5].

Carbon monoxide is known to have a slightly lower combustion rate compared to that of hydrogen and methane. This is in fact one of the main considerations behind the designed length of the furnace. The gas has to be given enough time for carbon monoxide to fully combust. There are governmental requirements regarding the residence time after the last air injection (i.e. after S2) with a lower limit of about 2 seconds as this is sufficient time to ensure oxidation of the carbon monoxide.

The kinetics of section 2.2.1 have a crossover temperature about 810° C. This led to some numerical problems when computing the rates, as there would be no reactions if the temperature went below the crossover temperature due to the mathematical nature of the expressions for the rates. With the new simplified kinetics we easily get away from this problem as there are no mathematical expressions to be solved.

However, a temperature dependence of the rates is realistic. All chemical reactions are affected by temperature, and so are combustion reactions. It is however, desired that the temperature never gets below the crossover temperature, hence these mathematical limitations are consistent with the requirements for normal operation.

[5]A mix of hydrogen and oxygen is sometimes referred to as “detonating gas”, just because that if such a mixture is ignited (it even autoignites at high temperatures) there will be an explosion.

To make the kinetics more similar to the previous model which is also more realistic, an exponential decay was included in the rates. More details on how the rates were implemented in section 2.3.

2.2.3 Stoichiometry

Stoichiometry describes the relationship between the reactants participating in a reaction. In our case the reactants will be classified as combustible species and oxygen, and the stoichiometry parameter will therefore tell us whether there is excess of oxygen or not. We denote this parameter λ defined as the total air entering the furnace to the total air needed for complete combustion of the syngas. This parameter characterises the overall process and carries information about the current operation conditions.

The gasification process in the primary chamber is sub-stoichiometric and the first part of the secondary chamber is ideally also operated sub-stoichiometricly, typically with a lambda value from 0.4-0.6 [4]. In the sub-stoichiometric region injection of air will lead to a temperature rise because there is enough fuel and when more oxygen is injected more combustion will take place. Thus it is desired to have shortage of oxygen and keep the first part of the secondary chamber sub-stoichiometric to always have control of the temperature.

In the final part of the chamber air is injected to make sure all combustible species are fully combusted. Even if the lambda value is exactly equal one, i.e. the number of oxygen molecules is exactly equal the number of oxygen molecules needed for complete combustion, it does not mean that there will be complete combustion; the molecules have to find each other in order to react as well. So to be sure, more oxygen than what is needed according to the stoichiometry is injected making the lambda value exceed one.

Further injection of air will lead to a temperature decrease as the air is cold and the shortage now is of fuel, hence no more combustion will happen with more air.

Figure 2.2 is an illustration of how the lambda value influences the temperature. Point A describes the desired operation condition for the first part of the chamber, point B describes the desired operation condition for the last part. The control problem is strongly related to keeping the stoichiometry in the desired regions for the different parts of the chamber.

Temperature dependence

Figure 2.3 shows the well-known fire triangle containing the three necessary components for combustion. The relation between fuel and oxygen is de-

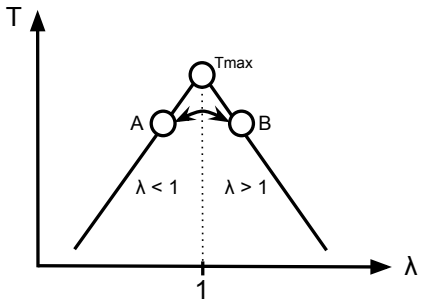

Figure 2.2: Stoichiometry

scribed by the lambda value, but the third part of the triangle, the heat, is also very important for the kinetics of this system. It is easily a forgotten factor when one considers a high temperature system like this, as it seems less likely that temperature is a problem.

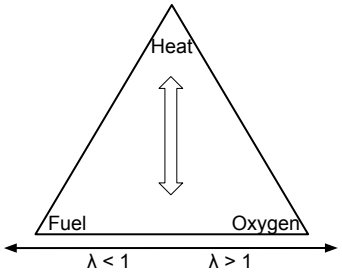

Figure 2.3: The classic fire triangle, showing the three necessary components for fire

It is however, observed in the real plant that if the temperature gets too low, the combustion will stop. This is part of the undesired quenching phenomenon.

Quenching occurs when for example the primary chamber produces less syngas, or the calorific value of the syngas decreases. Due to the lack of early measurements the control system is unaware of this, so there will be no reduction in the flow rates of recirculated flue gas. As mentioned, the purpose behind the injection of the recirculated flue gas is to keep the temperature down. The continued injection of recirculated flue gas will therefore increase its cooling effect, making the combustion stop and so also reducing the heat production. The overall result of this is a drastic drop in temperature of several hundred degrees. Often manual reduction of the recirculation flow rate is necessary to stop the quenching.

The syngas then travels as a cold front through the furnace and is gradually heated by the walls making the combustion start again, though in the final parts of the chamber. The combustion is designed to happen in the first part of the chamber and this behaviour is not desired.

The original kinetic equations were functions of temperature, and the reaction rates would go to zero if the temperature got too low. In the new simplified kinetics, the temperature dependence is not well incorporated. This means that the simplified model does not cover the quenching phenomenon. Instead, it is recommended to include a temperature constraint in the MPC controller, see section 2.5 for details.

2.2.4 Material balance

Using Reynolds transport theorem (see Appendix B) with molar holdup, n, being the property of interest we have:

$$\frac{d}{dt}n_{system} = \frac{d}{dt}\left(\int_{CV}\frac{dn}{dm}\rho\ dV\right) + \int_{CS}\frac{dn}{dm}\rho(v_m\cdot\vec{e})\ dA \tag{2.14}$$

The total change of the molar holdup in the system, $\frac{d}{dt}n_{system}$, is the formation/consumption of moles given by the reaction rates, $\vec{\Omega}V$ in moles per second. The formation of moles is given by the positive defined reaction rates. The consumption of a component results in a negative reaction rate.The first part on the right hand side of (2.14) denotes the change of moles inside the control volume, $\dot{n}$, and the flux term accounts for the sum of moles per second entering and leaving the control volume through its surfaces given by a molar flow rate, F. As there can be several inflows (both syngas, SG, and injection of air/recirculated flue gas, inj) the flux term will be:

$$\int_{CS}\frac{dn}{dm}\rho(v_m\cdot\vec{e})\ dA = -\sum F_{in} + \sum F_{out} = -F_{SG_{in}} - F_{inj} + F_{SG_{out}} \tag{2.15}$$

To find the change of each component the flow rates are multiplied with the molar fraction. Inserting for this and rearranging to get the final material balance:

$$\boxed{\frac{d\vec{n}_i}{dt} = F_{SG_{i-1}}\vec{x}_{i-1} + F_{inj_i}\vec{x}_{inj_i} - F_{SG_i}\vec{x}_i + \vec{\Omega}_i V_i} \tag{2.16}$$

where $\vec{n}_i$ is a vector containing the molar holdup of all components in control volume i, $F_{SG_{i-1}}$ is flow into control volume i, where the subindex SG stands

for syngas, a notation that will be used throughout the report[6]. F_{inj_i} is flow of secondary air/recirculated flue gas injected into control volume i. The subindex *inj* is short for *injection*, meaning the injection of either secondary air or recirculated flue gas. F_{SG_i} is flow out of control volume i, $\vec{x}_i$ is a vector with the molar fraction of each component in the syngas, $\vec{x}_{inj_i}$ is the molar fraction of air/recirculated flue gas into control volume i. $\vec{\Omega}_i$ is the formation rate of each component in volume i given in moles per unit time per unit volume, hence multiplied with the volume V_i which is the volume measured in cubic metres of the control volume i.

2.2.5 Energy balance

The first law of thermodynamics states that the total energy change of a system, dE, has to equal heat energy added to the system, dQ, minus work done by the system, dW:

$$\frac{dQ}{dt} - \frac{dW}{dt} = \frac{dE}{dt} \tag{2.17}$$

This is true for a fixed quantity of fluid, but as we here are working with a series of control volumes the laws become a little different. Fortunately Reynolds transport theorem makes it applicable for control volumes [5].
Here we want to consider energy and insert E for B and $e = \frac{dE}{dm}$ in (B.1) and get:

$$\frac{d}{dt}E_{syst} = \frac{dQ}{dt} - \frac{dW}{dt} = \frac{d}{dt}\left(\int_{CV} e\rho \; dV\right) + \int_{CS} e\rho(v_m \cdot \vec{e}) \; dA \tag{2.18}$$

The system's energy e is the total energy:

$$e = e_{internal} + e_{kinetic} + e_{potential} = u + \frac{1}{2}v_m^2 + gz \tag{2.19}$$

The heat term from equation (2.17) will here consist of heat transfer to or from the walls of the furnace. When the gas has a higher temperature there will be some heat loss to the wall, whereas if the gas is rapidly cooled by for instance a large intake of cold air, the wall will transfer heat to the gas.

The work term, W, in the same equation will reduce to work done only by the pressure forces because the fluid is not performing any work on its

[6]The subindex *SG* is used for the gas in the secondary chamber even if it in the last control volumes is more correct to denote it flue gas, as that is the actual composition in the final part of the chamber. But for notational simplicity and to avoid confusion this is not changed.

environment and other types of work like shear work due to viscous stresses are neglected so $\dot{W} = \dot{W}_p$ [5]. The pressure work, W_p occurs on the surface and for every small surface element dA the pressure times the normal velocity vector into the control volume gives the total work done by the pressure:

$$\dot{W}_p = \int_{CS} p(v_m \cdot \vec{e})\ dA \tag{2.20}$$

This can be added to the flux term of (2.18)

$$\int_{CS} e\rho(v_m \cdot \vec{e})\ dA + \int_{CS} p(v_m \cdot \vec{e})\ dA = \int_{CS} (e\rho + p)(v_m \cdot \vec{e})\ dA \tag{2.21}$$

and if we insert for e

$$\int_{CS} (u + \frac{1}{2}v_m^2 + gz + \frac{p}{\rho})(v_m \cdot \vec{e})\ dA \tag{2.22}$$

it can be seen that the enthalpy $h = u + p/\rho$ occurs.

From [5] we get the general form of the energy equation where the work is only done by pressure for a fixed control volume where Reynolds transport theorem, equation (B.1), is applied to the first law of thermodynamics, equation (2.17):

$$\dot{Q} = \frac{d}{dt}\left[\int_{CV} \left(u + \frac{1}{2}v_m^2 + gz\right)\rho\ dV\right] + \int_{CS} \left(h + \frac{1}{2}v_m^2 + gz\right)\rho(v_m \cdot \vec{e})\ dA \tag{2.23}$$

A quick look into the energy equation (2.19) shows that the kinetic and potential energy of the fluid in this model are so small compared to the internal energy that they are negligible and we are left with $e = u$ which from the definition of B in Appendix B gives

$$E = \int_{CV} e\ dm = \int_{CV} u\ dm = um = U \tag{2.24}$$

where U is the total internal energy. This also implies that $\dot{E} = \dot{U}$ and (2.23) reduces to:

$$\dot{Q} = \frac{d}{dt}\left(\int_{CV} u\rho\ dV\right) + \int_{CS} h\rho(v_m \cdot \vec{e})\ dA \tag{2.25}$$

Inserting for flux in and out and solving with $\vec{e}$ still being an outward normal unit vector so that inflow terms $v_m \cdot \vec{e}$ become negative $(-v_m)$ and outflow terms $v_m \cdot \vec{e}$ become positive (v_m):

$$\dot{Q} = \dot{U} + (-(\dot{m}h)_{in} + (\dot{m}h)_{out}) \tag{2.26}$$

where $\dot{m}$ is mass flow. Molar flow is more convenient as we are working with moles, and is found by dividing with the molar mass of the mixture M, $F = \dot{m}/M$. Also including a second input because of the air/recirculated flue gas injected and we have the final energy balance:

$$\frac{dU}{dt} = F_{in}\overline{h}_{in} + F_{inj}\overline{h}_{inj} - F_{out}\overline{h}_{out} + \dot{Q} \tag{2.27}$$

where h_{in} is the total enthalpy of the gas flow into the control volume, F_{in} is molar flow of gas into control volume, h_{inj} is the enthalpy of the air/recirculated flue gas flow into the control volume, F_{inj} is air/recirculated flue gas flow into control volume, h_{out} is the enthalpy of gas flow out of the control volume, F_{out} is the flow out of control volume and $\dot{Q}$ is heat transferred from the wall ($\dot{Q}$ will have a negative sign for heat loss to wall). Enthalpies for (2.27) are given as:

$$\overline{h}_{in} = \sum_{j=1}^{c} h_{in_j} = \sum_{j=1}^{c}(\int_{T_{ref}}^{T_{in}} C_{p_j}(T)\ dT + \Delta H_{f_j}) \tag{2.28}$$

$$\overline{h}_{inj} = \sum_{j=1}^{c} h_{inj_j} = \sum_{j=1}^{c}(\int_{T_{ref}}^{T_{inj}} C_{p_j}(T)\ dT + \Delta H_{f_j}) \tag{2.29}$$

$$\overline{h}_{out} = \sum_{j=1}^{c} h_{out_j} = \sum_{j=1}^{c}(\int_{T_{ref}}^{T_{out}} C_{p_j}(T)\ dT + \Delta H_{f_j}) \tag{2.30}$$

T_{ref} is a reference temperature of 298° K, T_{in} is the temperature of the gas entering the control volume, T_{inj} is the temperature of the injected air/recirculated flue gas, T_{out} is the temperature of the gas leaving the control volume, $\overline{C}_{p_j}$ is heat capacity of component j for constant pressure and ΔH_{f_j} is the heat of formation of component j. The values for ΔH_f are from [10] and can be found in table C.3.

$$\overline{C}_p = \sum_{j=1}^{c} C_{p_j} x_j \tag{2.31}$$

Each species have a C_p value dependent on temperature calculated with constants from [10] given in table C.2.

$$C_p(T) = a_0 + a_1 T + a_2 T^2 + a_3 T^3 + a_4 T^4 \tag{2.32}$$

2.2.6 Temperature

As we in this model assume approximately constant pressure and volume of the control volumes, we have that $\dot{U} = \dot{H}$ where H is enthalpy. The temperature is then found from the energy balance (2.27) using that

$$H = \sum_{j=1}^{c} h_j n_j \tag{2.33}$$

implying

$$\dot{H} = \sum_{j=1}^{c} \dot{h}_j n_j + \sum_{j=1}^{c} h_j \dot{n}_j \tag{2.34}$$

The definition of C_p as given in [11] where h is enthalpy and T temperature:

$$C_p = \frac{dh}{dT} \tag{2.35}$$

multiplying with the total number of moles, n_{tot}, [mol], and rearranging gives

$$n_{tot} C_p \dot{T} = \dot{h} n_{tot} \tag{2.36}$$

inserting this in (2.34) gives

$$\dot{H} = \sum_{j=1}^{c} n_j C_{p_j} \dot{T} + \sum_{j=1}^{c} h_j \dot{n}_j \tag{2.37}$$

Setting equation (2.37) equal equation (2.27) and rearranging gives the expression for the temperature in one control volume:

$$\boxed{\dot{T}_i = \frac{F_{SG_{i-1}} \overline{h}_{SG_{i-1}} + F_{inj_i} \overline{h}_{inj_i} - F_{SG_i} \overline{h}_{SG_i} + \dot{Q}_i - \sum_{j=1}^{c} h_{j_i} \dot{n}_{j_i}}{\overline{C}_{p_i} n_{tot_i}}} \tag{2.38}$$

where $\dot{T}_i$ is the temperature change of control volume i, F is molar flow rate, h is enthalpy, $\dot{Q}_i$ is heat transferred from the walls of control volume i, $\overline{C_p}$ as defined in (2.31) and $n_{tot_i} = \sum_{j=1}^{c} n_{j_i}$ the total number of moles in control volume i.

Because of assumptions and uncertainties in the modelling we insert a tuning parameter before the last part in the numerator of (2.38). The last part will then look like $\theta_1 \sum_{j=1}^{c} h_{j_i} \dot{n}_{j_i}$ where θ_1 is the parameter that will be estimated later. More on this matter in section 2.2.12.

2.2.7 Heat transfer with walls

Thermal energy is transferred from one place to another by three processes: conduction, convection and radiation. There is a continuous two-way heat transfer between the gas and the walls of the furnace and this will be discussed in more detail here.

The heat transfer with the wall, denoted $\dot{Q}$, i.e. heat transferred per time, is defined positive for heat added to the gas, i.e. $\dot{Q}$ has by definition a positive sign when the wall has a higher temperature than the gas.

Conduction

In conduction, energy is transferred as heat by interaction among atoms or molecules, although there is no transport of the atoms or molecules themselves [12]. The atoms/molecules with the highest temperature will vibrate with greater energy than the ones with low temperature. The interaction between them causes the energy to be transported.

The definition of the thermal current, i.e. heat conducted per time, $\dot{Q}$, is given as

$$\dot{Q} = \frac{\Delta T}{R_t} \tag{2.39}$$

where ΔT is the temperature difference $\Delta T = T_{wall} - T_{SG}$ and R_t is the thermal resistance defined as $R_t = \frac{\Delta x}{k_w A}$, k being a constant called the thermal conductivity. Δx and A are the thickness and the area of the cross-section of the wall respectively. The overall heat transfer coefficient for conduction through the wall, i.e. $\frac{k_w}{\Delta x}$, is 0.87 W m^{-2} K^{-1} [9].

The thermal conductivity of a gas is very small compared to that of a solid material.

Convection

In convection, energy is transported as heat by direct mass transport of a fluid [12]. For example when a gas is heated its density will decrease and it rises. The heat will here be transported along with the heated mass.

Heat transfer due to convection between a wall and its surroundings is typically given by

$$\dot{Q} = A_{wall} U_{htc_{wall}} (T_{wall} - T_{SG}) \tag{2.40}$$

where A_{wall} is the area of the wall and $U_{htc_{wall}}$ is a heat transfer coefficient.

The convection heat transfer coefficient, $U_{htc_{wall}}$, between the gas and the wall can be calculated with the Dittus-Boelter correlation given in the following equation:

$$U_{htc_{wall}} = 0.023 Re_{D_h}^{4/5} \; Pr^c k_g / D_h \tag{2.41}$$

Where $k_g = 0.0675$ W m^{-2} K^{-1} (heat conductivity of gas), D_h and Re_{D_h} are hydraulic diameter and Reynolds number based on hydraulic diameter. $D_h = 4A_c/P$, A_c is the cross section area and P is perimeter. $Re_{D_h} = \rho_g v_g D_h / \eta_g$ where ρ_g is the gas density, v_g is the gas velocity and η_g is the gas viscosity. Pr is Prandtl's number, c is 0.4 when the wall has a higher temperature than the gas and 0.33 when the wall has a lower temperature than the gas. Calculations done by Gonzalo del Alamo [9] shows that $U_{htc_{wall}}$ can be approximated to 8 W m^{-2} K^{-1}.

Radiation

In radiation, energy is transported as heat through space in the form of electromagnetic waves [12]. The rate at which energy is radiated is given by the Stefan-Boltzmann law:

$$P_r = e\sigma A_{wall} T_{wall}^4 \tag{2.42}$$

where P_r is the power radiated. e is the emissivity[7] of the walls, here approximated to be 0.9. σ is a universal constant called Stefan's constant which has the value [12]

$$\sigma = 5.6703 \times 10^{-8} \text{ W m}^{-2} \text{ K}^{-4} \tag{2.43}$$

The net power radiated by the walls to the gas is given by:

$$P_{net} = e\sigma A_{wall}(T_{wall}^4 - T_{SG}^4) \tag{2.44}$$

It should be noted that this is a simplified approach to model the radiation. Some of the radiation will not be absorbed by the gas but by the other walls. When the two walls have the same temperature they emit and absorb the same amount of energy.

The percentage absorbed by the gas will depend on both temperature and composition. A higher content of for example CO_2 would increase the energy absorbed by the gas (refer to the green house effect, global warming caused by an increased CO_2 content in the atmosphere).

[7] The emissivity of an object is a fractional quantity between 0 and 1 depending on the composition of its surface. Ideal "blackbodies" have emissivity equal to 1.

This percentage is not known and not further investigated here, so it should be kept in mind that further improvements could be done on this part of the model.

Total heat transfer gas/wall

The main heat transfer from gas to wall is done by convection. The main heat transfer from wall to gas is done by radiation.

The total heat transfer is found by adding the three processes together. We will add the heat transfer coefficients for convection and conduction and approximate $U_{htc_{wall}}$ to 9 W m^{-2} K^{-1}. $U_{htc_{wall}}$ will be used as a tuning parameter in the model. The expression for the total heat transfer then becomes:

$$\dot{Q} = A_{wall}(U_{htc_{wall}}(T_{wall} - T_{SG}) + e\sigma(T_{wall}^4 - T_{SG}^4)) \tag{2.45}$$

Let C_{p_w} be the heat capacity of the walls, here approximated to C_{p_w} = 1000 J kg^{-1}K^{-1} and m_w is the mass of the wall. The thermal mass of the walls, $C_{th_w} = C_{p_w} m_w$, can be regarded as a thermal inertia that resists fluctuations in the ambient temperature. This means that the walls of the furnace will act as a damper in the system because its time constant for temperature changes is much larger than that of the gas.

Because of the large thermal mass, the walls need a long time to become warm, so it takes some time to start up the plant, typically one-two days.

The important function of the walls is their damping effect on the system. The rapid combustions of e.g. hydrogen and methane will free a lot of thermal energy that will contribute to the heating of the walls. Then again if the gas is cooled too much, the walls will to some extent help damp this.

The temperature change in the wall is given by

$$\boxed{\dot{T}_w = \frac{-\dot{Q}}{C_{th_w}}} \tag{2.46}$$

Heat radiation from the walls of the furnace is of great importance as it flattens out rapid temperature changes and helps the system to recover from the quenching problem.

The wall temperature is not measured, neither on the inside nor the outside, making it more difficult to verify the model made of it. Thus is this model's wall heat transfer merely a way of predicting its effects on the process, but will not give a realistic picture of the temperature in the walls. The wall temperature will also probably affect the temperature measurements of the gas in a damping way. It can be seen from the process data that the measured gas temperature varies very slowly.

2.2.8 Temperature sensor modelling

It is generally not advisable to compare a process measurement directly with a calculated value and expect them to be the same. Most measuring devices will have some low-pass filtering effect, they might be biased, saturated and/or have other sources of errors. To make calculated values comparable to measured values, a measurement/sensor equation should be derived, to better describe the dynamics of the sensor. This will here be done for the four temperature sensors, and we introduce four new states to our model, T_{sensor}, which will represent the temperature displayed by the sensor. T_{sensor} is then the value that will be compared to the actual measured values from the process data.

The temperature sensors are thermo elements mounted in protective pockets. This pocket represents the biggest mass of the sensor element and the main heat transfer happens between the gas and the pocket. The total mass of the sensor element is typically 500-1000g.

The sensors are modelled assuming that most of the heat transfer happens as convection from the gas. The temperature change in the sensors then given by the following equation:

$$\dot{T}_{sensor} = \frac{A_{sensor} U_{htc_{sensor}}}{C_{p_{sensor}} m_{sensor}} (T_{SG} - T_{sensor}) \tag{2.47}$$

where A_{sensor} is the surface area of the sensor, $U_{htc_{sensor}}$ the heat transfer coefficient, $C_{p_{sensor}}$ is mean heat capacity of sensor + cover, m_{sensor} is the mass of the sensor element, T_{SG} and T_{sensor} the temperature of the gas and the sensor element respectively.

As neither area, heat transfer coefficient, heat capacity nor mass of the sensors are known, these will be regarded as one parameter to be estimated to fit to measured data, i.e.

$$\dot{T}_{sensor} = \theta_{sensor} (T_{SG} - T_{sensor}) \tag{2.48}$$

The temperature sensors are fixed to the walls and even if they are sticking out a bit and to some extent shielded from wall radiation, the temperature measurements will be affected by the wall temperature as well as the gas temperature. In addition, the calculated gas temperature, T_{SG}, is only an average temperature for the entire control volume. These two conditions indicate that using T_{SG} in (2.48) may not be the best choice. This because (2.48) will update T_{sensor} to try to follow T_{SG}. It is probably more influenced by the wall temperature so the expression should include the wall temperature T_{wall}.

It is likely that during normal operation the highest temperature is in the middle of the chamber: the furthest away from the walls that lose heat to the surroundings. The temperature of the gas in the plant is assumed to have a temperature profile similar to the parabola shown in red in Figure 2.4. The temperature is lowest close to the walls (shown as dashed lines) and highest in the middle. The circle (green) shows where the temperature sensor is and the blue line is the calculated gas temperature, i.e. the average temperature T_{SG}. The parabola is exaggerated to illustrate the idea. A parabola profile is valid for laminar pipe flows, turbulence will in the real plant lead to a much flatter profile. Determining the temperature profile in a turbulent flow is not straight forward, so the parabola profile will be used for modelling as it is thought that doing this approximation is better than doing no further adjustments to (2.48).

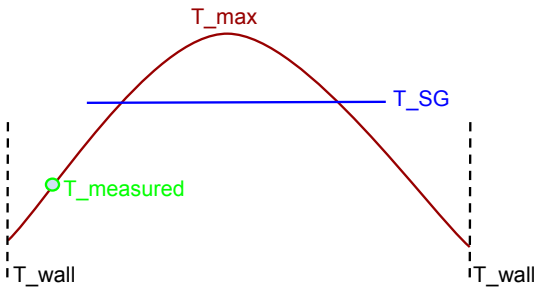

Figure 2.4: The assumed ideal temperature profile of the gas.

The the temperature profile for the gas can be found from the equation of a parabola:

$$T_{profile} = -a(x - l/2)^2 + T_{max} \tag{2.49}$$

where l is the length across the chamber, taken as a coarse guess of $l = 5$ meters. x is the distance from the walls. The boundary conditions for the parabola will be the wall temperature T_{wall} (this condition increases the importance of correct wall temperature modelling). The average, T_{SG}, is determined to be 3/4 of the maximum temperature, T_{max}. The relation 3/4 is an approximation only and is not tried fitted to any data. Note that T_{max} does not represent the real maximum value of the gas.

The constant a can be found from the boundary conditions by setting $x = 0$ which is when $T_{measured} = T_{wall}$

$$a = \frac{T_{max} - T_{wall}}{(l/2)^2} \tag{2.50}$$

Let us now introduce another variable: $T_{measured}$. The previously mentioned T_{sensor} is what will be used for comparison with the real measurement data. We don't want T_{sensor} to be updated based on T_{SG} so we need to calculated an imaginary measurement that can be used for this update. $T_{measured}$ denotes a calculated measured temperature. It is not a state of the system, only an internal variable used to update T_{sensor} in (2.48). We can think of T_{sensor} as the variable representing the temperature displayed by the sensor, i.e. the temperature of the sensor element itself, whereas $T_{measured}$ is the thought temperature of the gas just next to the sensor in the furnace, i.e. the temperature that is more likely to change the measurements.

If we assume that the sensor sticks out 0.5 meters into the furnace we can find $T_{measured}$ by setting $x = 0.5$ into (2.49).

When inserting this into (2.48) we get the final equation for the temperature sensor update:

$$\boxed{\dot{T}_{sensor} = \theta_{sensor}(T_{measured} - T_{sensor})} \tag{2.51}$$

Equation (2.49) also works for the case where the walls have a higher temperature than the gas, and the sensors are likely to show a too high temperature.

The code that shows how this was implemented is shown in Appendix F.2.

2.2.9 Flow rate calculations

From the equation of state, here the ideal gas law, the pressure of each control volume, p_i, is computed.
Ideal gas law:

$$pV = nRT \tag{2.52}$$

giving us

$$p_i = \frac{n_{tot_i} R T_i}{V_i} \tag{2.53}$$

where p_i is the pressure, n_{tot_i} is the total number of moles, R the universal gas constant, T_i the temperature and V_i the volume, all for control volume i.

The internal flows between the control volumes are calculated using (2.54) from [13] where $\dot{m}_i$ is the mass flow rate out of control volume i and $\dot{m}_{inj}$ is the mass flow rate of the air/recirculated flue gas injected into control volume i (the flow rates are converted to molar flow rates before used in the state update equations).

$$\dot{m}_i = \dot{m}_{i-1} + \dot{m}_{inj_i} + K_p(p_i - \tilde{p}) \tag{2.54}$$

The variable $\tilde{p}$ can be though of as an approximation of a global pressure for the entire chamber. It is set to 200 Pa below atmospheric pressure, as this is approximately the pressure out of the secondary chamber. The objective of the flue gas fan before the stack is to keep the pressure in the primary chamber 90 Pa below atmospheric pressure, this gives approximately 200 Pa below atmospheric pressure at the end of the secondary chamber.

The constant K_p should be large enough to incorporate the effect of pressure differences between the control volumes in the flow model, but small enough not to make its effect too large. A large K_p leads to a stiff model, as the rate of pressure change is much higher than that of the flow. If the pressure in some of the control volumes falls below the set global pressure, the pressure part of (2.54) will contribute in a negative way and reduce the flow. This is also a reason for not selecting K_p too large, as that could lead to a negative flow, i.e. flow in the backward direction. The local pressures in the control volumes can occasionally get a lower pressure, and the model will then reduce the flow until the pressure has increased again.

Here K_p is set to 0.0001.

The flow from the primary chamber is not measured, but so is the flow out of the plant. The flow from the primary chamber is calculated based on this. Here this is done by first converting all rates to mass flow rates, i.e. with the unit [kg s^{-1}], and the mass flow from the primary chamber, $\dot{m}_{prim}$, is then equal to:

$$\dot{m}_{prim} = \dot{m}_{out} - \sum \dot{m}_{inj} - \dot{m}_{bias} \tag{2.55}$$

where $\dot{m}_{out}$ is mass flow out of the combustion chamber, $\sum \dot{m}_{inj}$ is the sum of the two secondary air inlets and the two recirculated flue gas inlets, all these flow rates are measured and the measurements are used in the calculations. As the plant is operated slightly below atmospheric pressure and is not completely airtight, some air will leak into it. $\dot{m}_{bias}$ is a tuning parameter and represents the mass flow of this ingress air leaking into the process after the combustion chambers.

For the bias flow, some simple calculations are made to find its initial value. Energos knows from experience that the extra air inlet to the model increases the oxygen level by maximum 1%, from a typical 5% in the flue gas from the secondary chamber to 6% going out through the chimney. We let the air inlet have 21% oxygen and calculate the bias. Two relations are then known:

$$0.05F_{SG} + 0.21F_{bias} = 0.06F_{out} \tag{2.56}$$

$$F_{SG} + F_{bias} = F_{out} \tag{2.57}$$

inserting (2.57) in (2.56) and get

$$\begin{aligned} 0.05F_{out} - 0.05F_{bias} + 0.21F_{bias} &= 0.06F_{out} \\ 0.16F_{bias} &= 0.01F_{out} \\ \frac{F_{bias}}{F_{out}} &= \frac{1}{16} \end{aligned}$$

where F_{SG} is the flue gas from the secondary chamber, F_{bias} is the ingress air and F_{out} is the flue gas going out of the chimney, all rates are volumetric rates (unit [$\mathrm{Nm^3\ h^{-1}}$]) and volumetric % equals molar %. The typical flow rate out through the chimney is about 40,000 $\mathrm{Nm^3\ h^{-1}}$, hence the initial guess for the bias flow is $\frac{40000}{16} = 2500$.

2.2.10 Composition sensor modelling

The composition of the flue gas is measured just before the flue gas is let out to the atmosphere, i.e. after the flue gas has travelled through the plant and some excess air has leaked in. This will affect the measurements mainly by an increased oxygen level. To incorporate this into the model and make the predicted outputs comparable to the measured values, the bias flow (that has a composition equal to that of only air) is added. As already mentioned the bias flow, F_{bias}, is a parameter that will be used also to adjust the oxygen level in the output, but it will increase the level of maximum 1%.

To find the composition of the "new" flue gas, x_{mix}, a simple equation is derived. We assume that there are no reactions after the flue gas leaves the and no flow variations due to pressure/temperature differences. Then we have the following relation describing the composition of the flue gas:

$$F_{SG_{out}} x_{SG_{out}} + F_{bias} x_{bias} = F_{measured} x_{mix} \tag{2.58}$$

where $F_{SG_{out}}$ and $x_{SG_{out}}$ are the flow and composition calculated out of the furnace, i.e. out of CV6, F_{bias} is the flow parameter (converted to molar flow) with the composition x_{bias} being only air and $F_{measured}$ is the measured flue gas flow out.

The predicted measured compositions out, $x_{measured}$, are taken as extra states in the model, and the state update law is written as

$$\boxed{\dot{x}_{measured} = (x_{mix} - x_{measured})K} \tag{2.59}$$

where the constant K was chosen to 0.02 based on visual inspection of the plotted curves.

2.2.11 The unknown syngas composition

The composition of municipal waste is hard to guess with high precision because waste can contain just about anything. This fact represents one of the biggest challenges in controlling a plant where municipal waste is the fuel. It is hard to determine the amount of combustion air needed for optimal conditions in the furnace at any given time.

The constantly varying flow rate and composition of the syngas coming from the primary chamber are unknown disturbances that also represent a big challenge when modelling the secondary chamber. The flow rate is straight forward to calculate based on the other flow measurements.

The process model is simulated with only a vague idea of a typical syngas composition and the results are compared to measurement data from the plant. With no more knowledge of this disturbance the model cannot be expected to produce a good prediction of the process behaviour. In order to get better predictions it is absolutely necessary to estimate the syngas composition. To do this we have to check if we get enough information from our measurements to uniquely identify all seven components. If the components can be determined from the measurements and the inputs within finite time they are said to be observable. For any MPC application to make sense, the composition should at least be steady-state observable.

We will now address the steady-state observability of the syngas composition.

The relevant measurements are the final composition and temperature out of the combustion chamber. Here we have one temperature measurement and four composition measurements, i.e. five equations. If the measurement vector is $\mathbf{y}$ and the composition vector is $\mathbf{x}$ we have a simple steady-state representation given by

$$\mathbf{A}\mathbf{x} = \mathbf{y} \tag{2.60}$$

where $\mathbf{A}$ is a constant matrix. The components are steady-state observable if $\mathbf{A}$ has full rank, i.e. if it is invertible.

Let's take a closer look at this $\mathbf{A}$ matrix. For the measured components we can set up the following set of steady-state equations based on equation (2.11)-(2.13):

$$nCO_{2_{out}} = xCO_{combusted} + yCO_{2_{in}} + aCO_{2_{air}} \tag{2.61}$$

$$mCO_{out} = zCO_{in} + wCH_{4_{in}} - xCO_{combusted} + bCO_{air} \tag{2.62}$$

$$kH_2O_{out} = vH_2O_{in} + uH_{2_{in}} + 2wCH_{4_{in}} + cH_2O_{air} \tag{2.63}$$

$$qO_{2_{out}} = pO_{2_{air}} - \frac{3}{2}wCH_{4_{in}} - \frac{1}{2}uH_{2_{in}} - \frac{1}{2}zCO_{in} \tag{2.64}$$

The variables of interest here are y, z, w, v and u that represent the number of moles from the primary chamber of CO_2, CO, CH_4, H_2O, and H_2 respectively. a, b, c and p are the sums of the known number of moles of CO_2, CO, H_2O, and O_2 respectively injected to the process with the air and recirculated flue gas. k, m, n and q are the measured number of moles of H_2O, CO, CO_2 and O_2 respectively out of the plant.

It is important to note that we assume here that the process is at steady-state, i.e. that CH_4 and H_2 are fully combusted and that there is excess of oxygen. The equations (2.61) - (2.64) will not be valid otherwise.

x is the number of moles of CO that are combusted during the process, and is not of interest here, so we insert (2.61) in (2.62) and rearrange and use only the letter variables:

$$\begin{aligned} y + z + w &= m + n - a - b \\ v + u + 2w &= k - c \\ 3w + u + z &= 2(p - q) \end{aligned} \tag{2.65}$$

Here we have five unknowns and only three equations. Even if all equations are linearly independent this system is impossible to solve uniquely. But we have another measurement, the temperature, giving us yet another equation. We look at the steady-state of (2.27), i.e. when $\dot{U} = 0$ and the sum of all energy coming into the system has to equal all energy going out of the system. h is the enthalpy which is a function of temperature, with the unit [J mol^{-1}].

$$\begin{aligned} h_{in_1}y + h_{in_2}z + h_{in_3}v + h_{in_5}w + h_{in_6}u = \\ h_{out_1}n + h_{out_2}m + h_{out_3}k + h_{out_4}q - \\ h_{air_1}a - h_{air_2}b - h_{air_3}c - h_{air_4}p + \\ h_{out_7}r - h_{air_7}d - h_{in_7}(r - d) - \dot{Q} \end{aligned} \tag{2.66}$$

h_{in_j} is the enthalpy function for component j coming from the primary chamber, h_{out_j} is the enthalpy function for component j going out of the secondary chamber, h_{air_j} is the enthalpy function of the injected air and recirculated flue gas (it's important to note that there are four such injections, so they have to be summed) and $\dot{Q}$ is the heat transferred with the wall.

For easier notation we introduce some variables to represent the different parts of (2.66). The entire right hand side is known from measurements, and we denote it simply Π. We also replace the h_{in_j}s by α, β, γ, η and ϕ respectively. (2.66) can then be written as

$$\alpha y + \beta z + \gamma v + \eta w + \phi u = \Pi \tag{2.67}$$

By adding (2.67) to the system of (2.65) we have the new system

$$\begin{aligned} y + z + w &= m + n - a - b \\ v + u + 2w &= k - c \\ 3w + u + z &= 2(p - q) \\ \alpha y + \beta z + \gamma v + \eta w + \phi u &= \Pi \end{aligned} \tag{2.68}$$

But still we have five unknowns and only four equations. Thus we add an extra assumption regarding the relation between the combustible species CH_4 and H_2. Based on experiments done by Energos on typical compositions [4], the relation CH_4:H_2 is assumed to be 7:4, so $w = 1.75u$. When adding this to (2.68) and writing it on matrix form, we get

$$\begin{bmatrix} 0 & 1 & 1 & 1 & 0 \\ 1 & 2 & 0 & 0 & 1 \\ 1 & 3 & 1 & 0 & 0 \\ -1.75 & 1 & 0 & 0 & 0 \\ \alpha & \beta & \gamma & \eta & \phi \end{bmatrix} \begin{bmatrix} u \\ w \\ z \\ y \\ v \end{bmatrix} = \begin{bmatrix} m + n - a - b \\ k - c \\ 2(p - q) \\ 0 \\ \Pi \end{bmatrix} \tag{2.69}$$

where the last row consists of the enthalpies for typical temperatures in the primary chamber and has to be scaled down to an order of magnitude closer to that of the other rows to avoid the matrix from being ill-conditioned for inversion. (2.69) is the system written on the form of (2.60). This $\mathbf{A}$ matrix has full rank, i.e. rank = 5 so these components are steady-state observable. Note that this is only valid when we have the assumption about the constant relation between CH_4 and H_2, thus it will only be possible to estimate four independent variables uniquely.

To summarise; it is possible to estimate the syngas composition based on measurements when some assumptions are made, otherwise the composition

is not even steady-state observable. Steady-state observability is a requirement for MPC to make sense in the long run.

The assumptions made to make it possible to estimate the composition from the primary chamber are:

- we assume no oxygen from the primary chamber
- we assume a constant relation between CH_4 and H_2
- we assume that nitrogen, N_2, is all that's left when the first six species are calculated, i.e. no other components are present.

In this way all the seven components can be found provided that we don't lose any measurements.

2.2.12 Constant parameter estimation

This section deals with constant parameter estimation and has nothing to do with the previous section about the syngas components. The syngas components will be considered as time varying parameters, i.e. not constant parameters.

Parameter identifiability

In order to identify a system's constant parameters from process data, it is necessary that the data contains sufficient information. This is easily illustrated by considering the system equations in steady-state

$$\dot{x} = f(x, u, p) = 0 \tag{2.70a}$$
$$y = h(x, u, p) \tag{2.70b}$$

If we have n_x states and n_y measurements, (2.70) gives a total of $n_x + n_y$ equations. In general, n independent equations are necessary in order to obtain a unique solution of an equation system consisting of n unknowns. The only information known is the process inputs and available process measurements. The unknown variables in (2.70) are then the state vector and the parameters we wish to estimate. This results in a total of $n_x + n_p$ parameters to be identified from $n_x + n_y$ equations [14]. Hence, we may only expect to find a unique solution when:

$$n_y \geq n_p \tag{2.71}$$

If more variables are to be identified, we need to consider multiple data points. In order to achieve the required amount of independent equations, the data series must be *sufficiently rich* for our problem. By sufficiently rich we mean that the data series provides sufficient variations in the variables to provide at least $n_x + n_p$ independent equations which are solvable for our $n_x + n_p$ unknowns. This means that the system has to be excited, and the excitation needed to get it sufficiently rich is called persistent excitation. Identifiability for systems that are linear in unknown parameters is treated thoroughly in the literature, for example in [14]. For nonlinear systems, the analysis becomes more complex as the system may be locally identifiable, although not globally.

In applications depending on on-line parameter estimates, it is wise to choose $n_p \leq n_y$ [15]. The parameters are then identifiable, independent of signal richness, if the equations in (2.70) are linearly independent and solvable for the chosen parameter set. This reduces the requirement for persistent exciting inputs, which is especially important in industrial applications where high excitation is achieved at the expense of optimal operation [16]. In off-line parameter identification, however, it is often possible to identify more parameters than available measurements. In such cases, it it safe to exploit the richness of the recorded data series to identify more parameters.

The choice of which parameters to estimate is not always obvious, and often requires deep process knowledge. One approach to the choice of parameters is to look at the system's parameter sensitivity, namely how changes in the parameters affect the process outputs. It is not possible to estimate a parameter if it has no direct effect on any of the measured outputs.

The parameter vector, θ should normally be a set of parameters which is identifiable from stationary data and which do not require any particular excitations in order to obtain convergence. Typical choices are heat and mass transfer coefficients, kinetic parameters, etc. By carefully selecting a number of parameters equal to the number of output measurements, zero steady-state deviations in all predicted output measurements can normally be achieved [15].

Parameters to be estimated

As mentioned in the previous sections, there are some constant parameters to be estimated for this process. Cybernetica's ModelFit does the estimation using the least squares method to minimise the error between calculated and measured values. This may become a non-linear optimisation problem, thus not convex, and minimas found by that algorithm may be only local minimas, not global ones, hence initial values are important. A bad choice of initial

values is therefore not likely to give the optimal results.

An important thing to note is that the new values of the estimated parameters don't necessarily have a physical meaning, but it is a way of compensating for modelling errors. For example, as seen at an early stage of the parameter estimation, before a model of the temperature sensors was incorporated, when the calculated temperature values were tried directly matched with the measured ones. The estimated value for the heat transfer coefficient of the walls then became extremely large, i.e. a hundred times bigger than initially thought. This showed the model's desire for slower changes of the gas temperature so that they could be more comparable to the already low-pass filtered measured ones. The high value for the heat transfer to the walls damped the changes of the gas temperature a bit, but was not at all closer to the real value of the heat transfer coefficient.

So the estimated parameters are not necessarily more correct than the original ones (in the sense that they are more physically correct), but they will, if chosen carefully, improve the overall result from the model to make the calculated values closer to measured values. As all sensors have some uncertainty, the measured values will neither represent the exact true state of the process, but it's the closest we can possibly get to it. Another important thing to remember is to only compare comparable values, i.e. the calculated gas temperature cannot be directly compared to the measured temperature; we need a sensor model to make it more realistic, the same applies to the composition measurements.

Table 2.1 shows all constant parameters to be estimated.

Parameter	Description	Init. value
$U_{htc_{wall}}$	Heat transfer coefficient, walls	9 W m^{-2} K^{-1}
θ_{sensor}	Constant for temperature sensors	1 s^{-1}
θ_1	Constant for eq. (2.38)	1

Table 2.1: Parameter vector, $\boldsymbol{\theta}$

Process noise

In a process there will always be some process noise. In this work a simple additive process noise model is used. The process noise is incorporated into the model by adding some noise to the parameter vector $\boldsymbol{\theta}$ of (2.1), i.e.

$$\tilde{\theta}_k = \theta_k + v_k \tag{2.72}$$

$\tilde{\theta}_k$ being closer to what we would observe in the process than the ideal θ_k. v_k is chosen to a reasonable value based on visual inspection of the plotted results.

2.2.13 Assumptions and simplifications

The pressure is assumed to be approximately constant. The heat capacities, C_p, are calculated based on the assumption of constant pressure. The pressure changes with only about 20 Pa between the control volume, so it has negligible effect on the calculation of C_p. The assumption on constant pressure means that we assume that the flue gas fan works infinitely fast and manages to control the pressure perfectly.

Only three reactions are modelled. There are probably hundreds of reactions actually taking place, but these three reactions are thought to capture the main dynamics of the process. The composition of the syngas from the primary chamber was shown to be steady-state observable, so this model would only be valid at steady-state, but it should be possible to make an algorithm that will give a future MPC application a somehow sensible behaviour in transient periods as well.

The gas is assumed to be ideal, a common assumption for gases at low pressures and high temperatures.

The wall and gas temperatures are different for each control volume, as if there were some physical limit dividing them, but in the plant it is not so. The temperatures will have a gliding transition, but as we assume a series of CSTRs we lose this transition.

A mathematical model describing a physical process will always be simplified. Numerous assumptions have to be made to make it manageable. In that respect every equation mentioned is a simplification, though some more coarse than others.

2.3 The implemented model

The model was programmed using the programming language C in the development environment Microsoft Visual C++. C is quite different from Matlab, and with Cybernetica's tools there were a lot more options, like

estimation of constant parameters, tracking varying parameters and state estimation. Here follows a description of the implementation of the model.

Cybernetica's software

Cybernetica has developed their own software for (nonlinear) model based control; CENIT. The process model was implemented in a simplified CENIT user interface that is typically used by Cybernetica's customers, student or others working with them.

The CENIT kernel consists of a model component (that includes the model equations, the ODE solver etc.), an estimator and a model predictive controller. CENIT communicates real time with the plant based on the OPC communication protocol[8].

ModelFit is Cybernetica's own simulation platform and is here used for model validation, simulations of the system, estimation of constant parameters and implementation of a Kalman filter for the estimation of slowly varying model parameters such as the composition of the syngas from primary chamber.

The process data had to be conditioned and made suitable for use in ModelFit, this was done in Matlab and the .mat file loaded into ModelFit.

States

The model has 65 states in total: 7 components $\times$ 6 control volumes = 42 molar hold-ups, 1 gas temperature $\times$ 6 control volumes = 6 gas temperatures, 1 wall temperature $\times$ 6 control volumes = 6 wall temperatures, 4 sensor temperatures and 7 sensor components.

These variables were chosen as states because they directly represent what we're after; composition and temperature out of the furnace.

The equations for the state updates are (2.16), (2.38), (2.46), (2.51) and (2.59).

[8]OPC stands for 'OLE for Process Control' which again stands for Object Linking and Embedding (OLE) for Process Control. This is the original name for a standards specification developed in 1996 by an industrial automation industry task force. The standard specifies the communication of real-time plant data between control devices from different manufacturers. As of November 2011, the OPC Foundation has officially renamed the acronym to mean "OPen Connectivity". [17]

ODE solver

In Cybernetica's interface the default solver is a second order Runge-Kutta with fixed time step.

Before the kinetics were removed, the system was very stiff, and when working on finding a solution an eighth order Runge-Kutta solver was used to simulate the system. The eighth order Runge-Kutta solver is not a stiff solver, but a lot quicker than the default second order Runge-Kutta. The solver gsl_odeiv2_step_rk8pd was found in the on-line GSL library [18] and is an explicit embedded Runge-Kutta Prince-Dormand (8,9) method. It is similar to Matlab's ode45 (which is Runge-Kutta Prince-Dormand (4,5)). A wrapper function was made to incorporate this solver into the existing model.

The GSL library methods use variable step size, which is good in the sense that they probably run quicker than a method with fixed step size. The fixed step method would have to find the smallest step needed for the most stiff part and use this throughout the simulation, whereas the variable step size method would increase the step size and hence run quicker in smooth areas. The drawback is that the variable step size can lead to variable run time, which is not desirable for an on-line MPC application. During simulations while debugging the system, the eighth order method was used, but later the second order was used again as it provides a predictable runtime.

The Runge-Kutta methods is a family of iterative methods for the approximation of solutions of ODEs. A first order Runge-Kutta is the same as the classic Euler formula, whereas the second order Runge-Kutta method is the same as the Improved Euler method (also called Heun's method)[19].

Let us consider the following initial value problem:

$$x_{k+1} = f(x_k), \quad x(0) = x_0 \tag{2.73}$$

At point x_k we want to find x_{k+1}. Euler method finds the next x by the formula $x_{k+1} = x_k + hf(x_k)$ where h is the integration time step. The second order Runge-Kutta method has the following algorithm:

Let us define

$$\begin{aligned} k_1 &= hf(x_k) \\ k_2 &= hf(x_k + k_1) \end{aligned} \tag{2.74}$$

h still being the integration time step. Then x_{k+1} is found by

$$x_{k+1} = x_k + \frac{1}{2}(k_1 + k_2) \tag{2.75}$$

Measurements

The measurements of the composition out has a 1-2 minutes time delay, so the process data had to be shifted correspondingly. For the convenience of round numbers the data was shifted 100 samples, which is equal to 100 seconds as the true delay is not known. This is a coarse approximation and should be investigated further to get a more precise number.

Recirculation

The composition of the recirculated flue gas is taken as the calculated measured composition out. A 10 second delay is incorporated as that is approximately the time it takes for the flue gas to be recirculated [9].

The calculated composition is the low-pass filtered composition out of CV6 mixed with the ingress air. This low-pass effect suits the recirculated composition well as this corresponds to what happens in the real plant as well. Any rapid changes will be smoothed out because the gas is being recirculated for some time. The recirculation will lead to a natural smoothing process happening before it is being injected back into the furnace.

Kinetics

A function was made to calculate the change of molar hold-up caused by the reactions. The code for this function is included in appendix F.1 if the reader is interested.

As described in section 2.2.2 there are only three reactions. Hydrogen is combusted first, then if there is still oxygen left methane burns and finally carbon monoxide. For each control volume there are two flows in: the syngas, containing combustible species, and air/recirculated flue gas containing oxygen, both flows necessary for combustion.

The "reaction rates" for this are calculated by finding which is the limiting factor, the oxygen or the combustible species, and setting the rate to whichever is smallest. E.g. if there is more combustible species than oxygen, the reaction rate will be set equal to the number of moles of oxygen and all oxygen will disappear along with the corresponding amount of combustible species. The combustion products will also increase accordingly. There are no dynamic reactions involved, the combustion is assumed to happen instantaneously, and mathematically this is done even before the species enter the control volume.

However, it was seen from the process measurements that the temperature typically increased in the control volume after the oxygen injection, meaning that when air is injected it will locally cool the volume, but given

some time the oxygen will combust and hence increase the temperature. The temperature rise is consequently observed in the next control volume. The need for a delay in the combustion is hence evident. This was solved by making a bypass for the oxygen entering through the secondary air or recirculated flue gas to the next control volume. The amount of oxygen available for combustion is removed from the air and recirculated flue gas flows and will thus not be combusted in the control volume where it enters. This removal does not mean that the oxygen itself is removed, it is just not given the permission to react in the control volume where it first enters the process. In this control volume it will be mixed with the other components, gaining the same temperature as the rest. It enters the next control volume as part of the syngas, and here everything can be used for combustion.

As previously mentioned the reactions are dependent on the temperature. A simple temperature dependence is incorporated in the reaction rates by multiplying with an exponential rate of change (first order step response): $(1 - \exp(-T/200))$. This expression will give a number between 0 and 1, 0 for low temperatures and 1 for high temperatures. As the temperature T gets large, this expression goes to 1, i.e. the reaction rate remains unchanged for high temperatures (the reaction rate is simply multiplied with this expression, so at high temperature the reaction rate will be multiplied with 1). The reaction rates will be a little bit reduced at lower temperatures.

At approximately 1000° K it is desired not to have reduction in the rates, and the "time constant" of 200 was chosen based on the rule of thumb that a first order system will have reached about 99% of its steady-state value after $5 \times$ the time constant. A simple ramp function could also do the same job.

It is not realistic to assume that the reactions happen instantaneously. Therefore only a certain percentage of the combustible species are allowed to react at any given time. Hydrogen combustion is a very quick reaction, hence 99% of the hydrogen is combusted instantaneously. 80% of the methane and 60% of the carbon monoxide are combusted instantaneously. Mathematically this is the same as done for the temperature dependence, i.e. multiplying with a factor between 0 and 1, but has another physical motivation.

Other functions

One function was made for flow conversions, i.e. for converting between the different units for the flow rates; [mol s^{-1}], [kg s^{-1}] and [Nm^3 h^{-1}]. Based on the flow in the original units and the composition of this flow the new flow was calculated. Assuming ideal gas, the ideal gas law (2.52) gave volume

conversions and the known molar masses gave conversion between moles and kilos.

The molar fraction of the components is used several times during the main calculations. It is found as described below.

n_{tot} is total number of moles for one control volume

$$n_{tot} = \sum_{\forall j} n_j \tag{2.76}$$

The molar fraction x for component j is calculated as follows:

$$x_j = \frac{n_j}{n_{tot}} \tag{2.77}$$

Constant parameters

The constant parameters are calculated in ModelFit. An upper and a lower limit has to be chosen for the parameters that ModelFit cannot cross. Also a perturbation step is chosen, typically around 1/100 of the initial guess. ModelFit will then try to both decrease and increase the parameter with the perturbation value, simulate the entire time period and see what gives the smallest error. This will be done repeatedly with the new parameter values until it converges to some constant value, solved as an optimisation problem. The initial values are chosen based on knowledge of the process.

Initial conditions

The initial composition in the combustion chamber is chosen to be a typical flue gas composition with a temperature of 900° C. The initial value for the composition from the primary chamber is also chosen to be a typical syngas composition, as found by Energos [4]. Initial pressure is 150 Pa below atmospheric pressure.

The initial conditions of the states are later estimated to individually fit each dataset used.

Time steps

The time sample in the model was set to one second, hence one step on the plotted graphs in chapter 3 corresponds to one second. This also corresponds well to the measured data that has a (minimum) sampling time of one second, and can thus be used directly.

The integration time step was quite small, 0.01 second.

2.4 Comments to model changes

The model developed during last semester has here undergone some changes. This section will only explain clearly what was changed during this semester and why. The main idea behind the model changes was to get a lower run time and to and make the reimplementation in C easier.

Matlab has a very intuitive way of handling vectors and matrices, but this is not as straightforward in C, so e.g. the way of solving the entire problem was changed from a huge and messy matrix problem (DAE system) to only ODEs. This was made possible by calculating the internal flow between the control volumes explicitly based on the flow equation described in section 2.2.9.

One model error that was not found and understood last semester was now found and corrected. This removed the problems of large overshoots during simulation of transient periods that we had before and enabled the use of temperature directly as a state of the model, not internal energy as used before.

The gas kinetics were removed and this drastically reduced the program's runtime. The quickest measurement is done every one second, i.e. anything happening faster that that cannot be measured anyway, so there is no point in simulating dynamics that fast. For a control purpose, the model has to simulate at least 50 $\times$ real time, this was impossible to achieve earlier, but is now more than satisfied.

The heat transfer with the walls is modelled in a better way than before. The physical properties of the walls have been investigated and the model is made more realistic.

The temperature sensors are also modelled to get the right low-pass filtering on the temperature so it can be compared to measured temperature.

Now real process data is used as inputs, before the input was assumed to be known and constant. The use of Cybernetica's tools enabled parameter estimation and estimation of the composition from the primary chamber.

2.5 Model predictive control

2.5.1 Notation

Table 2.2 shows an overview of some typical notations for systems that will be used for the explanation of basic concepts in section 2.5 and 2.6.

MPC will be presented for a common linear system:

Symbol	Description
$\mathbf{x}$	State vector
$\boldsymbol{\theta}$	Parameter vector
$\mathbf{u}$	Input vector
$\mathbf{y}$	Measured output vector
$\mathbf{z}$	Predicted output vector
$\mathbf{v}$	Process noise
$\mathbf{w}$	Measurement noise
$\mathbf{d}$	Disturbances

Table 2.2: Notations

$$\begin{aligned} \mathbf{x}_{k+1} &= \mathbf{A}\mathbf{x}_k + \mathbf{B}\mathbf{u}_k + \mathbf{E}\mathbf{d}_k \\ \mathbf{z}_k &= \mathbf{C}\mathbf{x}_k + \mathbf{D}\mathbf{u}_k + \mathbf{F}\mathbf{d}_k \end{aligned} \tag{2.78}$$

2.5.2 MPC basics

Model Predictive Control, MPC, is currently one of the most popular advanced control methods (that is, more advanced than the standard PID) [20]. The theory originates from optimal control theory. There are several variants of the MPC, but they all share the common trait that an explicit process model is used to predict and optimise future process behaviour [21]. The internal model is usually based on physical/chemical relationships, but can also be found empirically based on experiments.

Many processes work quite well with only PID control, but could benefit from a more advanced control. The introduction of MPC is thus not necessarily only for stabilising a process, but to control it in an optimal way. MPC is thus often put on top of the regulatory control. The regulatory control is typically simple PID loops stabilising the process. The MPC is at a higher level and does supervisory control, e.g. determining the set points of the PID loops.

Because of the MPC's abilities to predict the future there will be less wear and tear on actuators and the control action would look more intuitive, more as if an operator was doing it. The knowledge of the process constraints will make it possible to operate closer to the limits and hence possibly increase the profit, which in many cases can be one of the main motivations behind a better control system.

One of the main advantages of MPC is that it handles constraints on

equipment, states and other variables. Because the MPC is aware of equipment constraints, it removes the problem of integer wind-up. It can also be easily applied to control multivariable systems. It is usually a good choice to use MPC when there exist constraints and it is e.g. desired (usually for economical reasons) to operate close to these. MPC can also be a good idea where there are dynamic characteristics that are difficult for regular PID controllers to handle. Common dynamic include large time delays and high-order dynamics. Such elements can be incorporated in the internal model of the MPC.

For the MPC to take sensible action, it needs to predict the plant response for a certain amount of time steps into the future, called the prediction horizon, H_p. It uses the current plant measurements, the current dynamic state of the process, the MPC models, and the process variable targets and limits to calculate future changes. The control inputs are calculated for the control horizon, H_u. Typically $H_u \leq H_p$.

The changes are calculated to hold the dependent variables close to target while not violating any constraints. The MPC controller essentially controls the process model by optimising the use of the inputs in order to remove the predicted deviation from some desired state (or output) trajectory [21]. The optimisation problem is recalculated at each sample to cope with changes in operational conditions, like unmodelled disturbances etc..

The optimisation problem of the MPC is to minimise the objective function. The objective function typically contains all the inputs and outputs of interest, but can also include states that directly affect an output that can be difficult to measure correctly. The objective function is also referred to as the cost function, making it more obvious that we want to minimse it. A typical objective function might take the form [20]:

$$J = \sum_{i=i}^{N} [(x_i - x_{ref,i})^T Q (x_i - x_{ref,i}) + (u_i - u_{ref,i})^T R (u_i - u_{ref,i})] \qquad (2.79)$$

where Q and R determines how much to penalise deviation of the states x_i from the reference trajectory $x_{ref,i}$, and the deviation of the input u_i from some desired input trajectory $u_{ref,i}$ respectively.

There is a trade-off between the weight on Q and R, one cannot have both the states and input trajectories followed perfectly, and the relation between Q and R is something to tune to achieve the best possible result. Relatively large values of Q increases the aggressiveness of the controller.

In general, the MPC problem may be formulated with both equality and inequality constraints. With all constraints written explicitly, the linear quadratic optimization problem may be formulated as in [20]:

$$\min_{\Delta U} \; J(\mathbf{z}, \mathbf{u}, \Delta \mathbf{u})$$

$$s.t. \quad \begin{array}{rcl} \mathbf{x}_{k+1} & = & \mathbf{A}\mathbf{x}_k + \mathbf{B}\mathbf{u}_k + \mathbf{E}\mathbf{d}_k \\ \mathbf{z}_k & = & \mathbf{C}\mathbf{x}_k + \mathbf{D}\mathbf{u}_k + \mathbf{F}\mathbf{d}_k \\ U_{min} & \leq U \leq & U_{max} \\ \Delta U_{min} & \leq \Delta U \leq & \Delta U_{max} \\ Z_{min} & \leq Z \leq & Z_{max} \\ X_{min} & \leq X \leq & X_{max} \end{array} \tag{2.80}$$

$$U = \left[\mathbf{u}_k^T \dots \mathbf{u}_{k+H_u-1}^T\right]^T \quad \Delta U = \left[\Delta\mathbf{u}_k^T \dots \Delta\mathbf{u}_{k+H_u-1}^T\right]^T$$
$$X = \left[\mathbf{x}_{k+1}^T \dots \mathbf{x}_{k+H_p}^T\right]^T \quad Z = \left[\mathbf{z}_{k+H_w}^T \dots \mathbf{z}_{k+H_p}^T\right]^T$$

where H_w is a window horizon determining from what time step errors in z shall be penalised. If there is no delay in the process, $H_w = 1$ and errors are penalised from the first step. H_p is how far into the future the predictions go and H_u is how far into the future we calculate changes in the control input. Δu is assumed to be 0 for all time steps after H_u.

Figure 2.5 (made by [22]) illustrates the basic principles of the MPC.

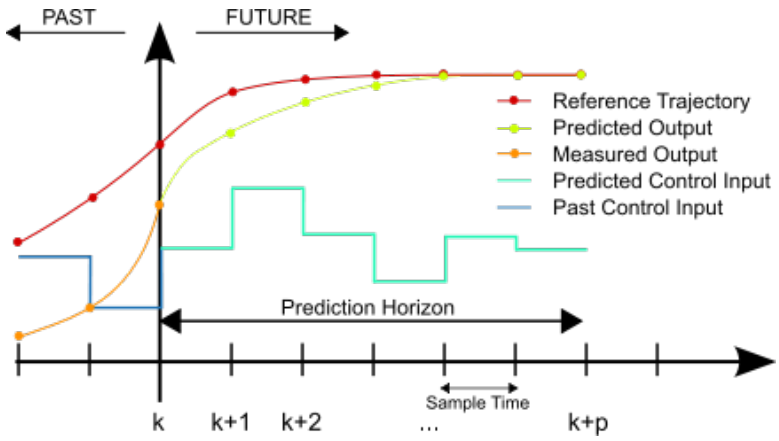

Figure 2.5: The basic idea of MPC

At the current time step, the MPC controller optimises the process behaviour over a finite horizon. The first element of the input sequence is then

applied to the process input. The procedure is repeated at regular intervals, resulting in moving horizon optimisation. The resulting controller can easily be configured to possess qualities of several basic control structures, such as feedback, integral action, anti windup and feed forward. Feedback is achieved implicit when recalculating the optimization problem, feed forward is achieved by adding a priori knowledge in the prediction equations and anti windup is handled by constrained optimisation theory. Integral action is achieved through choice of free optimisation variables, disturbance model and model update strategy [20]. [20] gives a thorough introduction on how the MPC problem should be formulated in order to create a controller with such qualities.

The biggest "problem" with the MPC is that it need a fairly good model for predictions. Many systems are very complex and it can be hard to model them sufficiently simple. Few and poor measurements can also make potential state estimations difficult.

2.5.3 Model based furnace control, objectives

The task of the control system of the furnace is to keep the temperature inside the furnace approximately constant and to have a complete combustion ensuring that the air emissions are within governmental regulations. The two main objectives are to keep the temperature out of the furnace around 900°C and have an oxygen content of about 6-7% at the end of the process.

The temperature inside the furnace is important for many reasons. One is that there is a risk of the refractory of the combustion chamber cracking if the temperature changes too quickly. Another important reason is that the temperature needs to stay high enough for complete combustion of all combustible species, especially carbon monoxide that burns slower than methane and hydrogen, and to ensure thermal destruction of dioxins and furanes [1]. There is a governmental requirement to have a minimum temperature of 850° C and a residence time of at least 2 seconds after the last air injection to ensure this [23].

At the same time it's not desirable to have the temperature much higher than that because formation of NO_x gases and sintering[9] happen at high temperatures. To control these parameters, the air/recirculated flue gas injection has to be controlled to balance the temperature and combustion.

[9]Sintering is a phenomenon where for instance a powder or another collection of smaller particles is heated until it becomes a solid object. It is not desirable that this occurs e.g. with the dust in the chamber as that could clog the temperature sensors and/or deposit on the walls, becoming difficult to remove.

The current control system consists of many PID loops. One problem with a PID controller is that it can be challenging to tune well, but just as important is the restriction given by the very structure of several individual control loops together. The selection of an optimal structure is not necessarily easy, maybe not even feasible. MPC can coordinate the use of multiple control signals and can take more explicitly into account the limitations of the process, though it would be optimistic to expect that it is easier to tune than a PID. In addition the MPC allows for operation closer to constraints, which often leads to more profitable operation [20]. It would be desirable to increase the amount of waste that can be treated and maximise the steam generation and thus have a higher and more stable energy production. Other expected benefits of MPC include faster response to fuel variations, thus a better and faster control of the temperature and O_2 level [23].

It is never known what comes from the primary chamber. The composition of the flue gas is measured and it is desired that this information can be used to estimate the composition from the primary chamber. Without measurements, the flow from the primary chamber can be viewed as only noise making future predictions difficult for the model predictive controller.

One of the biggest concerns in today's operation of the plant, is the quenching problem. There are various reasons for this happening (as discussed in section 2.2.7), and it is clearly not desired. An example of quenching will be shown in section 3.1.2, where the temperature falls until an operator manually reduces the injection of recirculated flue gas.

It is desired that a potential model predictive controller will take action similar to that of the operator, namely reducing the recirculated flue gas injection if the temperature goes too low. This is something the PID today does not handle.

However, the best would be to introduce a temperature constraint in the MPC such that the temperature is not allowed to go below a certain limit. As mentioned in previous sections, the simplified model does not capture the quenching problem. With a temperature constraint we would hopefully never get quenching and thus no need to model it.

2.5.4 This control problem

Manipulated variables

The relevant control inputs for the secondary chamber is the flow of secondary air and recirculated flue gas into the secondary chamber, in total four flows.

The recirculated flue gas has both a cooling and a heating effect. The cooling effect is due to its relatively low temperature (compared to the gas in the chamber), but as it contains some oxygen the recirculation can lead to an increase in temperature caused by combustion in the under stoichiometric areas of the furnace, i.e. control volume CV1-CV3. Nevertheless, the overall effect of the injection of recirculated flue gas, observed at the exit of the secondary chamber (i.e. what goes out of control volume 6), is no change or a decrease in temperature.

The secondary air also has an initial cooling effect because its temperature is much lower than that of the gas, but because it contains a lot of oxygen, combustion will occur thus the effect of secondary air injection is temperature rise in the under stoichiometric region. However, after the last injection of secondary air, the combustible species are fully consumed and there is excess of oxygen. Thus further secondary air injection at S2 will lead to a decrease in the temperature at the outlet, but a rise in the oxygen level.

In todays control system the recirculated flue gas (R1 and R2) are used to control the temperature of the flue gas leaving the furnace. The first secondary air injection, S1, and the combustion air through the last zone of the primary chamber are used to control the temperature in the first part of the secondary chamber. The last secondary air injection, S2, is used to control the oxygen level in the flue gas leaving the furnace.

The auxiliary burner is automatically turned on if the temperature gets too low.

Pressure in the primary chamber is supposed to stay just below atmospheric pressure, this is measured and used in the PID that controls the fan at the chimney.

The primary air and fuel fed into the primary chamber has a large impact on the gasification process; the two chambers are strongly coupled, but that is not part of this project's scope.

Measured variables

The temperature and O_2 concentration out of the chamber are measured, and these are this projects main objective to keep constant. The temperature is also measured several places in the chamber.

The flue gas quality, i.e. content of NO_x, CO, CO_2 etc. is measured before it leaves the chimney.

All secondary air/recirculated flue gas flows into the chamber are measured.

Constraints

Constraints on actuators are typically physical constraints that cannot be exceeded:

- Valve opening rates. A valve needs some time to go from fully closed to fully open.
- Max/min flow rates, for example due to pipe dimensions.
- Saturation. E.g. a valve can never be more than 100% open.

Constrained state variables:

The temperature out of secondary chamber should ideally be 900°C and the O_2 level about 6-7%, this will be a typical set point for the controller of the secondary chamber. Temperature changes inside the furnace should not be too quick, nor should the temperature violate the max/min limits. A governmental requirement is that the residence time after the last air injection should be at least 2 seconds with a temperature of at least 850°C.

One on the most important temperature constraints will be a lower limit on the temperature in the furnace. This with the idea that if the temperature never falls too low the quenching problem will be avoided.

A possible practical approach to find the lower temperature constraint could be the following: find out experimentally how much the temperature sinks per second (as minimum time step between measurements is one second) with maximum flow rate on the inlets. If this is for example 20 degrees per second, set the lower temperature constraint 20 degrees above the desired minimum temperature. This will ensure that we don't lose control from one time step to the next even if the valve is opened maximum. The idea here is that this will make us able to in the next time step to correct for the decrease in temperature before it's too late.

Constraints on the compositions could include an upper limit on the concentration of combustible species out of the furnace. It is not possible to constrain the composition other places than out of the furnace, as this is the only place with composition measurement.

Disturbances

The main disturbance is the composition and calorific value of the waste and therefore of the syngas entering the secondary combustion chamber. The fuel input has to be regarded as unknown and should be estimated.

The ingress air leaking into the system is also an unknown disturbance taken as a parameter to be estimated.

The need for a good process model

The MPC controller essentially controls the process *model* and good control can only be achieved if the model is able to predict the behaviour of the true process with reasonably accuracy. As there will always be some model errors and unforeseen disturbances it will be necessary to update the model to maintain good quality predictions of the future process behaviour [21]. Here the Kalman filter will be used as the state estimator, more on this in the next chapter.

Another important property of the model, is the run-time for simulations. The on-line requirement places a limitation on the complexity of the model: it should be as simple as possible, but still capture the main dynamics of the process.

Implementation

As suggested by Cybernetica [23] the MPC algorithms could be run on an external Windows workstation which is not to be used for other critical tasks. The workstation should be connected to the existing control system for two-way communication between the MPC and the hardware [23]. A software that can communicate efficiently with the existing system is needed as it's not desirable to have to wait for the data to be sent.

2.6 On-line estimation

In most chemical processes the measured variables are too inaccurate to give useful information about the process states that can be applied directly into our calculations. This might be due to for example measurement noise, time delays on measurements etc. It is also common that only some of the states are measured.

In these cases (which is most of the time) we need a state estimator to estimate the states that are not measured or the ones with too much measurement noise. In addition we have some time varying parameters, i.e. the syngas composition, that will be estimated by the state estimator. These time varying parameters will be put at the end of the state vector and will for the state estimator be regarded as states.

The Kalman filter (and several variants of it) is currently one of the most popular algorithms for this purpose and is what is used in this work.

2.6.1 The Kalman filter

The original Kalman filter is simply an *optimal recursive data processing algorithm* that uses all available measurement data to produce an estimate of the current variables of interest of a system. It is optimal in the sense that it minimises the variance of the estimation error, i.e. it minimises the error between measured and calculated values statistically [24]. The word *recursive* in the previous description means that, unlike certain data processing concepts, the Kalman filter does not require all previous data to be kept in storage and reprocessed every time a new measurement is taken. Because of the algorithm's recursive nature, it can run in real time using only the present input measurements and the previously calculated state; no additional past information is required [24].

Kalman filter for linear systems

The main assumption of the basic Kalman filter is that the underlying system is a linear dynamical system and that all error terms and measurement noise have a Gaussian distribution.

The state estimation problem is to determine an estimate of the state given the chosen model structure, an a priori initial state estimate and a sequence of noisy measurements. This has to be done during the available sample interval of the system as each measurement becomes available.

Assume the following system equations:

$$\begin{aligned} \mathbf{x}_k &= A_k\mathbf{x}_{k-1} + B_k\mathbf{u}_{k-1} + \mathbf{v}_{k-1} \\ \mathbf{y}_k &= C_k\mathbf{x}_k + D_k\mathbf{u}_{k-1} + \mathbf{w}_k \end{aligned} \tag{2.81}$$

where $\mathbf{v}$ and $\mathbf{w}$ are state and measurement noise vectors respectively. We assume that both $\mathbf{v}$ and $\mathbf{w}$ originate from uncorrelated white noise sequences, thus having covariance matrices:

$$\mathbb{E}\left[\mathbf{v}_k\mathbf{v}_i^T\right] = \begin{cases} Q_k & i = k \\ 0 & i \neq k \end{cases} \tag{2.82}$$

$$\mathbb{E}\left[\mathbf{w}_k\mathbf{w}_i^T\right] = \begin{cases} R_k & i = k \\ 0 & i \neq k \end{cases} \tag{2.83}$$

$$\mathbb{E}\left[\mathbf{v}_k\mathbf{w}_i^T\right] = \quad 0 \qquad \text{all } i \text{ and } k \tag{2.84}$$

The estimates generated from open loop model predictions are written

$$\begin{aligned} \hat{\mathbf{x}}_k^- &= A_k\hat{\mathbf{x}}_{k-1} + B_k\mathbf{u}_{k-1} \\ \hat{\mathbf{y}}_k^- &= C_k\hat{\mathbf{x}}_k + D_k\mathbf{u}_{k-1} \end{aligned} \tag{2.85}$$

where the superscript minus sign denotes that this is an *a priori* estimate calculated prior to time t_{k+1}. If the predicted outputs $\hat{\mathbf{y}}_k$ deviate from measured process outputs $\mathbf{y}_k$, the measurements may be used to update the a priori estimates forming *a posteriori* estimates. This update may be performed as a linear feedback from the prediction error:

$$\hat{\mathbf{x}}_k = \hat{\mathbf{x}}_k^- + K_k \left(\mathbf{y}_k - C_k\hat{\mathbf{x}}_k - D_k\mathbf{u}_{k-1}\right) \tag{2.86}$$

where K_k is known as the Kalman gain. In order to find an optimal expression for the Kalman gain, we consider the variance of error covariance matrix:

$$P_k = \mathbb{E}\left[\left(\mathbf{x}_k - \hat{\mathbf{x}}_k\right)\left(\mathbf{x}_k - \hat{\mathbf{x}}_k\right)^T\right] \tag{2.87}$$

By inserting equations (2.85) and (2.86), the expression becomes

$$\begin{aligned} P_k = \mathbb{E}\,[\, &\{(\mathbf{x}_k - \hat{\mathbf{x}}_k) - K_k\left(C_k\mathbf{x}_k + \mathbf{w}_k - C_k\hat{\mathbf{x}}_k\right)\} \\ &\{(\mathbf{x}_k - \hat{\mathbf{x}}_k) - K_k\left(C_k\mathbf{x}_k + \mathbf{w}_k - C_k\hat{\mathbf{x}}_k\right)\}^T\,] \end{aligned} \tag{2.88}$$

By solving the expectation, we get [25]

$$P_k = (I - K_kC_k)P_k^-(I - K_kC_k)^T + K_kR_kK_k^T \tag{2.89}$$

that we expand and rewrite

$$P_k = P_k^- - K_kC_kP_k^- - P_k^-C_k^TK_k^T + K_k(C_kP_k^-C_k^T + R_k)K_k^T \tag{2.90}$$

where P_k^- is the error covariance matrix for the a priori estimates. The diagonal elements of the error covariance matrix represent the variance of the estimation error in each state estimate. Hence, it is desired to find the Kalman gain K_k that minimizes these elements. In [25], this is done by differentiating the trace of the error covariance matrix with respect to K_k:

$$\frac{d(trace\ P_k)}{dK_k} = -2(C_kP_k^-)^T + 2K_k(C_kP_k^-C_k^T + R_k) \tag{2.91}$$

The optimal gain is then found by setting the derivative to zero and solving for K_k. The optimal Kalman gain is then found to be

$$K_k = P_k^-C_k^T(C_kP_k^-C_k^T + R_k)^{-1} \tag{2.92}$$

By substituting the optimal gain into (2.90), it can be shown that the relationship between the a posteriori and a priori error covariance matrix is

$$P_k = (I - K_kC_k)P_k^- \tag{2.93}$$

Note that (2.93) is only valid for the optimal Kalman gain whereas (2.89) is valid for any gain, optimal or suboptimal.

The *a priori* covariance matrix at time t_{k+1} may be calculated from

$$P_{k+1}^{-} = A_k P_k A_k^T + Q_k \tag{2.94}$$

Together, equations (2.86) and (2.92)-(2.94) constitute the recursive Kalman filter for the system described in (2.81).

Kalman filter for nonlinear systems

The linear Kalman filter theory is extended to nonlinear systems in the Extended Kalman Filter (EKF) algorithm.

Assume that the process model is formulated in a time-discrete nonlinear stochastic state-space form as in [15]:

$$\mathbf{x}_k = \mathbf{f}(\mathbf{x}_{k-1}, \boldsymbol{\theta}, \mathbf{u}_{k-1}) + \mathbf{v}_{k-1} \tag{2.95a}$$
$$\mathbf{z}_k = \mathbf{g}(\mathbf{x}_k, \boldsymbol{\theta}, \mathbf{u}_{k-1}) + \mathbf{w}_k \tag{2.95b}$$

where $\mathbf{x}_k$ is the vector of states at time t_k, $\boldsymbol{\theta}$ is the vector of model parameters, $\mathbf{u}_{k-1}$ is the vector of measured process inputs, which are assumed constant over the time interval $[t_{k-1}, t_k]$, $\mathbf{y}_k$ is the vector of output measurements at time t_k, $\mathbf{v}_{k-1}$ and $\mathbf{w}_k$ are sequences of independent random process and measurement noise (white noise) variables respectively, for simplicity assumed to enter the equation linearly. $\mathbf{f}(\mathbf{x}_{k-1}, \boldsymbol{\theta}, \mathbf{u}_{k-1})$ is the nonlinear process model, here the solution to a system of ordinary differential equations (ODEs) between the sampling instants t_{k-1} and t_k. $\mathbf{g}(\mathbf{x}_k, \boldsymbol{\theta}, \mathbf{u}_{k-1})$ is a nonlinear measurement model.

The EKF algorithm consists of two parts: a prediction and an update/ correction part described in [15]. The prediction part is where the a priori state estimate $\hat{\mathbf{x}}(t_{k|k-1}) = \bar{\mathbf{x}}_k$ is determined from (2.95a) by propagating the state estimate $\hat{\mathbf{x}}(t_{k-1|k-1}) = \bar{\mathbf{x}}_{k-1}$ at time t_{k-1} and the mean process noise $\bar{\mathbf{v}}_{k-1}$ through the nonlinear model $\mathbf{f}$. The a priori predicted measurement $\bar{\mathbf{y}}_k$ is then calculated from (2.95b) based on the a priori state estimate $\bar{\mathbf{x}}_k$ and the mean of the measurement noise $\bar{\mathbf{w}}_k$. In the measurement correction part of the EKF algorithm the a posteriori state estimate is calculated as

$$\hat{\mathbf{x}}_k = \bar{\mathbf{x}}_k + \mathbf{K}(k)(\mathbf{y}_k - \bar{\mathbf{y}}_k) \tag{2.96}$$

where $\mathbf{K}(k)$ is the Kalman filter gain calculated from the process noise covariance $\mathbf{V}_{k-1}$, the measurement noise covariance $\mathbf{W}_{k-1}$, the a priori state

covariance estimate $\bar{\mathbf{X}}_{k-1}$ and from the partial derivatives of $\mathbf{f}$ and $\mathbf{g}$ in (2.95) with respect to stochastic variables. The Kalman gain is the particular $\mathbf{K}$ that minimises the mean-square estimation error [25]. The error can be written as $\mathbf{e} = \mathbf{y}_k - \bar{\mathbf{y}}_k$.

The EKF essentially linearises the nonlinear function around the current estimate using Taylor approximation, but it is in general not optimal. Some other shortcoming of the EKF is that it's unable to accurately incorporate physical state constraints. Moreover it can also easily fail due to nonexistence of partial derivatives in certain singular points of the state space [15] which makes it hard to find the Jacobian [26]. The on-line requirement produces a further limitation on what is achievable in state estimation.

The above mentioned problems are mainly solved by implementing a derivative-free filter, for example the Sigma Point Kalman Filter (SPKF). The SPKFs do not linearise the dynamic system for the propagation, but instead propagate a cluster of points centered around the current estimate in order to form improved approximations of the conditional mean and covariance [15].

In this work, a version of the SPKF was used: the divided difference filter of first order, hereafter called DD1. The divided difference filters are based on polynomial approximations of the nonlinear transformations obtained with a multi-dimensional extension of Stirling's interpolation formula. The filter is conceptually much like the EKF. The difference is that matrices of divided differences replace matrix products of Jacobian and Cholesky factors of covariance matrices. The state update is therefore the same as in the EKF [27].

Let the operators δ and μ perform the following operations where h denotes the interval length:

$$\delta f(x) = f\left(x + \frac{h}{2}\right) - f\left(x - \frac{h}{2}\right) \tag{2.97}$$

$$\mu f(x) = \frac{1}{2}\left(f\left(x + \frac{h}{2}\right) + f\left(x - \frac{h}{2}\right)\right) \tag{2.98}$$

Using these operators and Stirling's interpolation formula around the point $\mathbf{x} = \bar{\mathbf{x}}$ we get the following first order simple polynomial approximation:

$$f(x) \approx f(\bar{x}) + f'_{DD}(\bar{x})(x - \bar{x}) \tag{2.99}$$

where

$$f'_{DD}(\bar{x}) = \frac{f(\bar{x} + h) - f(\bar{x} - h)}{2h} \tag{2.100}$$

where h is a selected interval length.

See [27] for a detailed description of the DD1 method.

One of the main problems faced with the Kalman filter, was that it uses measurements for the current time only, making the large time delay of the composition measurement difficult to incorporate. An other on-line estimator that can handle both nonlinear models and time delays is the moving horizon estimator, MHE. The MHE is more powerful than the Kalman filter, but also correspondingly more complicated and has a longer computation time. One of the most evident advantage is the ability to handle varying measurement delays as well as constraints in a consistent manner. The ability to include constraints is also important since a nonlinear mechanistic model by definition includes physically related states and parameters, variables which often can be limited by a lower and upper bound [28].

Here the Kalman filtering was only done off-line, and the datasets shifted to remove the time delay, but for on-line estimation this cannot be done as the measurements will not be available. For an improved future estimation it is recommended to take a look into the MHE algorithm.

A discussion about the two state estimators with a practical approach is given in [15].

Chapter 3

Simulation results

This chapter presents the results of the simulations of the model.

First the model is simulated using process data as inputs without any parameter estimation, the results of this are shown in section 3.1. Then the model is simulated using the same input but with the Kalman filter active, i.e. with parameter estimation, the results of this are shown in section 3.2.1.

For all simulations the following applies:

- Inputs to the model are: the measured flow rate of flue gas out of the plant, the flow rates of recirculated flue gas and secondary air and the measured temperature in the primary chamber, all being process data from Energos. These are plotted for each dataset in Appendix D.
- The flow rate from the primary chamber is continuously calculated internally in the model.
- The temperature of the recirculated flue gas and secondary air is set constant.
- The composition of the secondary air is constant.
- The composition of the recirculated flue gas is the calculated flue gas composition (i.e. the calculated composition out of CV6 plus the ingress air) with a delay of 10 seconds.
- The initial conditions are chosen based on visual inspection and manually fitted to each dataset.

The simulations without estimation of the composition from the primary chamber use a constant composition close to the typical composition given by Energos [4].

In addition, for the simulations with parameter estimation/Kalman filter the following applies:

- The measurements of temperature and composition is used to update the model.
- Some of the components from the primary chamber are estimated.

3.1 Model simulations

3.1.1 Composition

This subsection will present the simulations done without Kalman filter with focus on the composition. The next subsection will deal with the same simulations but with the focus on temperature.

The composition for every control volume is calculated, but only the composition out of the furnace will be plotted as this is the only composition that can be compared to measurement data.

The composition is measured just before the flue gas leaves the plant through the chimney. The calculated composition is the composition that goes out of the furnace, i.e. out of CV6, plus the ingress air.

The measured composition from the process data will here be compared to the calculated composition. Only four out of seven components are actually measured. CH_4 and H_2 are supposed to be zero, CO, CO_2, H_2O and O_2 are measured and nitrogen supposed to be the rest when the four measured components are summed up. This means that the plots showing measured nitrogen from process data is not a real measurement, but found by setting 100% minus the sum of the four measured components.

Each dataset has one plot with an overview of all components, followed by two other plots where the measured value and the calculated value for each composition are showed in subplots.

The x-axis shows time measured in seconds and the y-axis molar percentages of the components.

An observation made for all simulations is that there is a small concentration of the combustible species CH_4 and H_2 in the flue gas. This is explained by looking at the reaction rates. At no time will 100% of the combustible species be combusted. The reactions use at maximum 99% of the combustible species, making it mathematically impossible to remove absolutely everything. The amounts recorded are anyway negligible small.

Another remark to the observation of CH_4 and H_2 in the calculated measurements is that is might as well be realistic to find traces of the original species in the flue gas. Even if there were sufficient amounts of oxygen molecules for complete combustion, we cannot know if absolutely all of the methane molecules found an oxygen molecule to react with.

Dataset 1

Figure 3.1 shows the calculated measured composition and the measured composition from the process data. Figure 3.2 and 3.3 contain the same information as Figure 3.1, but plot each component separately. The solid lines are the measured compositions from the plant and the dashed lines are the calculated measured composition from the model. The calculated values can be seen to follow the measured values with only minor deviations.

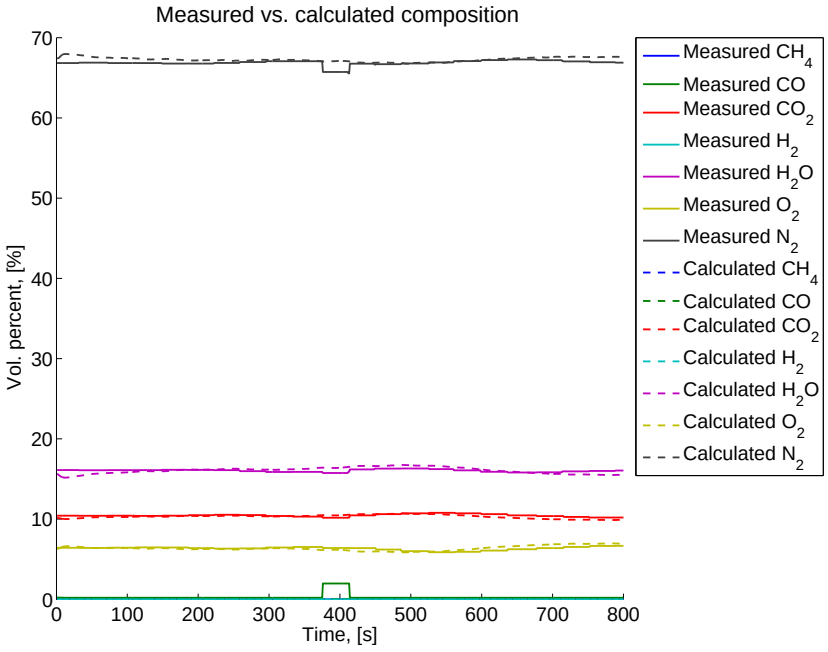

Figure 3.1: Calculated vs. measured components

A sudden increase in the measured CO level out is observed (see second subplot in Figure 3.2). This might be due to a sudden change in the composition, but a more likely explanation is that the CO steadily increases until

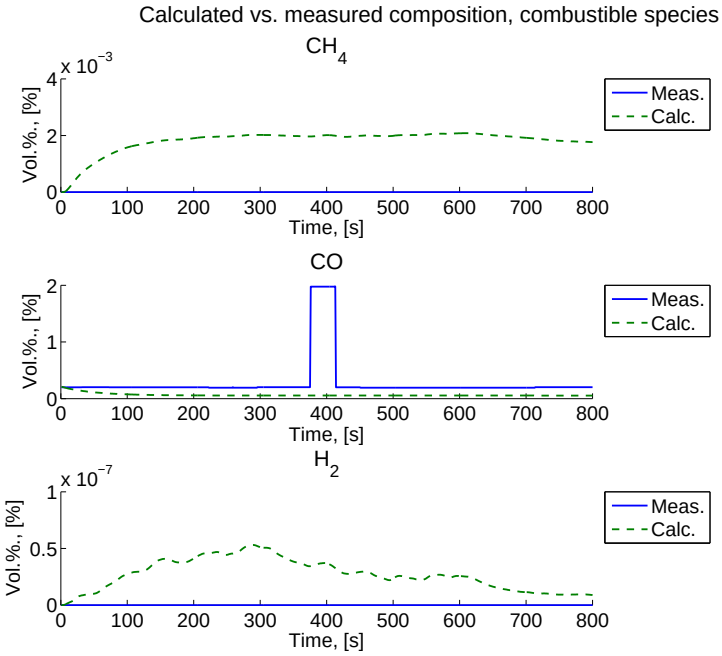

Figure 3.2: Calculated vs. measured components, combustible species

a new measurement is done, alternatively until the sensor's trigger point is reached. This is supported by the increase in temperature observed in CV2 and CV3, see Figure 3.13. The measured *CO* "pulse" might also be due to a measurement error, though the rise in temperature at the same time makes this less plausible.

The same pulse is observed in the measured nitrogen, see fourth subplot in Figure 3.3. This is explained by the fact that nitrogen is not measured, but found as the rest when the four measured components are summed.

It can be seen that the model follows the actual measured composition quite well. The *CO* pulse is the only phenomenon that the model does not follow.

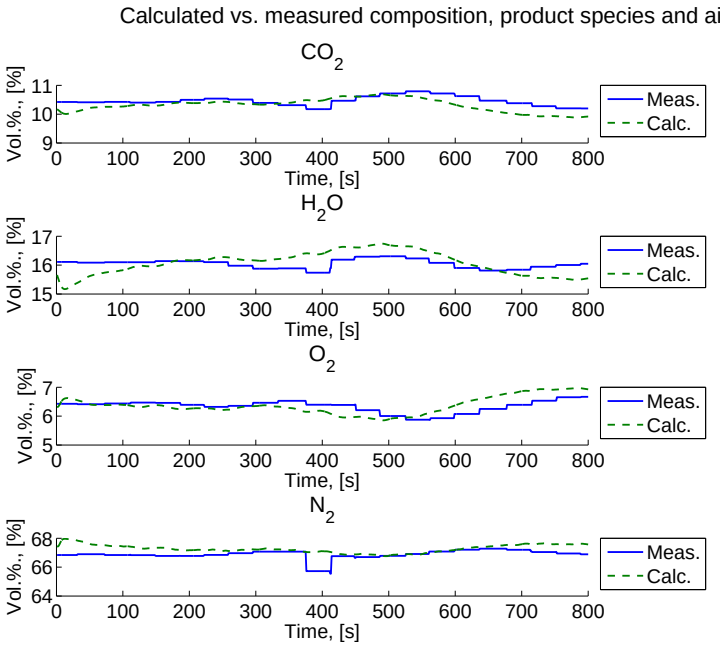

Figure 3.3: Calculated vs. measured components, product species and air

Dataset 2

There are more changes in the measured composistion in this dataset compared to Dataset 1. The model seems to follow this to some extent, but does not manage to follow the measurements exactly. Figure 3.5 and Figure 3.6 show the same as Figure 3.4 but plot each component separately. The solid lines are the measured compositions from the plant and the dashed lines are the calculated measured composition from the model.

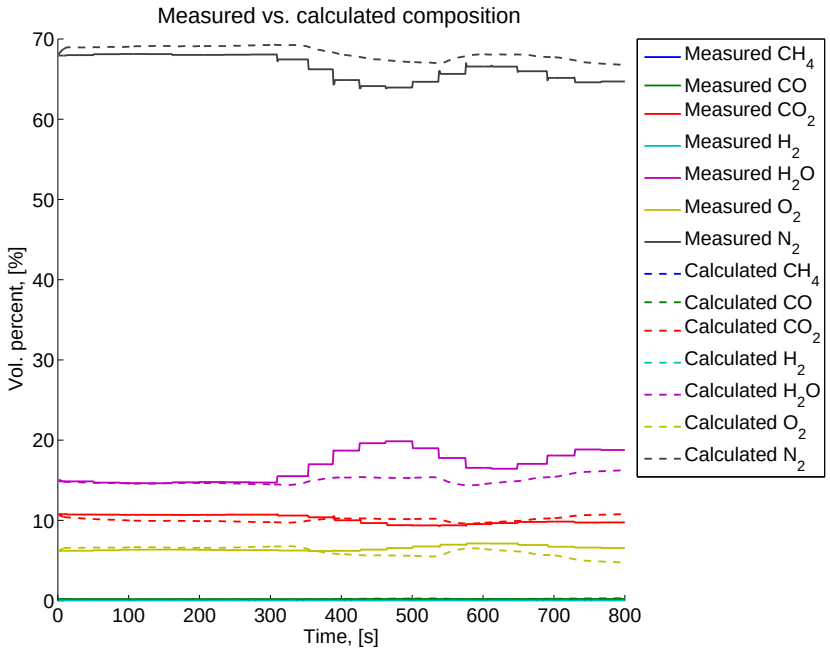

Figure 3.4: Calculated vs. measured components

Approximately between time $t = 350$ and $t = 550$ a small increase is observed for the calculated combustible species of Figure 3.5 and CO_2 and H_2O in Figure 3.6. At the same time the calculated O_2 and N_2 decrease. These observations witness of a model with a periodically higher content of syngas than air. This can be explained by looking at how the model uses the measured flow rates. The model uses the measured flow rates directly for calculations and does not have the natural smoothing effect as the real process. The measured components for the same time period do not exercise the same behaviour.

The measured flow out increases at $t = 300$ and decreases again about 200 seconds later, see Figure D.3. This change is not caused by any of the injection flows (see flow rates of S1/2 and R1/2, also in Figure D.3), meaning that this change is due to changes in the flow rate from the primary chamber. Since the flow rates of the air/recirculated flue gas are approximately constant, the content of syngas becomes relatively higher when the flow rate from the primary chamber is increased.

Note that this explains why the *model* behaves this way, as it depends on simple relations between the flows. The actual furnace has other mechanisms that are not modelled and does thus not behave in exactly the same way.

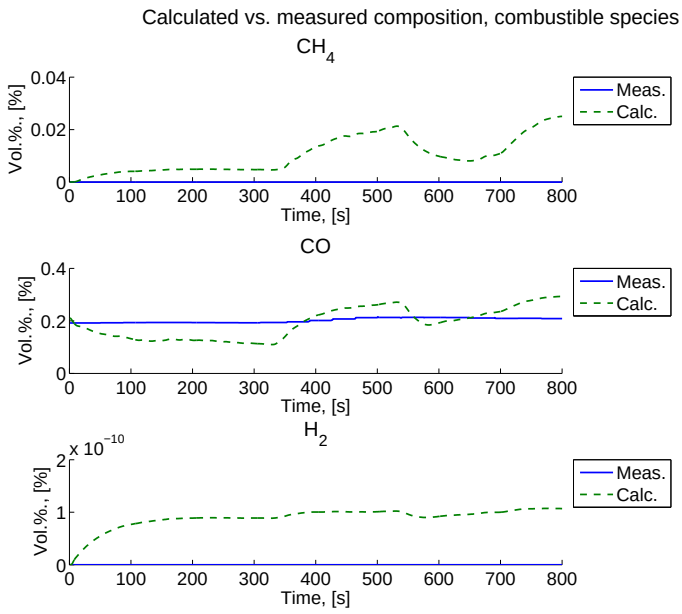

Figure 3.5: Calculated vs. measured components, combustible species

The change in the *measured* composition out of the furnace suggests that there were some changes in the syngas composition as well. As the model is simulated with a constant syngas composition, it is not surprising that the calculated values do not copy the measured ones perfectly.

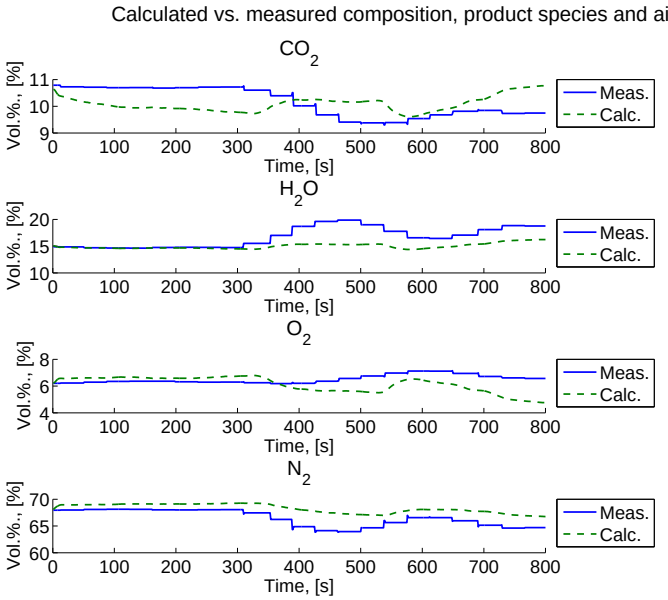

Figure 3.6: Calculated vs. measured components, product species and air

Dataset 3

This dataset shows a very stable period with only minor changes when it comes to the measured composition out of the furnace. The modelled comopsition follows the measured composition quite well. Of course, this is mainly due to a good initialisation.

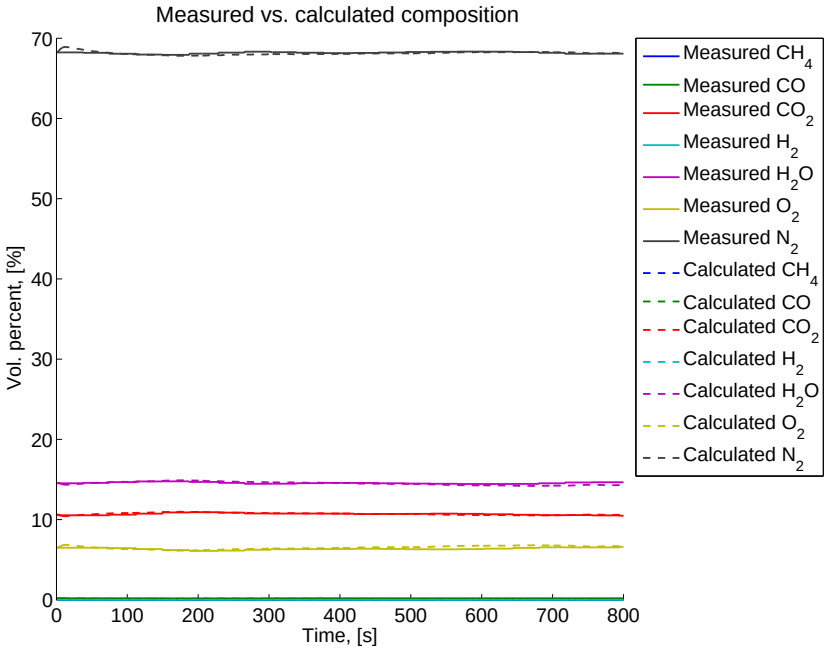

Figure 3.7: Calculated vs. measured components

The zoomed-in version of Figure 3.7, i.e. Figures 3.8 and 3.9, show that there are some small variations in the composition. The calculated composition follows the same trends as the actual composition does.

From the simulation done on this and other similar datasets from stable and calm periods, it was observed that the model has steady-state behaviour similar to that of the real plant, provided a reasonably good initialisation.

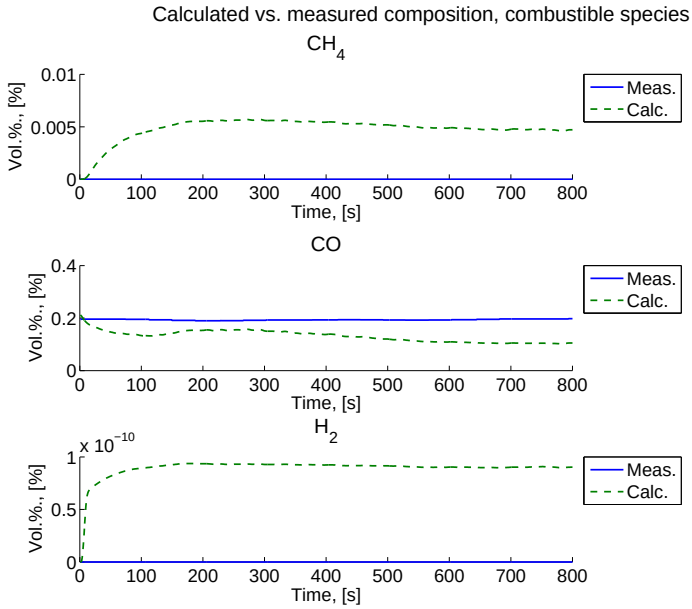

Figure 3.8: Calculated vs. measured components, combustible species

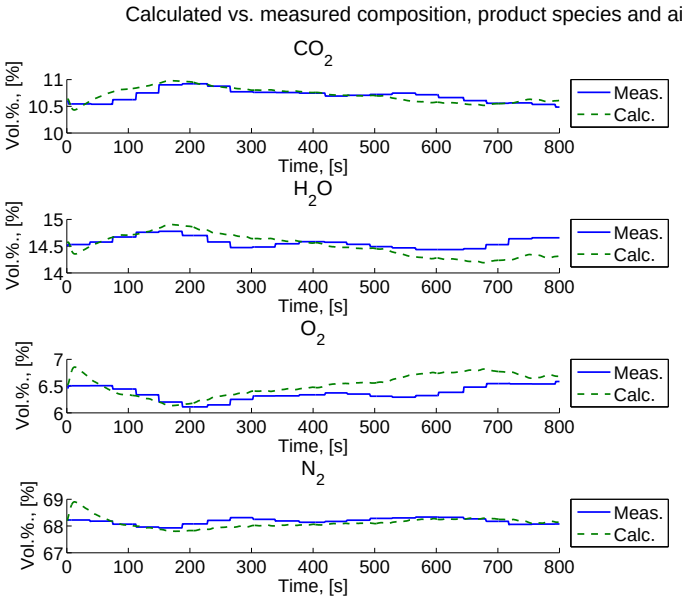

Figure 3.9: Calculated vs. measured components, product species and air

Special case, quenching

This dataset is taken from a period with quenching. The dataset is four times as long as the previous ones with a simulation length of 3500 seconds.

The quenching cannot be detected by looking at the measured composition, but is easily observed on the temperature plot in the next section, see Figure 3.20.

There are no large changes in the composition and the model follows the composition quite well.

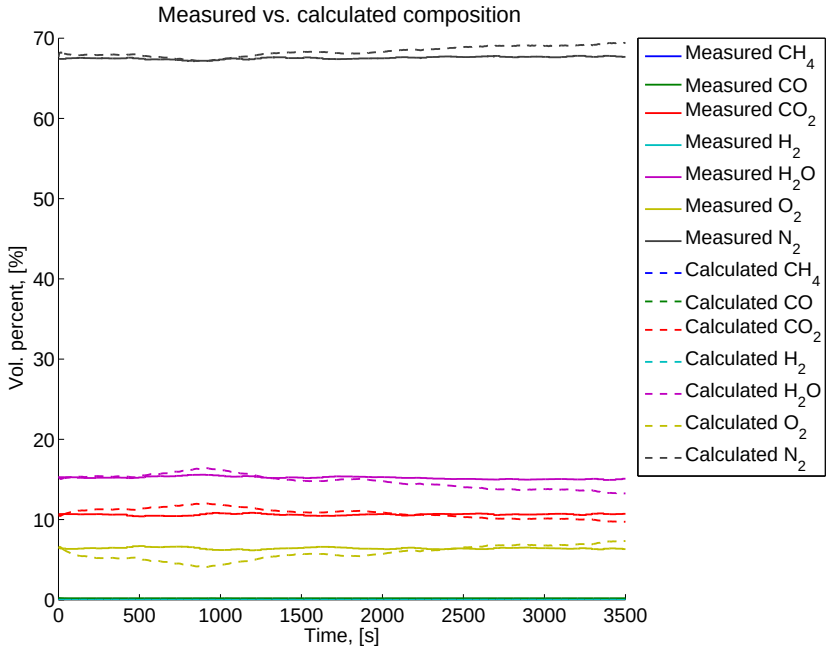

Figure 3.10: Calculated vs. measured components

In Figure 3.12 it can be seen that the calculated oxygen does not follow the measured value very well. This can be explained by looking at the flow of secondary air injected into the furnace, see especially S2 in Figure D.7. The calculated oxygen composition follows the trend of the injection of secondary air and it is surprising that the measured values don't. A likely reason for this is that the composition of the flue gas is smoothed much more during its flow through the plant than what is modelled here. Or alternatively it may suggest that the sensors are insensitive to such changes, though the latter is less likely to be the reason because the sensors are expected to detect changes this big.

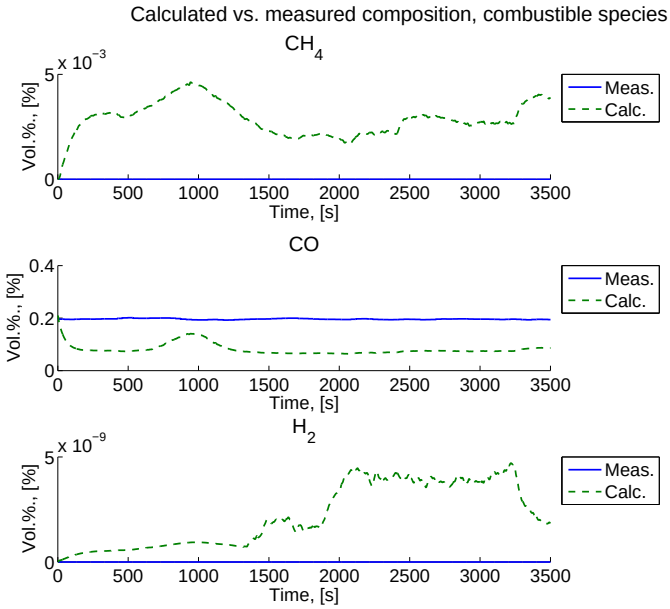

Figure 3.11: Calculated vs. measured components, combustible species

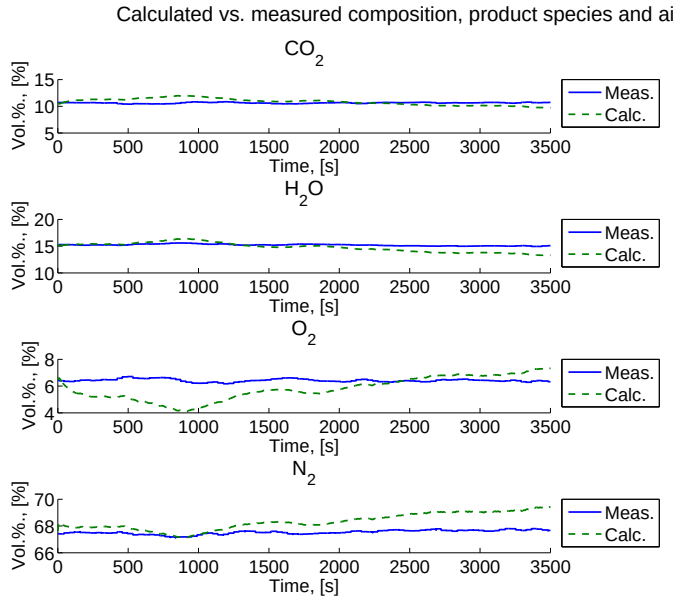

Figure 3.12: Calculated vs. measured components, product species and air

3.1.2 Temperature

The process datasets in this subsection are the same as in the previous subsection but here the focus is on the temperature.

The model has six control volumes and temperatures are calculated for all control volumes. There are only four temperature sensors, these are physically placed in what is modelled to be control volume 2,3,5 and 6, hereafter referred to as CV2, CV3, CV5 and CV6. Only calculated temperatures for CV2, CV3, CV5 and CV6 will be plotted.

The x-axis shows time in seconds and the y-axis shows temperature in degrees Celsius.

There are four different types of temperature that will be plotted in this section: one measured temperature from the process data given by Energos and three calculated temperatures that are states of the model: the temperature of the wall, the (average) temperature of the gas and the temperature of the sensor. The latter is the one that will be compared to the measurements from the real plant.

There are four different datasets that will be presented here. Each of them will have two temperature plots. One plot showing the temperature states of the model and one comparing measured temperature to calculated sensor temperature. A zoom-in of the latter can be found in Appendix E where it is shown in more detail how each calculated temperature compares to the corresponding measured temperature.

Dataset 1

Figure 3.13 shows the three temperature states of the model. The dotted lines represent the wall temperatures, the dashed lines represent the sensor temperatures and the solid lines the gas temperatures. Each control volume has three temperatures plotted in the same colour.

It can in figure 3.13 be seen that the gas temperature changes quite rapidly compared to the almost constant wall temperature. The time constant for temperature changes in the wall is much higher than that of the gas and during the 800 seconds simulated it does not change much. The sensor temperature is also very low-pass filtered and has no rapid changes. The sensor temperature is dependent on the wall temperature as well the gas temperature and can be seen to lie between these two.

The temperatures of the wall, gas and sensor of CV3, CV5 and CV6 are seen to coincide to some extent, whereas there is a quite large gap between

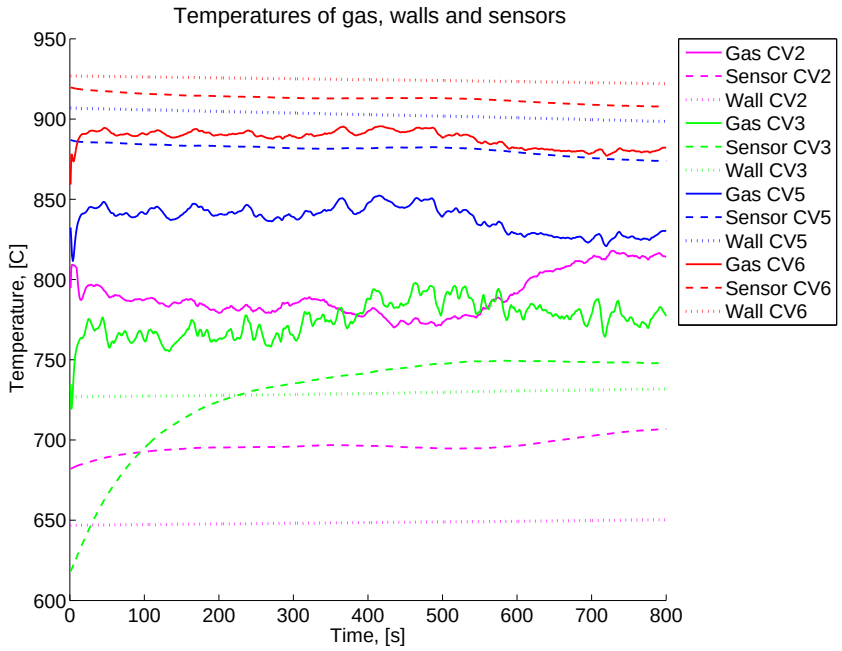

Figure 3.13: Calculated wall temperature, calculated gas temperature and calculated measured gas temperature

the calculated temperature of the wall and gas of CV2.

Figure 3.14 shows the calculated sensor temperature (the same as shown in dashed line in Figure 3.13) plotted with the measured process data.

It can be seen that the predictions follow the temperatures that don't change much, i.e. CV5 and CV6, but cannot cope with the changes in CV2 and CV3. The temperature increase in CV2 and CV3 are thought to be caused by an increase in combustible species from the primary chamber. This assumption is supported by the measured pulse in the CO measurements. The composition from the primary chamber here is set constant and it is thus impossible for the model to follow such changes.

The temperature in CV2 stays quite constant whereas the temperature of CV3 increases. This increase is solely due to the higher initial temperature of the walls of CV3. These initial values are set manually. The wall temperature is crucial for the measured temperature, hence a good initialisation is important. As seen in Figure 3.14 the initial value for the walls of CV2 are chosen as if both wall and gas were in a steady-state from the beginning,

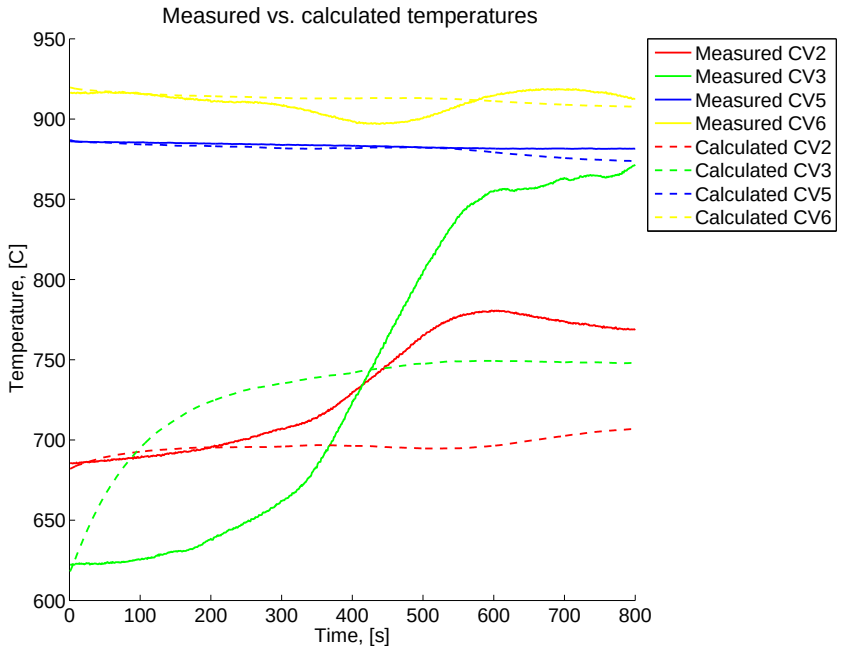

Figure 3.14: Predicted vs. measured temperature

whereas the walls of CV3 have a higher temperature and the gas temperature increases until it reaches a steady-state with the wall.

Dataset 2

The calculated gas temperature in Figure 3.15 can be seen to vary quite a lot. This can be explained by looking at the measured flow rates for the flue gas out of the furnace. See Figure D.3. The variations of the gas temperature are in accordance with the measured flow out of the furnace. The variations seen suggest that the flow rate of syngas from the primary chamber was changing, as no other flow rate changed much.

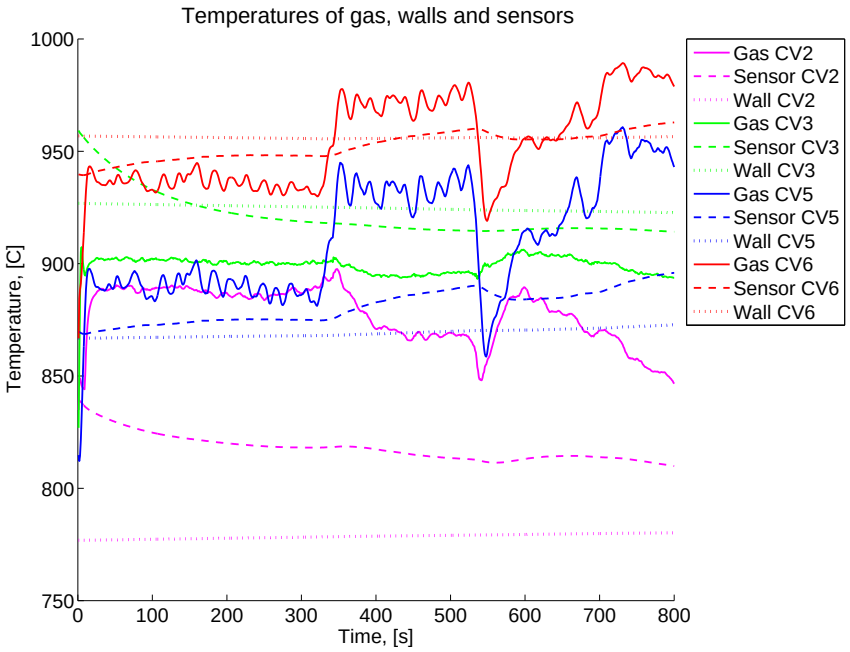

Figure 3.15: Calculated wall temperature, calculated gas temperature and calculated measured gas temperature

Because of slow response of the temperature sensors the variations are not caught in the measurements.

The measured temperatures in Figure 3.16 show that quite a few changes in the tempearture is detected, but these changes are not observed from the model.

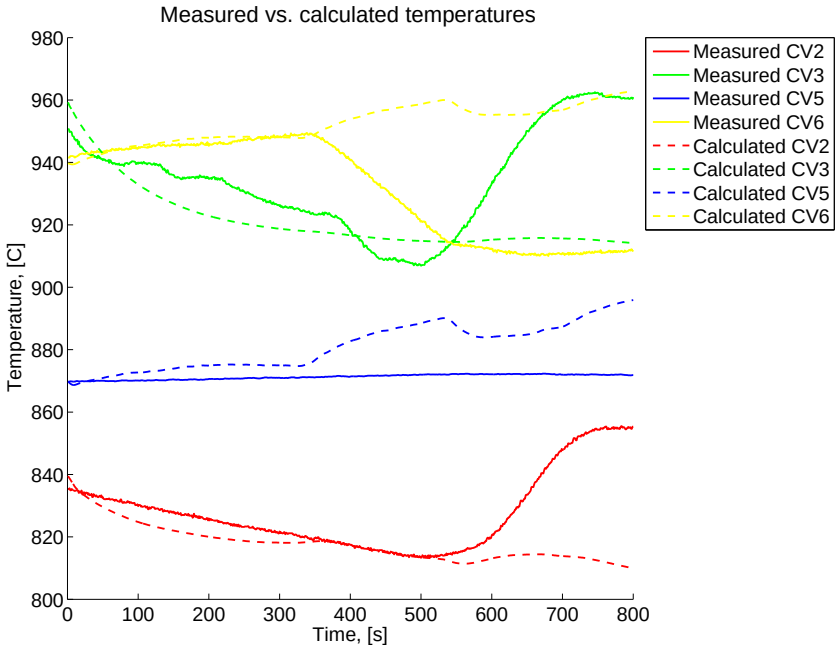

Figure 3.16: Predicted vs. measured temperature

Dataset 3

This dataset is from a very calm and stable period, and it can be seen that the measured temperatures do not vary much. There are only minor deviations between the measured temperatures and the calculated measured temperatures as seen in Figure 3.18.

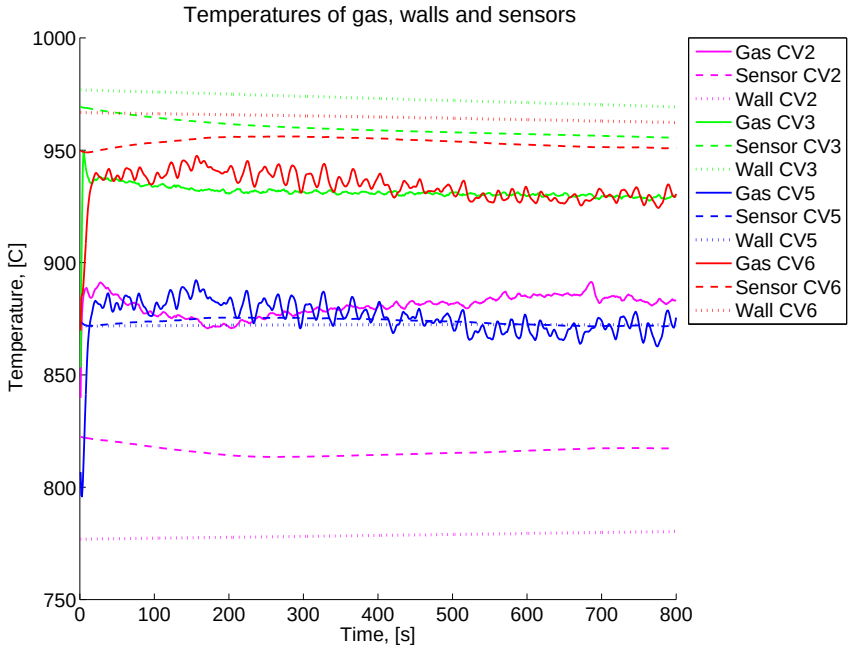

Figure 3.17: Calculated wall temperature, calculated gas temperature and calculated measured gas temperature

However, the calculated gas temperature for CV2 is quite a lot higher than the wall temperature of CV2 as seen in Figure 3.17 showing that the model is not in steady-state even if the measured values may indicate that the plant is in a steady-state.

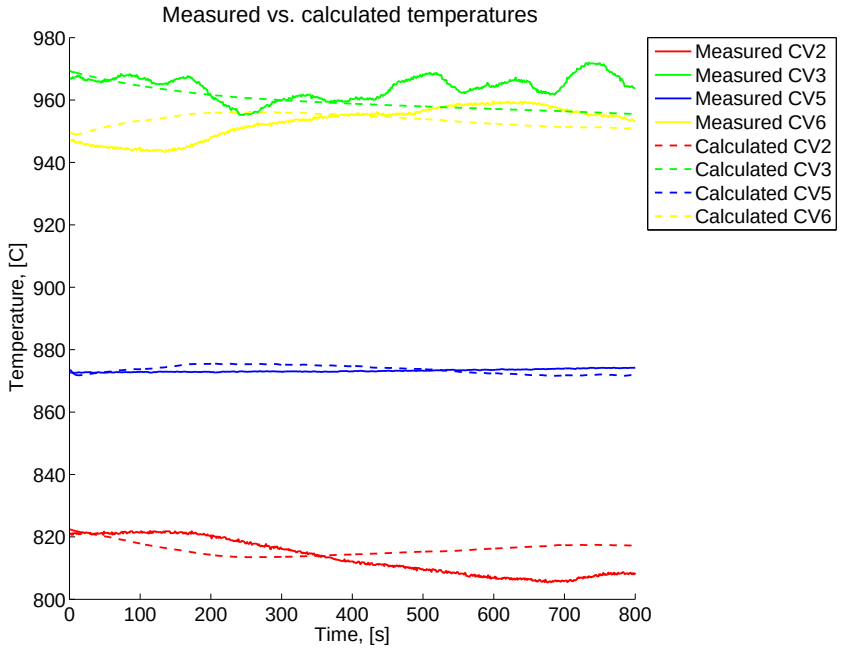

Figure 3.18: Predicted vs. measured temperature

Special case, quenching

This dataset differs from the other datasets in that it shows the quenching problem. To capture the entire quenching the dataset is four times longer than the others, nearly an hour is recorded and simulated.

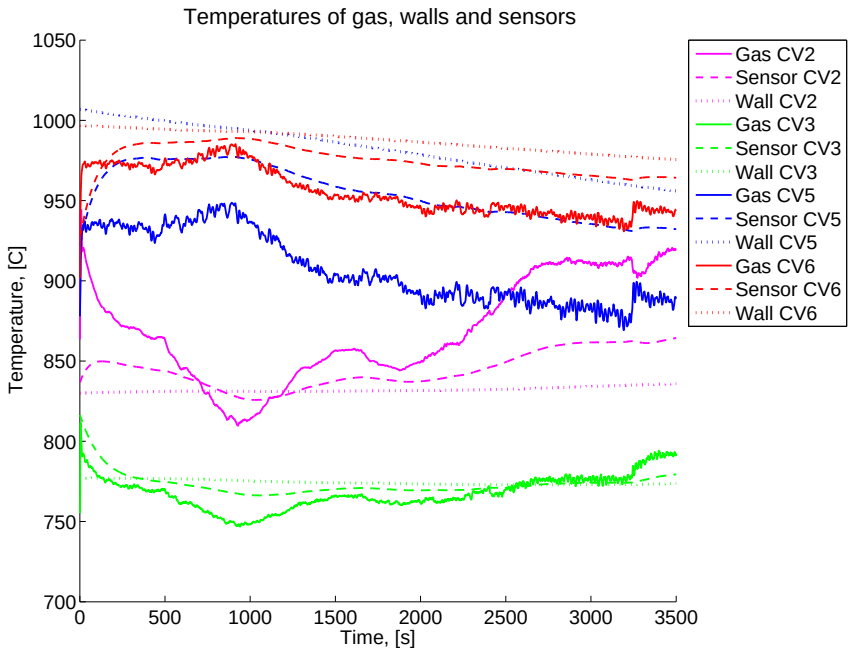

Figure 3.19: Calculated wall temperature, calculated gas temperature and calculated measured gas temperature

The measured gas temperatures of CV2 and CV3 in figure 3.20 can be seen to drop down around time $t = 1500$. The calculated measured temperatures do not follow this temperature fall and do in fact show very little sign of a quenching taking place.

However, the calculated gas temperature of Figure 3.19 shows that the gas temperature of CV2 and CV3 decreases, but not nearly as much as the measured temperature.

Figure 3.20 shows how the quenching is strongest in the beginning of the chamber. The measured temperature of CV2 drops down approximately 150 degrees at $t = 1500$. The temperature of CV3 drops by about 100 degrees. The cold front even reaches the final parts of the camber and the measured temperature of CV5 can be seen to decrease by about 40 degrees. This

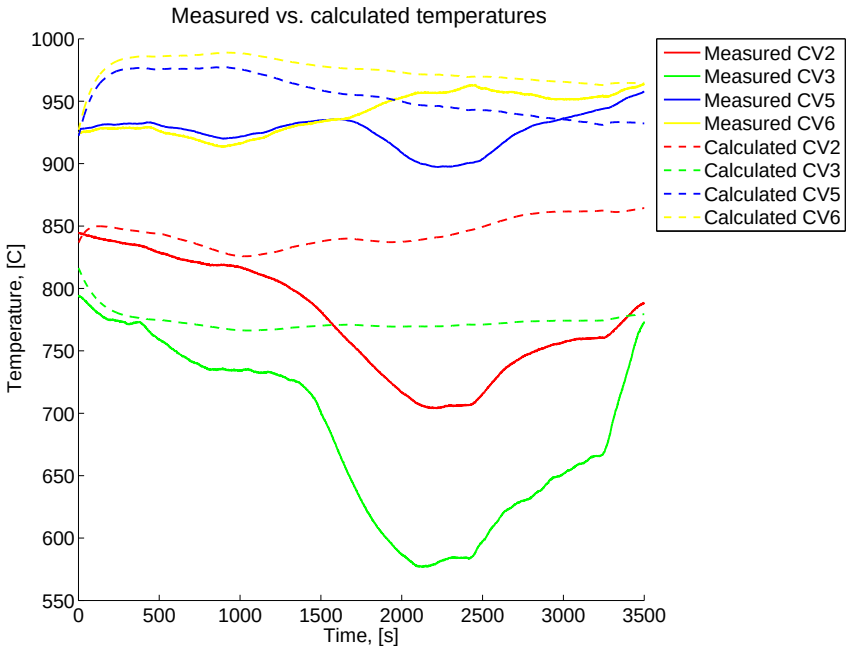

Figure 3.20: Predicted vs. measured temperature

decrease is not very significant and suggests that the gas has been heated by walls during the flow through the chamber. The temperature of CV6 can be seen to increase a little bit at the same time, indicating that the combustion finally started again.

The calculated temperatures (dashed lines of figure 3.20) do not exercise this behaviour.

Recirculation as temperature control

The main reason behind the injection of recirculated flue gas is to control the temperature. The injection of recirculated flue gas has a cooling effect. It is here verified that the model has this behaviour.

Figure 3.21 shows the two recirculated flue gas flows, R1 and R2, and the calculated temperature in CV1 (where R1 is injected) and CV3 (where R2 is injected), T1 denotes temperature in CV1 and T3 denotes temperature in CV3.

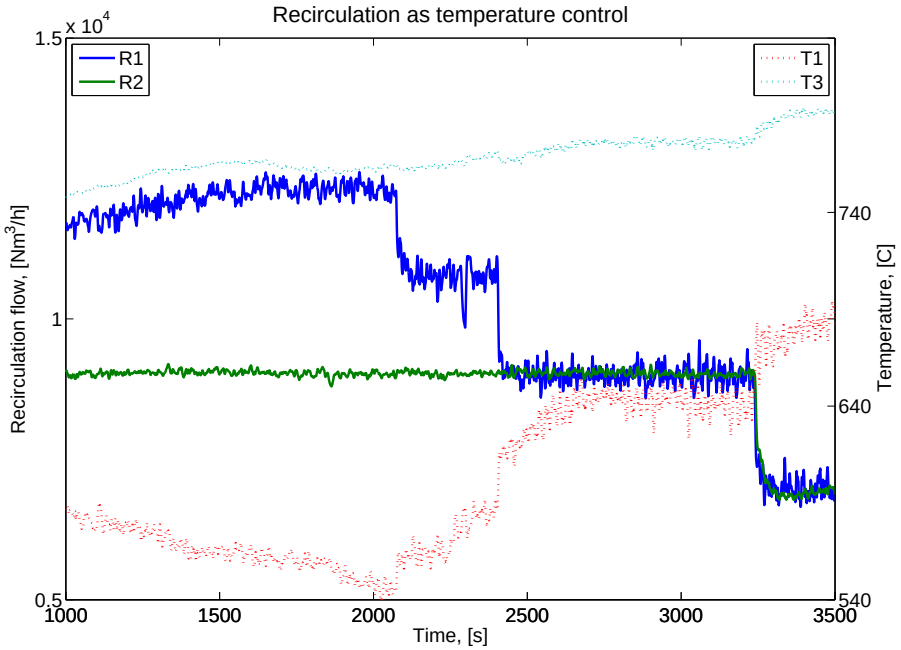

Figure 3.21: How recirculation affects temperature

In Figure 3.21 it can be seen how the temperatures are influenced by the recirculated flue gas flow. First the temperatures are slightly decreasing or not changed until the recirculation is reduced around time $t = 2000$ and they stop decreasing. Then the recirculation is decreased further around $t = 2400$ and the temperature starts increasing again. When both recirculation flows are reduced around $t = 3200$ all temperatures rise with even steeper gradient.

T1 can be seen to change a lot more than T3. This is because the flow rate of recirculated flue gas is the same into both control volumes, but the volume of CV1 is much smaller than CV3, and the effect of the recirculation

becomes relatively much larger. There is less thermal mass in the walls of CV1 to damp the temperature change.

3.2 Parameter estimation

3.2.1 Kalman filter

The main motivation behind introducing the Kalman filter was to be able to continuously estimate the composition of the syngas from the primary chamber. This was done with a positive result as will be showed in this section. All datasets and simulations are the same as in the previous section, but this time the Kalman filter is active. Both temperatures and compositions will be shown as the previous sections, and the final plot for each dataset is the estimated composition from the primary chamber.

Only four components are being estimated, i.e. CH_4, CO, CO_2 and H_2O. O_2 is supposed to be zero and H_2 is a constant fraction of CH_4. Only the estimated components will be plotted. The estimates are within reasonable limits.

When the Kalman filter is being used some uncertainty, i.e. measurement noise, has to be added to each measurement. This weighting is done explicitly in ModelFit by adding noise manually to the measurements with the same units as the measurement itself. Choosing the uncertainties implies an evaluation of the sensors in order to find the most reliable, i.e. to find the sensor assumed to be less biased for the given dataset. The other measurements will be weighted with more measurement noise and the Kalman filter tries to update the model in order to follow the measurement with the least measurement noise.

The choice of measurement noise to be added to each measurement is also a way of indicating what is considered to be the most reliable; the measurements or the model. Little measurement noise implies that the measurements are assumed to be more reliable than the model and vice versa.

Dataset 1

Dataset 1 in this section is the same as Dataset 1 in the previous section. The difference between the two simulations is that this time the simulations are run with the Kalman filter. The estimated syngas composition from the primary chamber is shown in Figure 3.24.

In Figure 3.14 from the previous section it was seen that the calculated temperature of CV2 and CV3 did not follow the measured temperature rise. When using the Kalman filter it can in Figure 3.23 be seen that the temperature of CV2 and CV3 increase a little more. This happens because the concentration of methane is increased, see Figure 3.24. The temperatures of CV5 and CV6 do not change much, but the temperatures of CV2 and CV3 increases, just as measured.

Nevertheless, the increased accuracy on the calculated temperature comes at the expense of composition accuracy. Figure 3.22 illustrates how the calculated composition deviates more from the measured composition than when the model was simulated without the Kalman filter, see Figure 3.1.

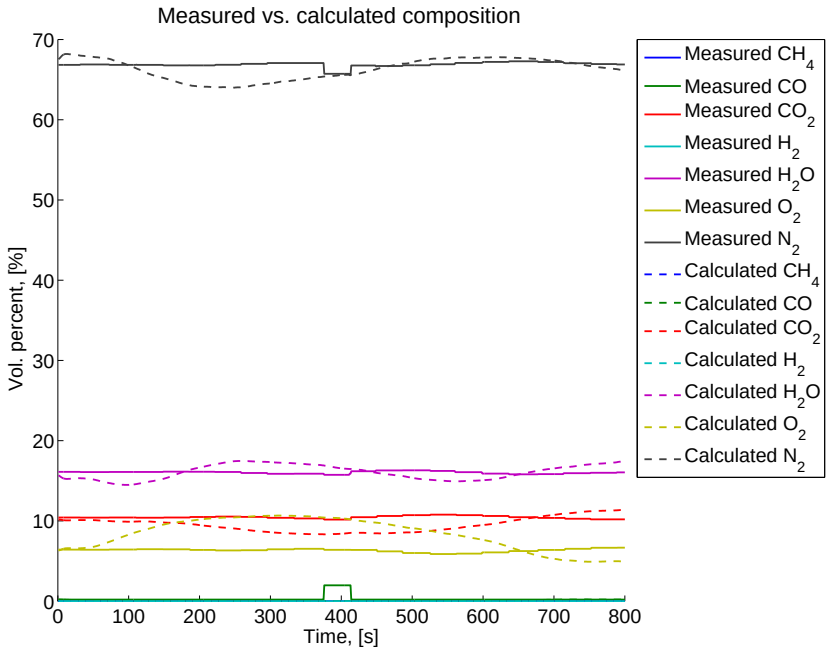

Figure 3.22: Calculated vs. measured components

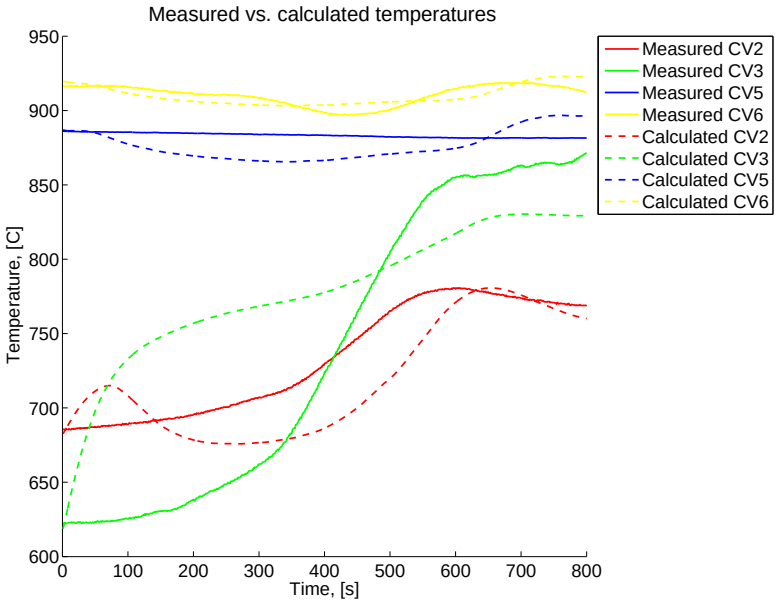

Figure 3.23: Predicted vs. measured temperature

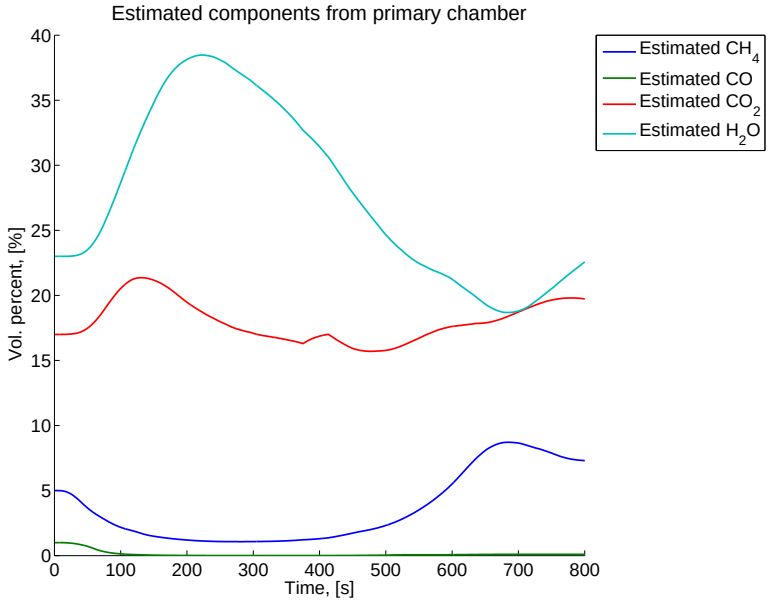

Figure 3.24: Estimated components from the primary chamber

Dataset 2

From the simulations done on this dataset it can be seen that the model follows the compositions better than without the Kalman filter, see Figure 3.4 compared to Figure 3.25. The calculated composition, showed by dashed lines, exhibits changes in the same direction and with approximately the same magnitude as the measured composition.

The temperatures are not significantly better predicted as seen in Figure 3.26.

The estimated syngas components can be seen in Figure 3.27.

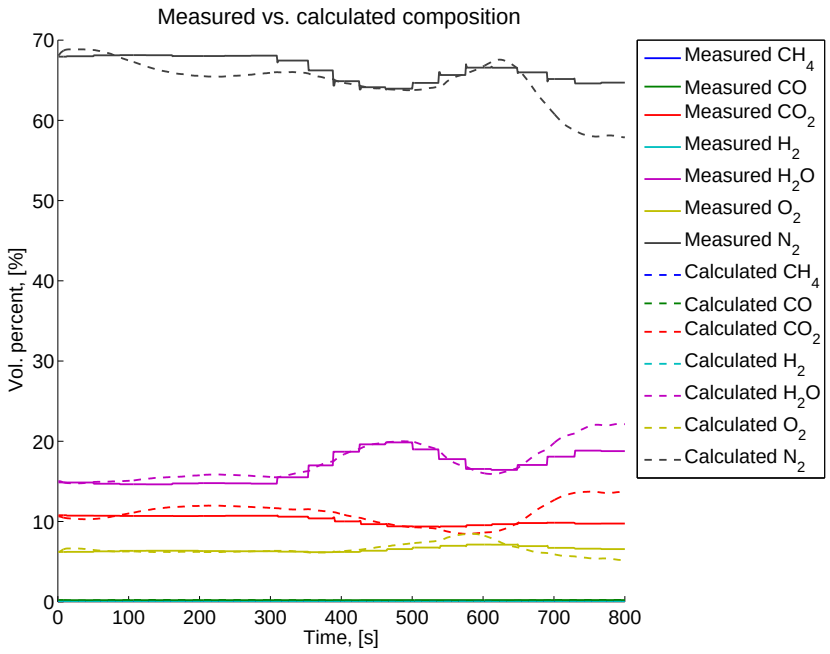

Figure 3.25: Calculated vs. measured components

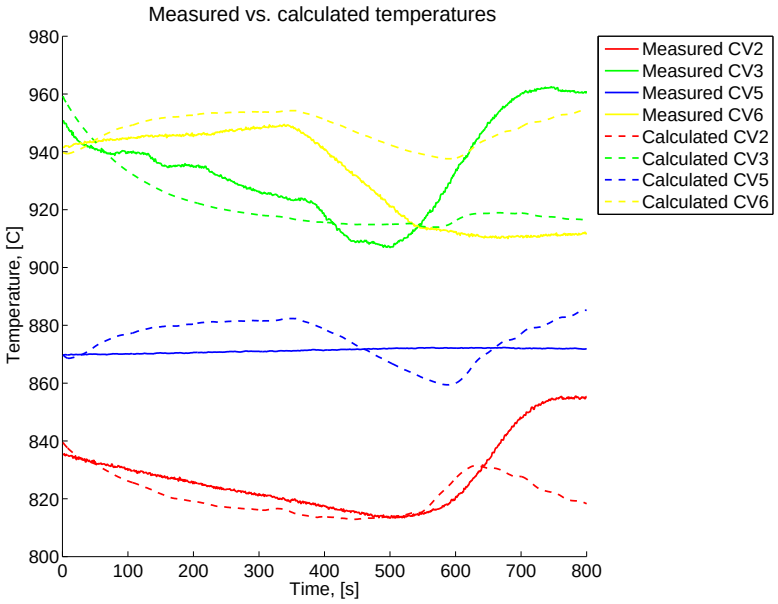

Figure 3.26: Predicted vs. measured temperature

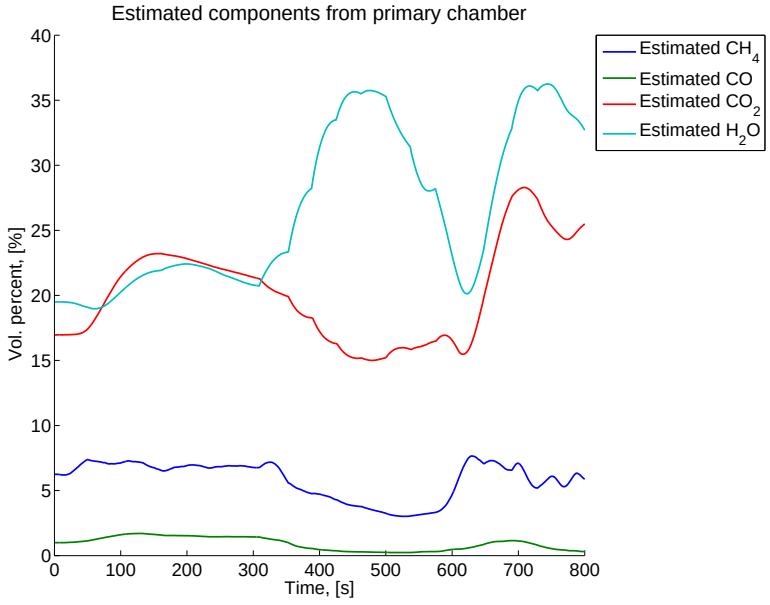

Figure 3.27: Estimated components from the primary chamber

Dataset 3

As seen in the previous section (simulations without Kalman filter), this dataset is from a very calm period. Both the composition and temperature follow measured values quite well and the use of the Kalman filter will probably not yield any improvements in this case. The overall result from simulating this dataset with the Kalman filter was not considerably better than running it without the Kalman filter.

Therefore we will show an example of what happens when the Kalman filter is tuned a little bit too hard to illustrate the importance of sensible measurement noise weighting. If we are too strict on how much deviation from the measurements we can allow the Kalman filter will update the parameters too aggressively. A small deviation will lead to a massive correction of a parameter. This correction may be so big that we get a deviation the other way and the Kalman filter has to correct even more. This leads to instability, as can be seen in all figures plotted for this dataset, it's especially easily detected the increasing oscillations on the estimated methane shown in Figure 3.30. Some beginning oscillations can also be observed on the calculated temperature of CV5 in Figure 3.29. If the simulations were allowed to run for a longer time the system would probably go off to infinity.

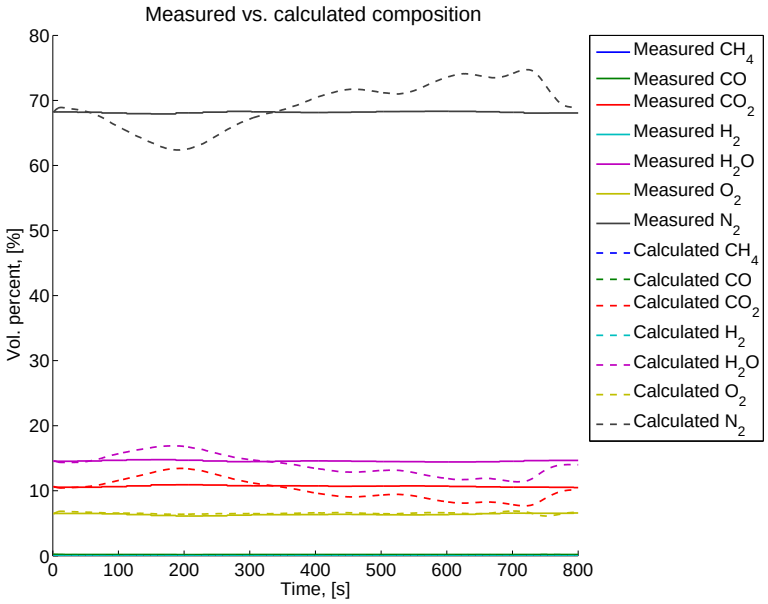

Figure 3.28: Calculated vs. measured components

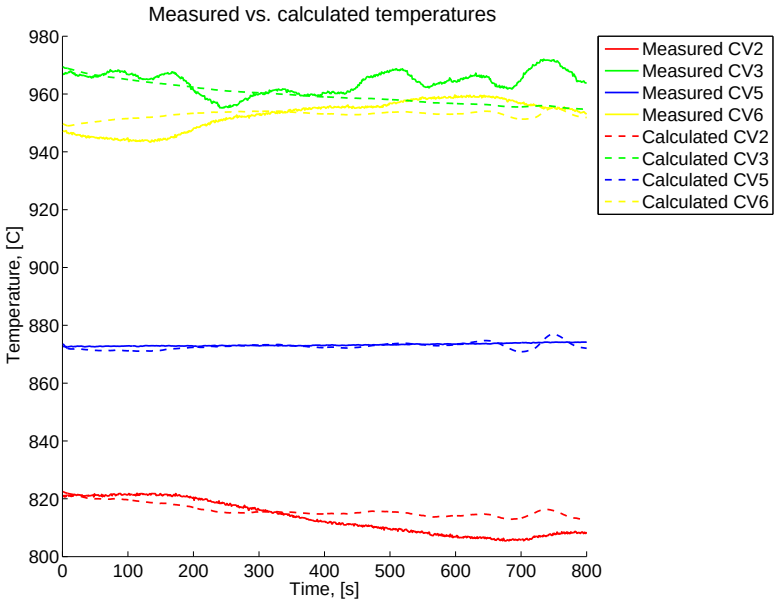

Figure 3.29: Predicted vs. measured temperature

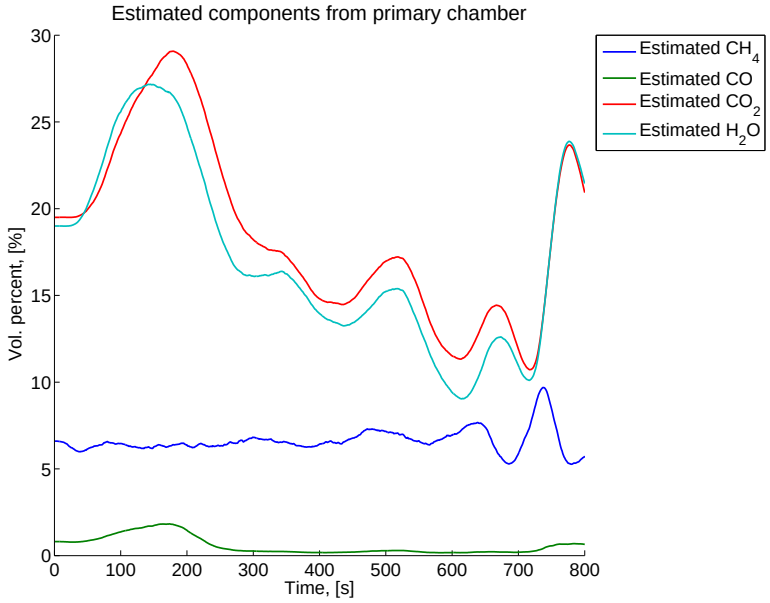

Figure 3.30: Estimated components from the primary chamber

Special case, quenching

This dataset is longer than the other datasets because more time was needed to record the quenching. By inspecting the measured temperature in Figure 3.32 it can be seen that the temperature of CV2 and CV3 fall drastically around time t=1500s. Without Kalman filter, this decrease in temperature was not at all followed by the model. The calculated temperature exercise a similar response to the measured temperature when the Kalman filter is active.

The accuracy of the compositions were not considered important for this case, as it was more interesting to see if the model managed to simulate a quenching. The weights for measurement noise were set to 50% for the composition, i.e. the estimated compositions may have an additive deviation of 50%. The measurement error has the same unit as the measurement itself, so 50% uncertainty means that 50% can be added to/subtracted from the calculated composition, i.e. not a multiplication of 0.5 with the calculated composition.

In practice this means that the composition will not be assigned any importance and the focus of the Kalman filter is on the temperature. In addition, the highest uncertainty was added to the temperature of CV5 and CV6, so these two temperatures were not followed in any great detail either. It was tried to restrict the measurement noise on these two temperatures as well, but that resulted in instabilities.

When the temperature stars decreasing around t=1500 the Kalman filter responds by decreasing the amount of combustible species in the syngas from the primary chamber. The combustible species are reduced by the Kalman filter until they reach zero, see Figure 3.33. The results in an increase of the oxygen content as there will be no combustion consuming it, see Figure 3.31. The result of the reduction of CH_4 and CO leads to a decrease in temperature of CV2 and CV3 as seen in Figure 3.32. The temperatures of CV5 and CV6 are also decreased as there is no more combustion releasing heat.

The quenching phenomenon is described in section 2.2.3 and the reason for it is not a sudden stop in the combustible species coming from the primary chamber. This statement is supported by the measured temperatures in CV5 and CV6 and the measured oxygen level out of the furnace. The measured temperature in CV5 and CV6 do not decrease. Neither is the oxygen level increasing. These two observations give evidence of that the combustion is continued further out in the secondary chamber.

Nevertheless, reducing the content of combustible species is the only ac-

tion the Kalman filter can take in order to reduce the temperature. Given the current model setup the action taken is rather intuitive.

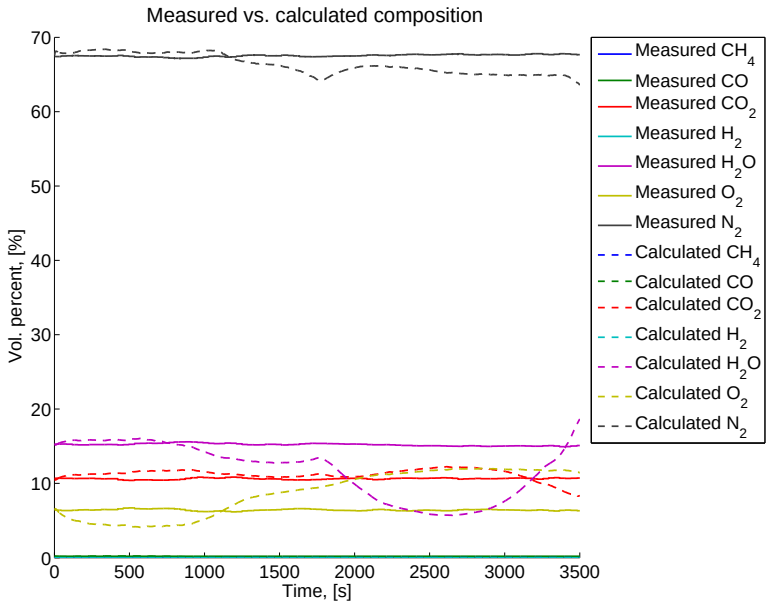

Figure 3.31: Calculated vs. measured components

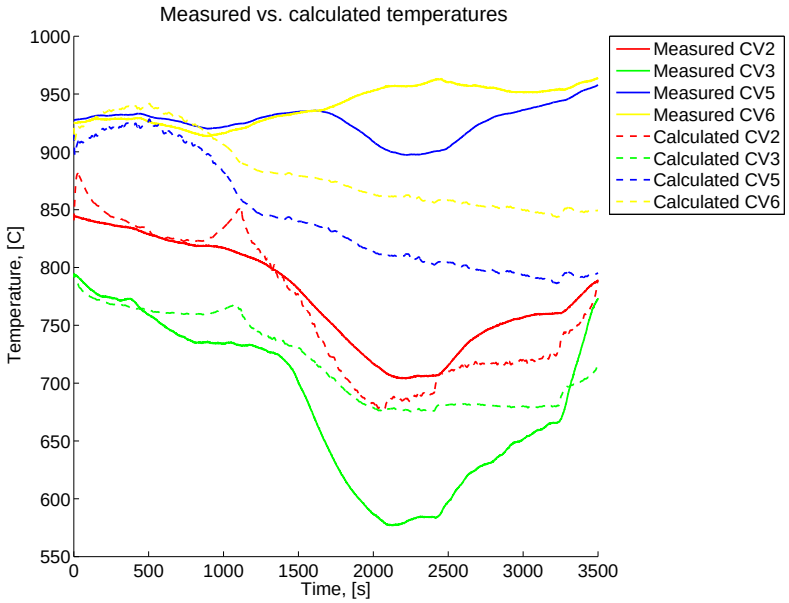

Figure 3.32: Predicted vs. measured temperature

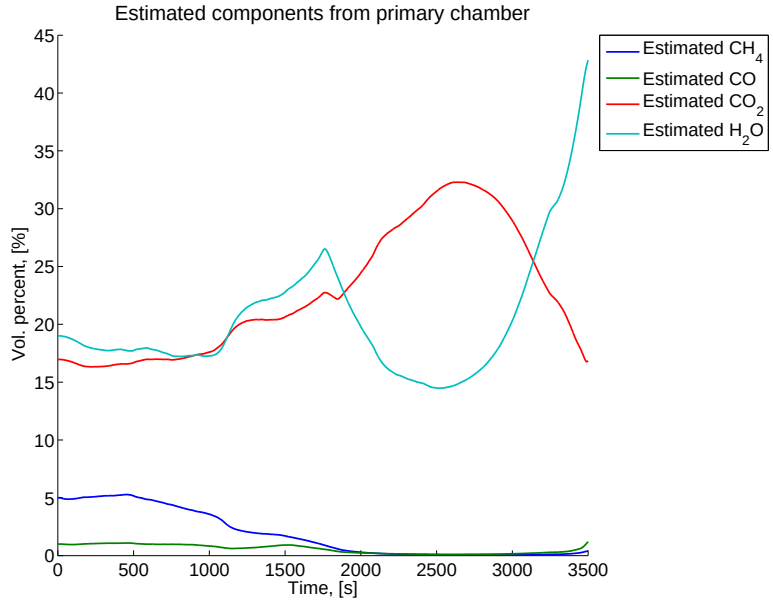

Figure 3.33: Estimated components from the primary chamber

3.2.2 Estimation of constant parameters

This subsection shows the result of the constant parameter estimation. The estimations are done off-line based on a least squares algorithm and have nothing to do with the Kalman filter.

The constant parameters chosen were shown in table 2.1. Initial values were also tried estimated, though not always with a good result. The algorithm minimises the error over all samples and if the calculated values do not match the measured values very well, the algorithm might try to choose initial values quite far from the starting point just to try to compensate for this. Therefore most of the initial values were set manually.

To estimated the constant parameters process data from calm and stable periods was used, i.e. periods where the measured states (temperature and composition) had quite constant values. Table 3.1 shows the result after parameter estimation based on five datasets from Energos. The process data is from the Hafslund plant, each with a duration of 15 minutes.

Parameter	Description	Init. value	Est. value
$U_{htc_{wall}}$	Heat transfer coefficient, walls	9 W m^{-2} K^{-1}	17
θ_{sensor}	Constant for temperature sensors	1 s^{-1}	0.01
θ_1	Constant for eq. (2.38)	1	1.01

Table 3.1: Constant parameters, estimation result

The almost negligible change of parameter θ_1 from 1 to 1.01 may indicate that the model was insensitive for changes in this parameter and hence a better estimate could not be found.

The initial value of 1 chosen for θ_{sensor} was a random starting point as none of the physical properties of the temperature sensors were known.

After the parameter estimation, the calculated response was still not the same as the measured response, the Kalman filter was introduced to estimate the states and slowly varying parameters, i.e. the composition from the primary chamber.

Chapter 4

Discussion

This chapter will discuss the results of this project. The understanding of the process leading to the model is the main result. Simulation results will be used to illuminate the result.

4.1 Model development

A mathematical model is in itself a simplification of reality, and in this work a coarse model was derived. The model had to be accurate yet simple enough to be used for control purposes. It is very difficult to combine these two as real process reaction rates give a very stiff mathematical problem.

In general terms, this work's simulations showed that it is possible to get a model that has similar behaviour to the real plant, but only for steady-state periods with appropriate initialisation. Transient cases were reproduces to some extent, giving larger deviations for those showing a steep process operation.

4.1.1 Some physical assumptions

Dividing the entire furnace into 6 CSTRs is a very coarse simplification and is done solely for simplifying the calculations. The CSTR approach calculates an average of every variable such as temperature, pressure and concentration in each control volume. Assuming that the temperature and concentration is the same in the entire control volume is not realistic, but sufficient for calculations. No local variations, for example hot spots, will be modelled even if the injection of cool air and recirculated flue gas will lead to local differences in both concentration and temperature. This will affect the way we compare simulation results with measurement and can cause some of the

differences observed.

A way of increasing the discretisation of the model to enable more detailed simulations is to increase the number of control volumes. Several extra control volumes would make it possible to model more local temperature differences. This could involve a more distributed injection of the recirculated flue gas/secondary air. The control volumes could be chosen such that the injections happen over several control volumes.

On the other hand, the calculations of the composition would probably not benefit from a more detailed modelling because the composition is only measured at the end of the process, and it is thus not possible to validate the simulated composition elsewhere. The current sensors exist in limited numbers, and since measurements are needed for validation, there is an upper boundary on how many states that would be beneficial for this model.

An increase in the number of control volumes will lead to a more complex model as each extra control volume implies seven extra state in the model. As the local variations are generally not picked up by the sensors it could be argued that it is unnecessary to introduce more control volumes and thus increase the complexity of the model in order to model the small variations.

Assuming constant pressure is a reasonable simplification because the small pressure differences (typically around 20 Pa) are not large enough to affect the calculations significantly. This also means that the calculation of C_p based on the assumption of constant pressure will only yield minor deviations.

The material balance and flow calculations assume that no mass is lost. Some ashes will accumulate and deposit on the walls and sensors, though it should be noted that the violation of the mass balance because of this is negligible. The practicalities around the removal of the deposits stuck on the walls and especially on the sensors disturbing the temperature measurements is by far the greatest concern in this matter.

It was assumed that the gas is ideal. This introduces a source of errors to, for example, the flow conversions. The measured flows have the unit [Nm^3 h^{-1}] and this is converted to [mol s^{-1}] by assuming that the gas is ideal, i.e. that each mole, no matter what components it consists of, occupies the same amount of space.

Only three reactions are taken into account. These three are believed to represent the main dynamics when it comes to heat production and composition, but there are a lot more reactions taking place in the real process. More

measurements would benefit the model and validation of more reactions. The kinetics will be further discussed in section 4.2.4.

4.2 Temperature

The gas temperature is probably the most important aspect of this model as it affects the course of the process, the final composition and the wall. The complexity of the phenomena describing the different parts of the heat transfers in the real process combined with the uncertainties related to temperature measurement makes the temperature hard to model with a high level of accuracy.

4.2.1 Temperature measurements

The temperature sensor modelling is of great importance as the predicted measured temperature will be used to validate the model against measurement data.

The boundary conditions, i.e. the wall temperature, are not known, neither is the temperature profile of the gas. The turbulence makes it hard to assume a geometric shape/equation for the temperature profile, however a simple solution, i.e. a parabola temperature profile, was selected. The reason for choosing for the parabola was that this is how the temperature in an homogeneous conductive medium with exothermic reactions typically is modelled. Here the temperature will be highest in the middle of the pipe as the walls represent a heat drain. This temperature distribution in the chamber was shown to be better than having no temperature profile at all. See e.g. Figure 3.13 where the sensor temperature lies between the gas and the wall temperature.

The parameters of the parabola equation were found based on many assumptions, and are not possible to accurately determine with the limited information available, as mentioned in section 2.2.8.

Temperature sensors act as low-pass filters, smoothing out any rapid changes that may occur. See e.g. Figure 3.19 where the sensor temperature is a smoothed version of the gas temperature.

This is mainly due to the physics of the temperature sensor; the sensor itself has to change temperature before it displays a temperature change. Even then it is the temperature of the sensor that will be displayed, not the actual temperature of the gas, though they should be close. The material of

the sensor determines the heat capacity and heat transfer between the gas and the sensor. It is desired that the thermal mass, and thus the thermal inertia, of the sensor is as small as possible.

Deposits on the sensors can slow down the temperature change detection and bias the measurements. This is a problem currently observed in the plant where the sensors have been observed to be surrounded by several hundreds kilograms of dust. Compared to the small mass of the sensors this is a large increase of mass that will change the properties significantly. The build-up of dust around the sensor will happen over time. It is generally not known at what stage of this build-up process the sensor is in. This should be taken into account when selecting the weights on the measurements for the Kalman filter. The temperature sensor displaying the most accurate temperature is likely to change. It is not known how much (if any) built-up material there was on the sensors at the time the datasets used for simulation were recorded.

The location of the sensor is important. The sensor will display the temperature of the gas around it. An unfortunate placement of a sensor could be just where the secondary air is injected as the temperature there is assumed to be (locally) quite low, i.e. not representative for the average temperature.

The geometric design of the furnace is not known in much detail. The placement of the sensors is assumed to be such that the measured temperature represents the mean temperature for that control volume. This is a best case assumption, the sensor might have a more unfortunate placement e.g. in the warmest or coldest part of the control volume.

As seen from the simulations the predicted temperatures are not exactly the same as the measured temperatures. Even when the state estimator is used, it is only possible to follow one temperature closely, not all temperatures. This could indicate that the sensors may be assumed to represent a different temperature than what they actually do. The flow velocity past the sensor could also affect the measurement.

The influence from the walls is quite significant both in the real plant and in the model. The sensors (if clean and under normal operation) are likely to show a temperature somewhere between the temperature of the wall and that of the gas. This temperature influence is incorporated in the model and can be observed in the simulations, see section 3.1.

If the sensors are operating normally they are likely to show a temperature somehow close to the real temperature of the gas. The predicted temperature from the model is more dependent on correct initialisation and also of the composition of the syngas, and cannot be assumed correct without further

analysis.

4.2.2 Wall temperature

An average temperature for the walls is calculated based on values for mass, area, heat capacity and heat transfer coefficient proposed by Energos [9]. The different layers/materials of the wall are not known.

It is expected to have a temperature profile through the wall with decreasing temperature because of the heat loss to the surroundings. There are no measurements of the wall temperature, neither on the inside nor the outside of the furnace. The lack of measurements makes it hard to determine the temperature profile of the wall.

The wall has a very high heat capacity/thermal mass, hence the temperature changes very slowly. It can be observed to have a small damping effect on the gas temperature, though as mentioned it is more important for the predicted measured values.

During simulations it was seen that the initial condition of the wall determined whether the predicted measured gas temperature and the measured temperature matched. In practice this means that since we are free to choose any initial condition of the wall it can be chosen for each dataset to make the predictions coincide with the measurements. However, not realistic wall temperatures were never chosen.

Because the wall temperature is not known, it is not possible to validate/invalidate the chosen temperature of the wall without simulating longer periods than 15 minutes. During simulations as short as 15 minutes, the wall temperature does not behave as a state, but rather as a tuning parameter. Fouling sensors can be confused as clean sensors biased by wrong wall temperature.

4.2.3 Recirculation for temperature control

The main function of the recirculated flue gas is to avoid too high temperatures. The recirculated flue gas has a temperature of about 150° C and a relatively low oxygen content, hence it will have an overall cooling effect.

In the process data it can be seen how the reduction of recirculated flue gas injections stops the quenching, see Figure 3.21. It can in this figure be seen that the model produces results with the same trends as the measured temperature; the modelled temperature also increases when the recirculation is reduced.

4.2.4 Kinetics

The simplified kinetics are less realistic than the original kinetic. As this model is for control purposes, not simulation purposes, the simulation time has to be lower than real time. An example of the low runtime obtained: the model simulated a period of 800 seconds in less than 5 seconds.

The simplified kinetics give realistic results in the sense that the combustible species disappear and the product species increase. The simulations show that given the right initial conditions the predicted compositions are quite similar to the measured ones. When the typical syngas composition given by Energos is used, the output lies close to the typical flue gas composition, implying that the reactions modelled are capturing the main changes. The kinetic reactions are too quick to be measured, it can thus be argued that there is little gain in modelling a phenomenon that cannot be measured as that means that we will not be able to verify it.

The simplified kinetics are not dependent of the temperature and are based on steady-state operation. At steady-state there is no quenching, this means that the model will not capture the quenching problem, which is actually one of the most interesting phenomena to model. It should be investigated how a realistic temperature dependence can be incorporated without making the system very stiff.

Let's consider the fire triangle of section 2.2.3 again. The lambda parameter is easy to understand; we need to have sufficient amounts of oxygen for the combustion to happen. It appeared that the "third dimension" of the triangle, the heat, is of greater importance than first believed. The work conducted in this project contributed to a better understanding of the importance of the temperature for the kinetics. The fact that the current model cannot simulate quenching and hence failed to follow the real process data illuminated the importance of a temperature dependent kinetics.

4.3 Composition

The composition out is measured as vol% and the calculated values are mol%. As we assume ideal gas, one mole has the same volume no matter which component it is, hence mol% = vol% for the same pressure and temperature.

The concentrations of methane and hydrogen out of the furnace are not measured because they are assumed to be zero. The simulations show that

there is a small amount of methane left when the flue gas leaves the furnace. Even if it is quite certain that all methane and hydrogen is fully combusted, it is quite realistic to find traces of the combustible species in the flue gas.

4.3.1 Composition measurements

The composition sensors have a sampling time ranging from some seconds to nearly a minute. This means that rapid changes may not be displayed in the measurements.

The composition analysis of CO, CO_2, H_2O and O_2 takes one to two minutes and the flow of the gas also takes a few seconds. These delays are not known in any more detail and a total delay of 100 seconds is used to shift the composition measurements for simulations. These delays could be further investigated and better approximated if more precision is needed. Since the residence time in the chamber is some seconds only, measurement delays of minutes may play an important role. However, by inspecting the measurements, see e.g. Figure 3.20 it seems that the time constant is in minutes. This may indicate that some seconds difference in the measurements will not affect the calculations significantly.

4.3.2 Recirculation composition

The recirculated flue gas composition is the same as predicted measured out, i.e. the same as the composition out of the furnace, but with added ingress air. Alternatively, the measured composition out could have been used as the recirculation composition. Because of the mentioned time delay and the uncertainty of the measurements this was not done.

4.4 Parameter estimation

Inserting parameters for estimation in the equations is a way of correcting for modelling errors. When a parameter is being estimated, the estimated value is not necessarily more correct than the initial one, but it accounts for modelling errors and fit parameters to make calculated values as close to measured values as possible. The error is thus absorbed by the parameter and might not be more physically correct.

Some process noise was added to the parameters. The noise was introduced additively and a bigger effort could be spent on noise modelling. Better

knowledge of the process could suggest alternative ways the noise enters the process.

4.4.1 Constant parameters

The first estimations of the heat transfer coefficient for heat transfer with walls, U_{htc}, led to a great increase of its value. The sensors act as low-pass filters, the wall does also have a damping effect of the temperature change of the gas, it absorbs some fluctuation. A higher heat transfer coefficient means that the walls will absorb more heat so that the heat changes of the gas happens more slowly.

The estimation of initial values did not give satisfactory results. The likely explanation for this is that the rest of the dataset was too inaccurate, so the algorithm tried to compensate for this by adjusting the initial condition until the mean error was smaller. The initial values were therefore found manually for each dataset.

The constant parameter estimation can be done off-line as the parameters are always constant and can be found off-line first and then used in later datasets. It is here possible to remove degree of freedom by setting one constant equal for several datasets.

4.4.2 Kalman filtering

The main focus of the Kalman filter in this work was to estimate the composition of the syngas from the primary chamber. If this is not estimated and updated it has to be set to a constant value. Setting the primary chamber composition constant is not a very realistic choice. It is known that this composition changes quite a lot over time, and simulations show that the temperature is very dependent on the composition.

The syngas composition is calculated based on measurements, both temperature and composition measurements. Using temperature measurements for composition estimation can give misleading results as there are many uncertainties related to the temperature as already discussed. Many different compositions could give the same temperature and it is not possible to distinguish the different components.

The composition measurement at the end of the process does not carry enough information alone to estimate the syngas composition. Therefore the temperature measurements have to be used as well as they give an indication

about how much combustible species that entered.

When the composition from the primary chamber is unknown, it is the same as sending only noise through the model. It is unreasonable to expect the model to predict future process behaviour under such conditions. It is absolutely necessary to estimate the primary chamber composition.

Deriving a model for the primary chamber is a highly recommended way of getting more knowledge and give basis for a better starting point for the syngas estimates. This is though expected to be a hard task as the primary chamber is assumed to be even more complex than the secondary chamber.

The Kalman filter cannot be tuned too hard. Measurement time delays, modelling errors, unforeseen disturbances etc. are uncertainties that suggest that the parameters should not be updated too aggressively. Simulations showed that the model might become unstable if the Kalman filter is tuned too hard.

If one parameter is tuned to improve one prediction, this parameter is likely to affect another measurement as well. The composition of the syngas from the primary chamber affects all temperatures in the secondary chamber as well as the final composition out of the chamber.

Because the model is a simplification of the real process, it will not follow the behaviour of the real plant perfectly. Before activating the Kalman filter it has to be considered which measurement that is most important and let the Kalman filter update the model to follow this. The measurement chosen as most important may vary between the different datasets.

The Kalman filter manages to fit the predictions to only one measurement quite well. The choice of which measurement to follow is a trade-off between following several measurements more or less accurate, or following one measurement very well and accepting large deviations in the other measurements. Better temperature predictions typically come at the sacrifice of composition accuracy.

In general the simulations seemed to be better with Kalman than without, even if the action taken by the Kalman filter not necessarily are very realistic. Based on the current model structure and the parameters chosen for update, there are only a few parameters the Kalman filter can alter to change the result of the simulation. An example of this is the estimated methane content in the syngas. When simulating the model with the dataset that includes the quenching, it was observed that the Kalman filter reduced the amount of combustible species in order to reduce the temperature. An actual decrease in the concentration of combustible species is not probable,

but reducing the concentration is the Kalman filter's only choice to decrease temperature. The action performed by the Kalman filter is the most intuitive considering what parameters it is allowed to change for the given model.

As suggested by Cybernetica [23] a model of the primary chamber is almost inevitable as the two chambers are strongly coupled. Some preliminary knowledge of the composition of the waste entering the primary chamber would then be needed, and this would possible lead to a need for more instrumentation. A model of the primary chamber would give a much better basis for the syngas estimation.

4.5 Off-line predictions and on-line MPC

The Kalman filter regards measured values as now-values. For off-line predictions done in this work, this is not a problem, because the process data can be shifted so that all measurements correspond in time. However, if used in an on-line estimation, the large time delay on the composition measurements would represent a problem. The Moving Horizon Estimator, MHE, is better suited for this type of predictions, as it can better incorporate this time delay. The MHE was not considered further here, but is an idea that can be of future interest if the estimation is supposed to be done on-line.

For the MPC to take sensible action reasonably good model predictions are needed. Because of unmodelled disturbances and model errors a constant model update is necessary. This implies that the process should be well equipped with sensors. Measurement errors and inaccurate instrumentation makes it hard to get an optimal model, which also makes it hard to get optimal control. This illustrates the importance of investing in good and robust instrumentation and to carefully consider how it should be installed for the lowest chance of any biasing from the surroundings.

All problems mentioned in this thesis also represent problems for PID controllers. A model based controller is not expected to be any worse than PID. With this limited model the MPC might not be better than PID in transient periods, but could possibly optimise the steady-state operation.

4.6 Software

Some stiff ODE solvers exist, but this problem is so stiff that it would probably have a runtime far too large for any control application anyway. Though these solvers could be used for simulation purposes, if that was desired. Cybernetica has a stiff solver, but far from good enough for this problem. There are also some free software available on the internet, but many of these methods require the Jacobian matrix for the model, and for this highly non-linear model the Jacobian is cumbersome to find.

Finding valid simplifications of the model seems like the most straight forward and easiest option when the model is to be used for control purposes. If the model was to be used for simulation purposes only a stiff solver could be considered.

Chapter 5

Conclusions and further work

The purpose of this project was to investigate the possibilities and challenges related to the implementation of model based control of the secondary combustion chamber in an energy from waste plant. This thesis contributes with a study of different aspects on the matter, some seem promising and others still need further investigation. The main contribution of the work was the derivation of a mathematical model for the system and fitting the model to process data from the plant.

5.1 Conclusions

A first principles model was derived based on mass and energy balances. The kinetics of the system turned out to be so stiff that any real-time simulation was impossible. The approach chosen to avoid this problem was to remove all dynamics involved in the reactions and assume pseudo instantaneous combustion. The simplified kinetics had no incorporated temperature dependence, and could hence not model quenching.

A potential MPC will need to have a lower temperature constraint to prevent the temperature from decreasing too much. This will also avoid the need for a model that handles quenching as it presumable would not occur with such a constraint.

Process data provided by the plant operator was used as input to the simulation. The model showed similar behaviour to that of the real plant in steady-state periods. Assuming constant composition of the syngas from the primary chamber, the model did not follow the plant behaviour in transient periods. The composition of the syngas strongly affects the temperature.

A first order divided difference Kalman filter was used to estimate the composition of the syngas from the primary chamber. This improved the predictions to some extent, but the very limited model put a natural restriction on the possible achievements of the Kalman filter. The syngas composition is only steady-state observable if some assumptions are made and many uncertainties make it a hard task to estimate the composition. Both temperature and composition measurements out of the furnace are used for the syngas estimation.

For realistic simulations and for the implementation of MPC the composition from the primary chamber is needed. A possible improvement is to model the primary chamber at the same time as the two chambers are strongly coupled. Reasonably good predictions are needed for the MPC to take sensible action. The current model cannot be used for MPC before it is improved further to follow the process in transient periods.

The walls are assumed to influence the measured temperatures by damping temperature changes. The temperature sensors are in themselves a low-pass filter for the temperature measurements. This implies that no rapid and/or local changes will be measured. The calculated gas temperature is also made quite significantly influenced by the calculated wall temperature through the sensor model.

The model derived had a low enough run-time to be used for on-line control purposes. The previous version of the model with the original reaction kinetics could have been used for off-line simulations, but not for control purposes, so the simplifications done during this work were necessary to get a model with a lower-than-real-time run time.

Many of the simplifications done depend on a steady-state assumption, and some more realistic features should be incorporated for the model to have a better response in transient periods. The model is not valid for start-up or other periods where the conditions are far from those of normal operation.

5.2 Further work

Before MPC can be implemented the model could benefit from some improvements.

Some possible modifications could include:

- A model for the recirculation of the flue gas.

- A way of simulating the quenching without increasing the stiffness of the model too much.
- Increase the number of control volumes. Distribute the injection of recirculated flue gas.
- Include a slowly time varying clogging parameter to use for the temperature sensors. They are more or less clogged during operation, and this affects the measurements significantly.
- Incorporate back the water-gas-shift equation, as the equilibrium of this may affect the temperature.
- Investigate the wall properties further for a better estimate of the temperature profile in the wall in order to get at better understanding of the heat loss to the surroundings.
- Investigate the temperature profile of the gas for a more correct representation than the parabola equation.
- Derive a better model for the sensors. Both the composition and the temperature sensors now follow a linear model. There may be some nonlinearities describing the relation better and more knowledge about the sensors would reveal this.
- Investigate the composition measurement in more detail to get a more accurate time delay incorporated in the model.
- Implements MHE instead of Kalman filter to better handle the measurement delay.

Additional work that could be interesting to study at a second stage:

- Derive a model for the primary chamber as the two chambers are strongly coupled.

It is still early to determine if all these changes are necessary for the implementation of MPC.

Appendix A

Process description

Figure A.1 shows an overview of an Energos energy from waste plant. The numbers shown on the figure referring to the different parts of the process correspond to the numbers mentioned in this section.

Before entering the plant the waste is shredded and metals are removed with a magnet (no. 3). The fuel (shredded waste) will then be fed in a controlled fashion to the primary combustion chamber (no. 4) along with primary combustion air. In the primary chamber the fuel enters the grate and is gradually heated up. The heating is mainly caused by radiation from the warm gas and walls of the furnace, but also with thermal oil of approx. 180°C circulating in the grate. The thermal oil has two functions; cooling the last part of the grate and warming the first part. When the water has evaporated the temperature of the waste increases further because oxygen reacts with some of the hydrocarbons in a gasification process. Gasification is a process that converts heavier hydrocarbons to lighter ones in a combustion-like process with an amount of oxygen too low for normal combustion, hence the waste is being gasified instead of burned. It is not desirable that the gas is combusted in the primary chamber and the supply of primary air is therefore kept at an under-stoichiometric level[1].

Pyrolysis occurs at high temperatures in the absence of oxygen when higher-order hydrocarbons are cracked into smaller gaseous species such as CH_4, CO and H_2 [1]. The primary air supply is only sufficient for the first gasification to happen and the small amount of oxygen is consumed in the gasification process, but the released heat keeps the pyrolysis going.

The resulting gas mixture is called synthesis gas or simply syngas, and is

[1]Stoichiometry is the relation between the quantities of substances that take part in a reaction or form a compound. Here this is the ratio between oxygen and combustible species, and when the process is under-stoichiometric there are insufficient amounts of oxygen for complete combustion.

the fuel gas that enters the secondary combustion chamber for high temperature oxidation. The syngas typically consists mostly of methane, hydrogen, water, carbon monoxide, carbon dioxide and nitrogen, but the composition will vary depending on the composition of the waste and the temperature and residence time in the primary chamber. The bottom ash removed at the end of the primary chamber is typically 20% of the feed.

Combustion occurs in the secondary chamber where the syngas is mixed with air (secondary air) and recirculated flue gas from downstream the bag house filter (no. 8). There is one inlet for the syngas from the primary chamber, two inlets for secondary combustion air, two inlets for recirculated flue gas and one outlet. The combustion air is taken from the hall where the waste bunker is, keeping the hall slightly below atmospheric pressure to reduce the risk of foul odors escaping the plant. The combustion chambers are shown in more detail in figure A.2. There are two auxiliary oil burners that are used for start-up of the plant. One of them is also automatically turned on if the temperature in the furnace gets too low. Today the combustion process is controlled by a number of PID controllers.

The hot flue gas is sent to a boiler that generates steam which is utilised in a steam turbine where electricity is produced and/or some of the heat is used for district heating (no. 6,13,14). The flue gas is cleaned (no. 7-9) before it is let out to the atmosphere. The plant is equipped with a dry flue-gas cleaning system consisting of a bag-house filter, a storage silo for lime and activated carbon and a filter dust silo Lime and activated carbon is injected at the inlet of the bag house filter. The lime absorbs acid components in the flue-gas, while activated carbon adsorbs dioxin, TOC (total organic carbon) and heavy metals [2].

A flue gas fan (no. 10) is placed at the chimney and the flow through the fan is controlled by a PID controller with the objective of keeping the pressure in the primary chamber constant at 90 Pa below atmospheric pressure.

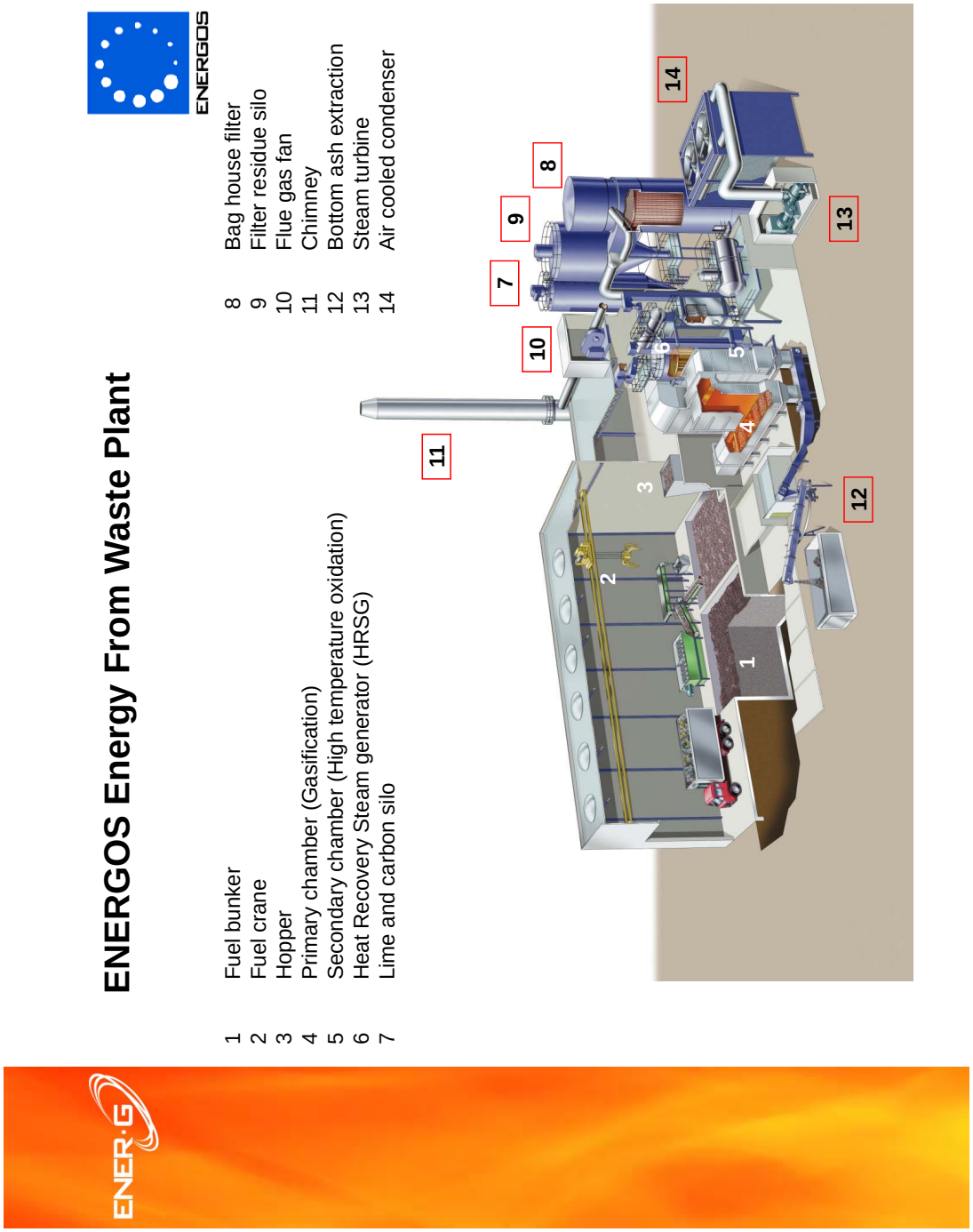

Figure A.1: Plant overview, used with permission from Energos.

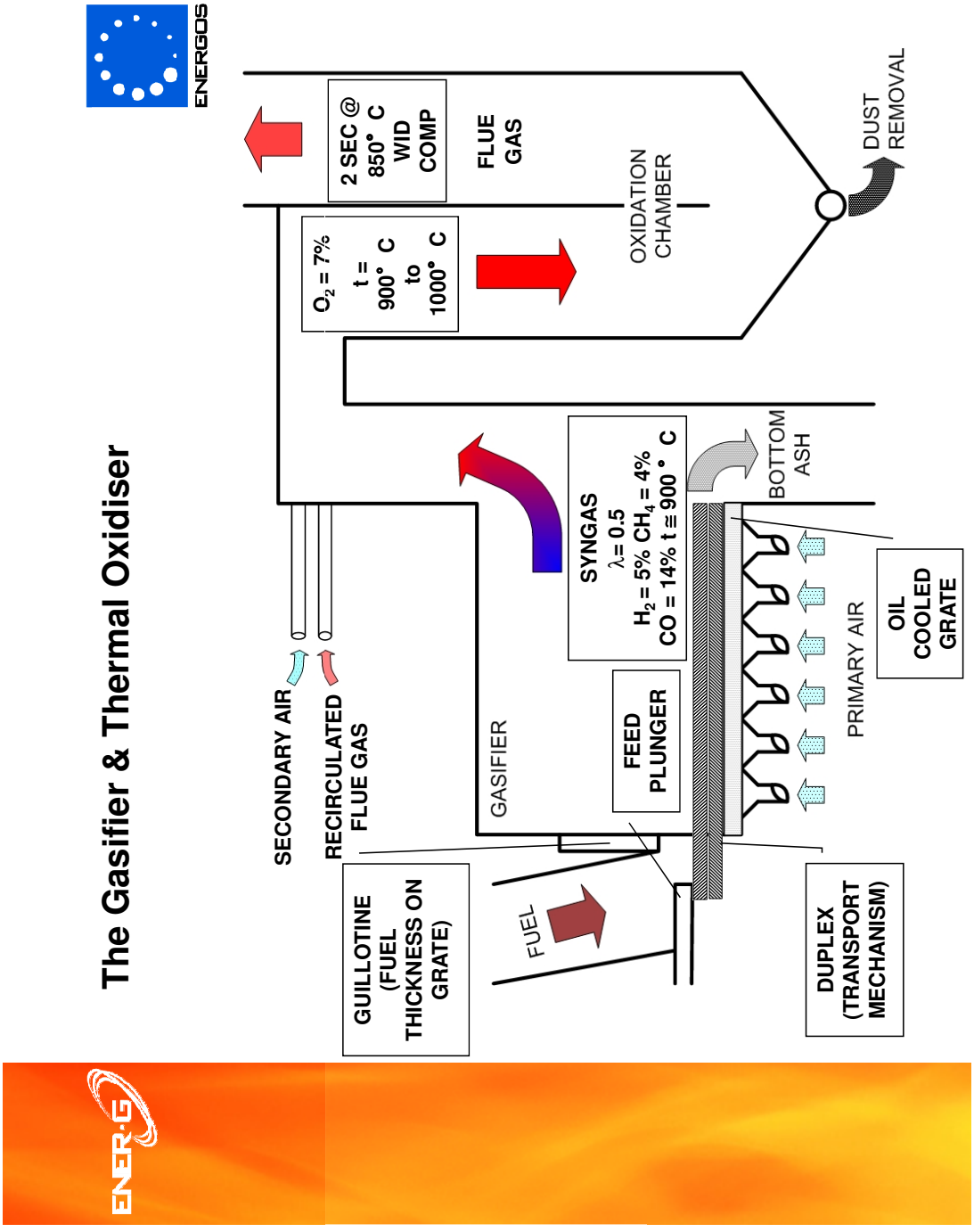

Figure A.2: Combustion chambers, used with permission from Energos.

Appendix B

The Reynolds transport theorem

All the laws of mechanics are written for a system, which is defined as an arbitrary quantity of mass of fixed identity. Everything external to this system is denoted by the term surroundings, and the system is separated from its surroundings by its boundaries [5].

To convert a system analysis to a control volume analysis, we must convert our mathematics to apply to a specific region rather than to individual masses. This conversion, called the Reynolds transport theorem, can be applied to all the basic laws [5].

Let B be the property of interest of the fluid (energy, mass, momentum etc.) and integrate over the control volume (CV):

$$\frac{d}{dt}B_{syst} = \frac{d}{dt}\left(\int_{CV} \beta\rho \; dV\right) + \int_{CS} \beta\rho(v_m \cdot \vec{e}) \; dA \tag{B.1}$$

On the right hand side we have the flux term

$$\int_{CS} \beta\rho(v_m \cdot \vec{e}) \; dA = -\int_{CS} \beta \; d\dot{m}_{in} + \int_{CS} \beta \; d\dot{m}_{out} \tag{B.2}$$

that is an inlet/outlet flux accounting for what goes in and out through the control surfaces (CS). β is the amount of B per unit mass m of the fluid, $\beta = \frac{dB}{dm}$, ρ is the density, $\dot{m}$ is mass flow, $\vec{e}$ is an outward normal unit vector, V is the volume of the control volume, dA is each differential area of surface and v_m the mean velocity of the flow. The equation (B.1) shows that the overall change of property B equals the change of B inside the control volume plus what comes in through its surfaces.

Appendix C

Constants

$k_{1f} =$	$1.40 \times 10^4\ T^3\ e^{-33.63/(0.008314T)}$
$k_{2f} =$	$4.40 \times 10^6\ T^{1.5}\ e^{3.1/(0.008314T)}$
$k_{2b} =$	$2.41 \times 10^{13}\ T^{0.222571}\ e^{-104/(0.008314T)}$
$k_{3f} =$	$5.75 \times 10^{19}\ T^{-1.4}$
$k_{4f} =$	$2(3.52 \times 10^{16}\ T^{-0.7}\ e^{-71.42/(0.008314T)})$

Table C.1: Arrhenius constants

	a_0	a_1	a_2	a_3	a_4
CH_4	4.568	-8.975×10^{-3}	3.631×10^{-5}	-3.407×10^{-8}	1.091×10^{-11}
CO	3.912	-3.913×10^{-3}	1.182×10^{-5}	-1.302×10^{-8}	0.515×10^{-11}
CO_2	3.259	1.356×10^{-3}	1.502×10^{-5}	-2.374×10^{-8}	1.056×10^{-11}
H_2	2.883	3.681×10^{-3}	-0.772×10^{-5}	0.692×10^{-8}	-0.213×10^{-11}
H_2O	4.395	-4.186×10^{-3}	1.405×10^{-5}	-1.564×10^{-8}	0.632×10^{-11}
O_2	3.630	-1.794×10^{-3}	0.658×10^{-5}	-0.601×10^{-8}	0.179×10^{-11}
N_2	3.539	-0.261×10^{-3}	0.007×10^{-5}	0.157×10^{-8}	-0.099×10^{-11}

Table C.2: Constants from [10] for calculating C_p

Species	ΔH_f° [kJ mol^{-1}]
CH_4	-74.51
CO	-110.53
CO_2	-393.51
H_2	0
H_2O	-241.81
O_2	0
N_2	0

Table C.3: Heat of formation

Species	Molar mass [g mol^{-1}]
CH_4	16.012
CO	28.01
CO_2	44.01
H_2	2.016
H_2O	18.016
O_2	32
N_2	28.02

Table C.4: Molar mass

Appendix D

Measured inputs

This appendix shows the measured flow rates of flue gas out, recirculated flue gas (denoted R1 and R2) and secondary air (denoted S1 and S2). Measured temperature from the primary chamber is also included.

Dataset 1

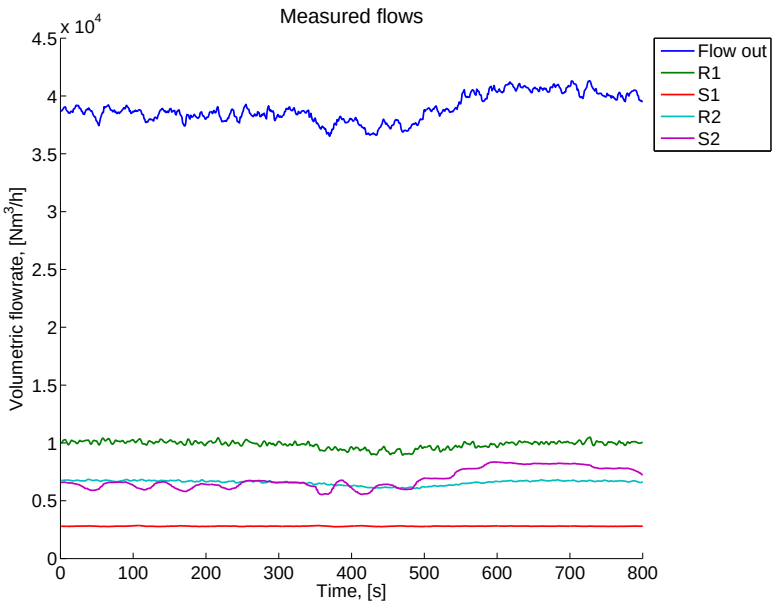

Figure D.1: Measured flow rates

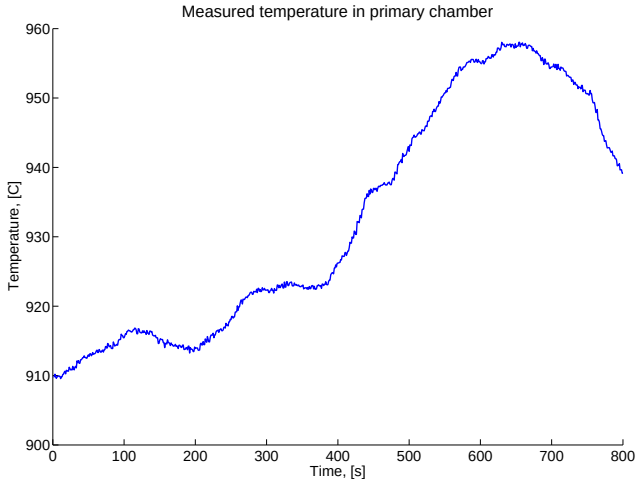

Figure D.2: Measured temperature primary chamber

Dataset 2

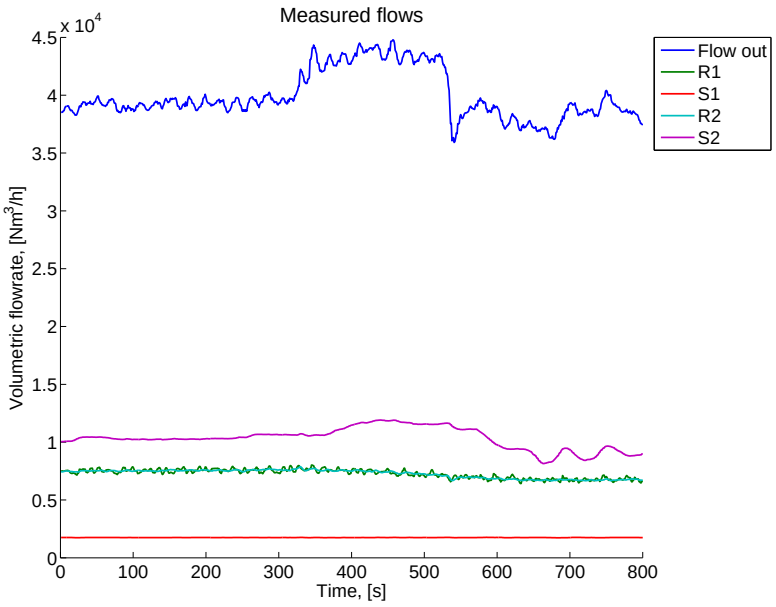

Figure D.3: Measured flow rates

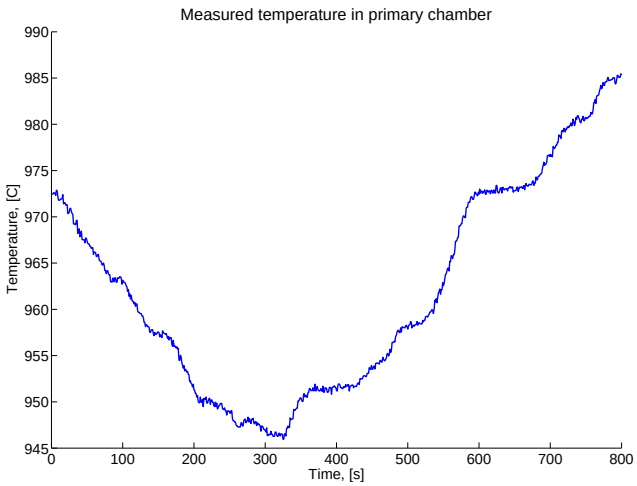

Figure D.4: Measured temperature primary chamber

Dataset 3

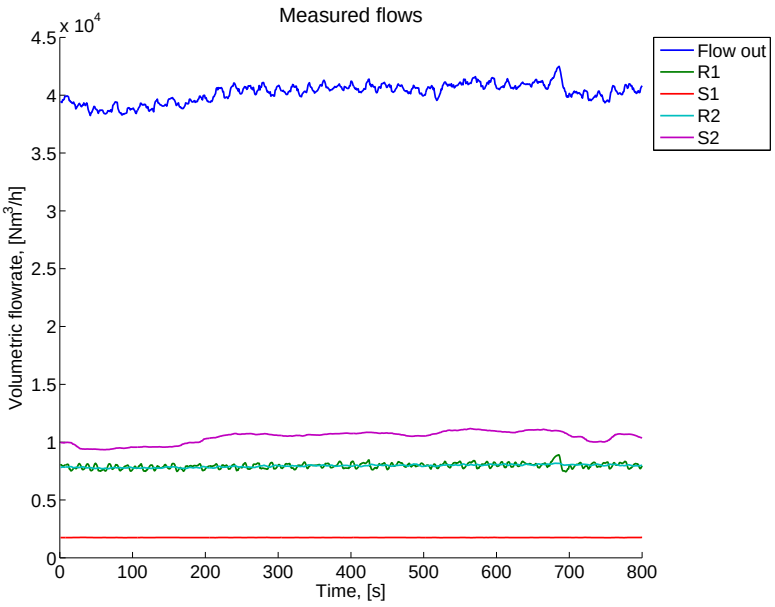

Figure D.5: Measured flow rates

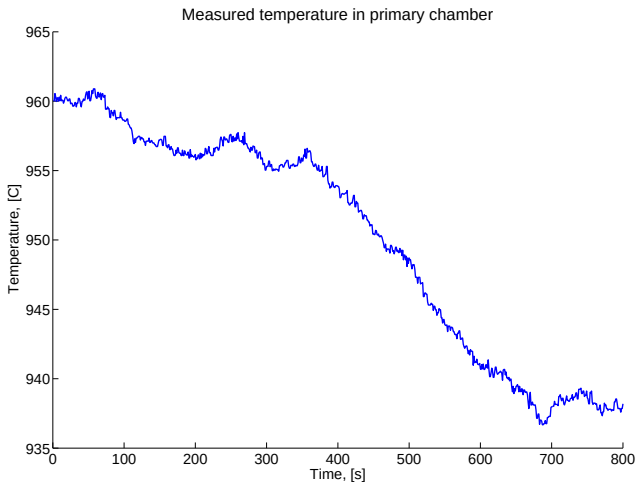

Figure D.6: Measured temperature primary chamber

Special case, quenching

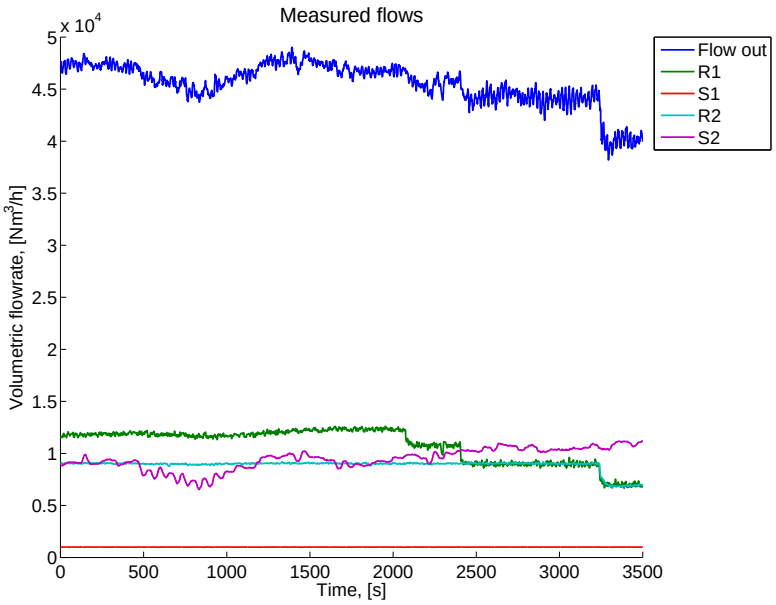

Figure D.7: Measured flow rates

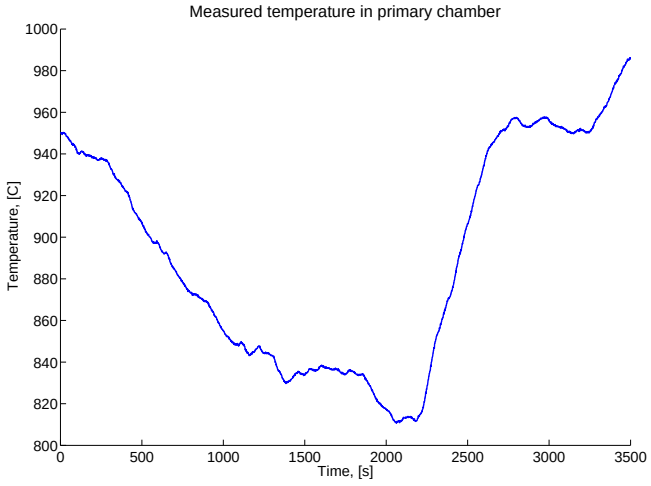

Figure D.8: Measured temperature primary chamber

Appendix E

Detailed temperature plots

E.1 Without Kalman filter

Dataset 1

Figure E.1 shows the same data as in Figure 3.14, but this time each control volume is shown in each subplot.

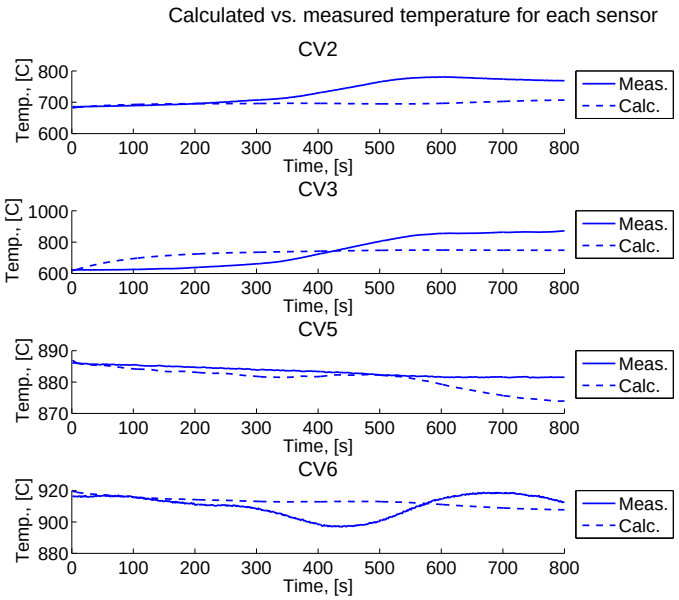

Figure E.1: A zoom-in of Figure 3.14, predicted vs. measured gas temperatures

Dataset 2

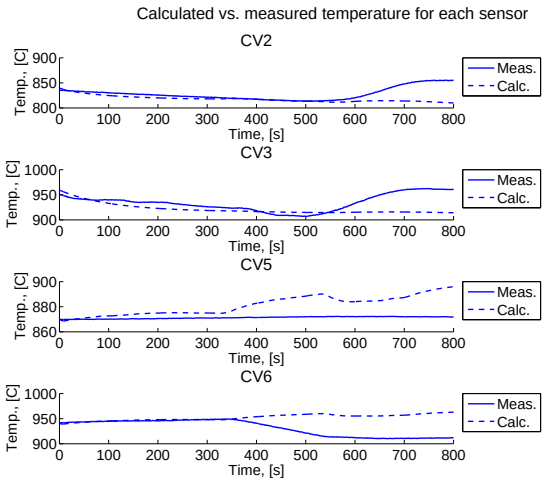

Figure E.2: A zoom-in of Figure 3.16, predicted vs. measured gas temperatures

Dataset 3

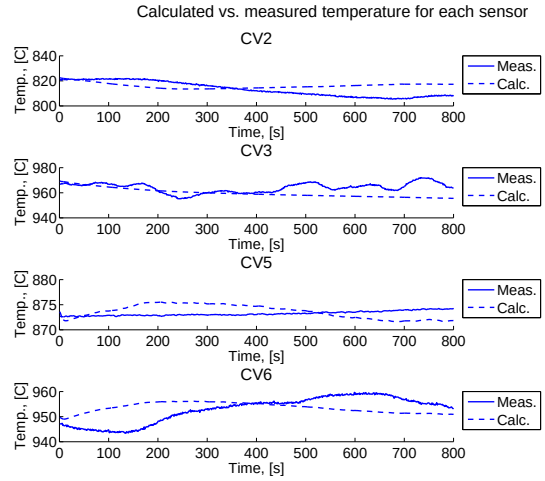

Figure E.3: A zoom-in of Figure 3.18, predicted vs. measured gas temperatures

Special case, quenching

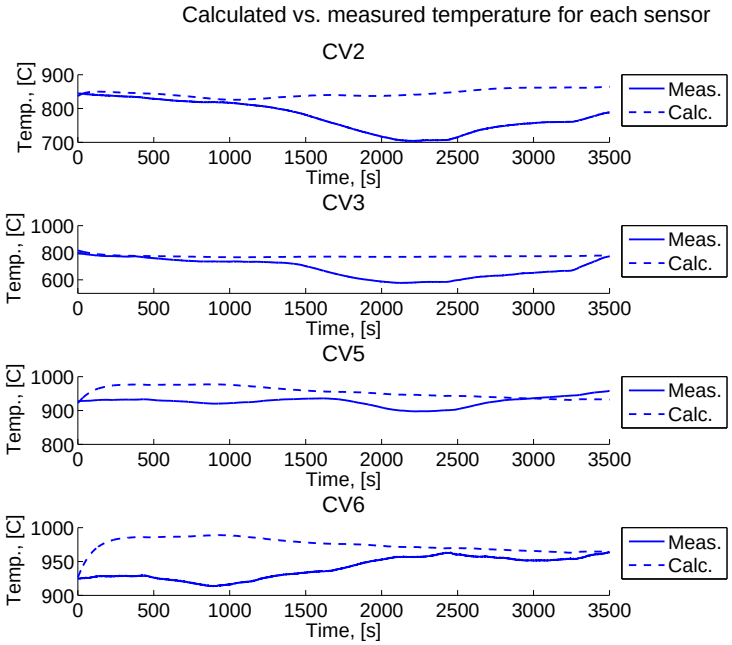

Figure E.4: A zoom-in of Figure 3.20, predicted vs. measured gas temperatures

E.2 With Kalman filter

Dataset 1

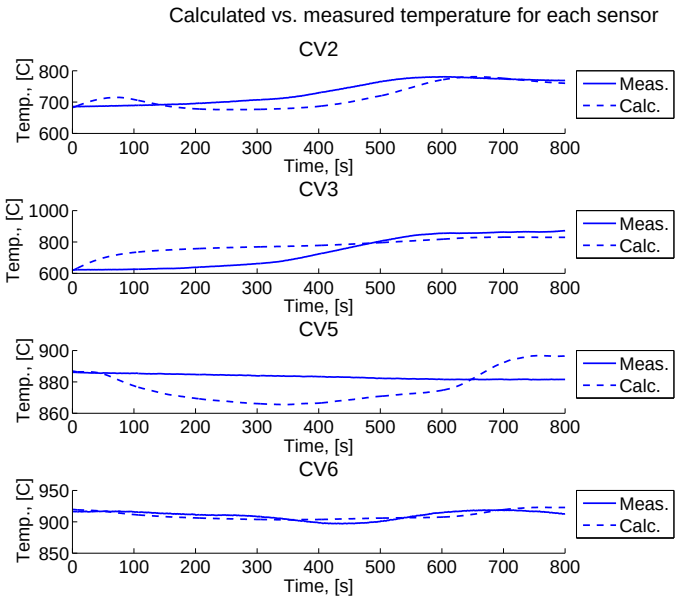

Figure E.5: A zoom-in of Figure 3.22, predicted vs. measured gas temperatures

Dataset 2

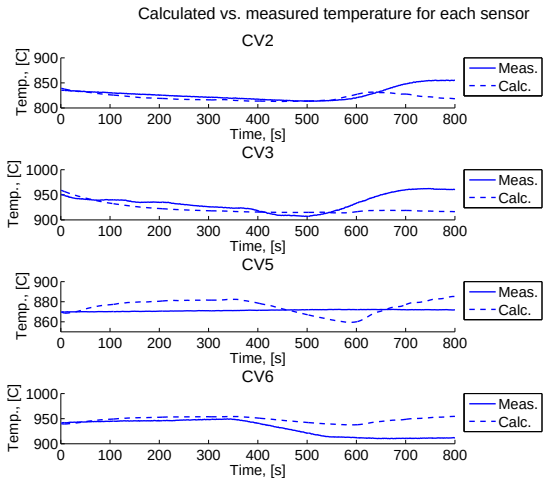

Figure E.6: A zoom-in of Figure 3.26, predicted vs. measured gas temperatures

Dataset 3

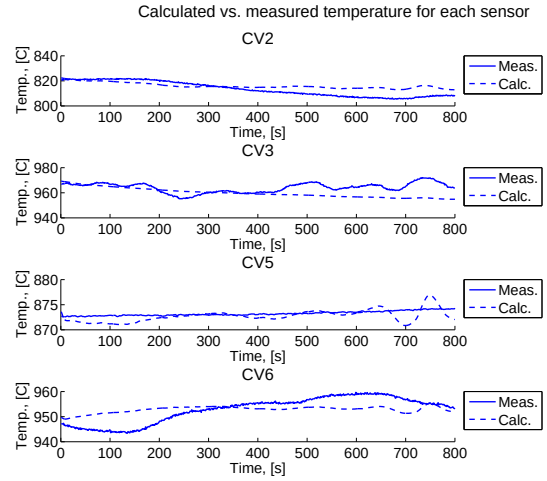

Figure E.7: A zoom-in of Figure 3.29, predicted vs. measured gas temperatures

Special case, quenching

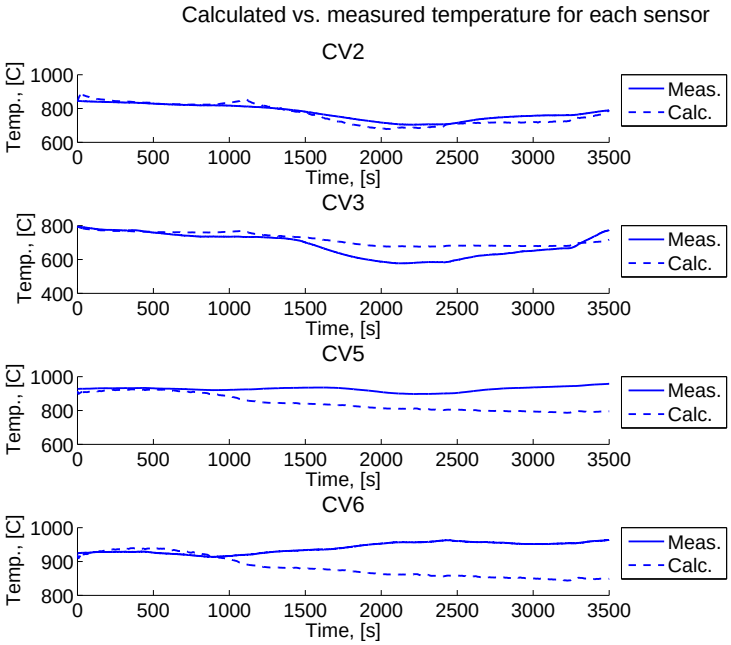

Figure E.8: A zoom-in of Figure 3.32, predicted vs. measured gas temperatures

Appendix F

Source code

Here follows the code for the functions calculating the kinetics and the calculated measured temperature.

F.1 Kinetics

```
1  void burning (double temp, double flow1, double flow2,
2    double *com1, double *com2, double *con,
3    double *par, double *burn, double valve){
4
5    if(valve == 0){
6      return;
7    }else{
8
9    //concentration of each species
10   double CH4, CO, CO2, H2, H2O, O2, N2;
11
12   double H2factor, CH4factor, COfactor;
13   double r1, r2, r3, factor2, factorSG, factorAir;
14   double Tcrossover = 800 + Tdiff, TzeroReaction;
15
16   factorSG = 1;
17   factorAir = 0.0;
18   CH4 = factorSG*com1[0]*flow1 + com2[0]*flow2;
19   CO =  factorSG*com1[1]*flow1 + com2[1]*flow2;
20   CO2 = factorSG*com1[2]*flow1 + com2[2]*flow2;
21   H2 =  factorSG*com1[3]*flow1 + com2[3]*flow2;
22   H2O = factorSG*com1[4]*flow1 + com2[4]*flow2;
23   O2 =  factorSG*com1[5]*flow1 + factorAir*com2[5]*flow2;
24   N2 =  factorSG*com1[6]*flow1 + com2[6]*flow2;
25
26   /*has to be below Tcrossover*/
27   TzeroReaction = 400+Tdiff;
```

```
28
29    factor2 = (1-exp(-temp/200));
30
31    H2factor = 0.99;
32    CH4factor = 0.8;
33    COfactor = 0.6;
34
35    if(O2>0){
36      /*Hydrogene burns first; H2 + 1/2*O2 -> H2O */
37      if(H2>0 /*&& temp > (820+273.15)*/){
38        r1 = (H2>(O2*2))?O2*2:H2;
39          r1 = r1*factor2*H2factor;
40        O2 -= 0.5*r1;
41      }else{
42        r1 = 0;
43      }
44
45      /*Methane burns second; CH4 + 3/2*O2 -> CO + 2*H2O */
46      if(CH4>0 && O2>0  /*&& temp > (820+273.15)*/){
47        r2 = ((CH4>(O2*2/3.))?(O2*2/3.):CH4);
48            r2 = r2*factor2*CH4factor;
49        O2 -= r2*3./2;
50        CO += r2;
51      }else{
52        r2 = 0;
53      }
54      /*Carbonmonoxide burns last; CO + 1/2*O2 -> CO2 */
55      if(CO>0 && O2>0){
56        r3 = (CO>(O2*2))?(O2*2):CO;
57        r3 = r3*factor2*COfactor;
58
59      }else{
60        r3 = 0;
61      }
62    }else{
63      r1 = 0;
64      r2 = 0;
65      r3 = 0;
66    }
67
68    burn[0]=  -r2;
69    burn[1]=  (r2-r3);
70    burn[2]=  r3;
71    burn[3]=  -r1;
72    burn[4]=  r1+2*r2;
73    burn[5]=  -0.5*r1 - 1.5*r2 - 0.5*r3;
74    burn[6]=  0;
75    }
76  }
```

F.2 Measured temperature

```
1  void measuredTemperature(double const *tempGas,
2    double const *tempWall, double *tempMeas){
3
4  int i;
5  //width across the chamber
6  double xmax = 5;
7
8  //how far out from the wall is the sensor placed
9  double xmeas = 1;
10
11 double xmid = xmax/2;
12 double Tmax[4], Tmin[4], Tavg[4], a[4];
13 Tavg[0] = tempGas[1];
14 Tavg[1] = tempGas[2];
15 Tavg[2] = tempGas[4];
16 Tavg[3] = tempGas[5];
17 Tmin[0] = tempWall[1];
18 Tmin[1] = tempWall[2];
19 Tmin[2] = tempWall[4];
20 Tmin[3] = tempWall[5];
21
22   for(i=0;i<4;i++){
23     Tmax[i] = Tmin[i] + 4/3*(Tavg[i]-Tmin[i]);
24     a[i]=(Tmax[i]-Tmin[i])/(xmid*xmid);
25     tempMeas[i] = f(Tmax[i],a[i],xmeas,xmid);
26   }
27 }
28
29 double f(double Tmax,double a,double x, double xmid){
30   return -a*(x-xmid)*(x-xmid)+Tmax;
31 }
```

Bibliography

[1] Silvia Bardi and Alessandro Astolfi. Modeling and control of a waste-to-energy plant. *IEEE Control Systems Magazine*, 30(6):27–37, 2010.

[2] The ENER·G group. Energy from waste, comercially proven energy recovery. www.energ.co.uk/energy-from-waste, December 2011.

[3] Kristin Guldberg. Modelling and control of the secondary combustion chamber in an energy from waste plant. Technical report, NTNU, 2011.

[4] G. Del Alamo, A. Hart, A. Grimshaw, and P. Lundstrøm. Characterisation of syngas produced from MSW gasification at commercial-scale energos plants. In *Thirteenth International Waste Management and Landfill Symposium*, 2011.

[5] Frank M. White. *Fluid Mechanics*. McGraw Hill, 6 edition, 2008.

[6] R.C. Flagan and J.H. Seinfeld. *Fundamentals of air pollution engineering*. Prentice-Hall, 1988.

[7] Marcus Bollig, Amable Liñán, Antonio L. Sánchez, and Forman A.Williams. A simplified approach to the numerical description of methane-air diffusion flames. *Symposium (International) on Combustion*, 27(1):595–603, 1998.

[8] Mechanical and University of California at San Diego Aerospace Engineering (Combustion Research). Chemical-kinetic mechanisms for combustion applications. http://combustion.ucsd.edu, September 2011.

[9] Gonzalo Del Alamo (employee at Energos). Personal communication, September 2011.

[10] Bruce E. Poling, John M. Prausnitz, and John P. O'Connell. *The Properties of Gases and Liquids*. McGraw Hill, 5 edition, 2001.

[11] Sigurd Skogestad. *Prosessteknikk*. Tapir Akademiske Forlag, 3 edition, 2009.

[12] Paul A. Tipler and Gene Mosca. *Physics for scientists and engineers*. Freeman, 5 edition, 2004.

[13] Peter Singstad. *Modelling and multivariable control of high pressure autoclave reactors for polymerization of ethene*. PhD thesis, Norges tekniske høyskole, NTH, 1992.

[14] Petros A. Ioannou and Jing Sun. *Robust adaptive control*. Tapir akademisk forlag, 2003.

[15] Tor Steinar Schei. On-line estimation for process control and optimization applications. *Journal of Process Control*, 18(9):821–828, 2008.

[16] Andreas Hammervold. Model based estimation and control of a bos converter. Master's thesis, NTNU, 2011.

[17] OPC Foundation. The interoperability standard for industrial automation & related domains. http://www.opcfoundation.org, May 2012.

[18] Free Software Foundation. Gsl - gnu scientific library. http://www.gnu.org/software/gsl/, April 2012.

[19] Erwin Kreyszig. *Advanced engineering mathematics*. Wiley international edition, 9 edition, 2006.

[20] J.M. Maciejowski. *Predictive control: with constraints*. Pearson Education. Prentice Hall, 2002.

[21] Morten Hovd. Lecture notes for the course advanced control of industrial processes, December 2011.

[22] Wikipedia. Model predictive control. http://en.wikipedia.org, June 2012.

[23] Halgeir Ludvigsen. Model based control of energos' waste-to-energy plants. pre-study report for development project. Technical report, Cybernetica, 2004.

[24] Peter S. Maybeck. *Stochastic models, estimation, and control*, volume 141 of *Mathematics in Science and Engineering*. Academic Press, 1979.

[25] Robert Grover Brown and Patrick Y. C. Hwang. *Introduction to Random Signals and Applied Kalman Filtering*. Wiley, 3 edition, 1997.

[26] S. Kolås, B.A. Foss, and T.S. Schei. Noise modeling concepts in nonlinear state estimation. *Journal of Process Control*, 19(7):1111–1125, 2009.

[27] Magnus Nørgaard, Niels K. Poulsen, and Ole Ravn. New developments in state estimation for nonlinear systems. *Automatica*, 36(11):1627–1638, 2000.

[28] Bjarne A. Foss and Tor S. Schei. Putting nonlinear model predictive control into use. *Assessment and Future Directions, LNCIS*, 358:407–417, 2007.